Université de Montréal

Fronto-parietal neural activity during multi-attribute decision-making

par Ayuno Nakahashi

Département de Neurosciences

Faculté de Médecine

Thèse présentée en vue de l'obtention du grade de Philosophiae Doctor (Ph. D.) en Neurosciences

Janvier, 2023

Université de Montréal

Département de neurosciences : Faculté de Médecine

Cette thèse intitulée

Fronto-parietal neural activity during multi-attribute decision-making

Présentée par

Ayuno Nakahashi

A été évaluée par un jury composé des personnes suivantes

Roberto Araya, Ph. D.
Président-rapporteur

Paul Cisek, Ph. D.
Directeur de recherche

Marina Martinez, Ph. D.
Membre du jury

Lawrence H. Snyder, M. D. Ph. D.
Examinateur externe

RÉSUMÉ

Cette thèse examine deux modèles alternatifs de prises de décision motrice à travers des données comportementales humaines et des données électrophysiologiques de singes obtenues lors d'une tâche de décision multi-attributs.

Les théories psychologiques classiques suggèrent que la prise de décision soit une fonction de l'exécutif central (EC). En accord avec cela, de nombreuses études ont montré des modulations neuronales concernant les décisions dans le cortex préfrontal (PFC), renforçant la notion que les décisions sont prises à un niveau abstrait dans l'exécutif central du cerveau : le PFC. Cependant, de telles corrélations neuronales se trouvent également dans les régions sensorimotrices, qui étaient traditionnellement considérées externes à l'EC. Cela a conduit à un modèle alternatif de prise de décision dans un EC, impliquant plusieurs zones cérébrales, y compris les zones exécutives et sensorimotrices. Ce second modèle suggère qu'une décision est prise lorsque les compétitions au sein et entre les aires cérébrales arrivent à une résolution, ce qui permet d'atteindre un consensus distribué (CD).

L'objectif principal de cette thèse est de tester les prédictions faites par ces deux modèles. Pour ce faire, nous avons conçu une tâche d'atteinte basée sur la valeur d'attributs multiples et créé une situation dans laquelle les deux modèles font des prédictions neuronales distinctes. Dans cette tâche, deux attributs visuels indépendants indiquaient le montant de la récompense associé à chaque cible. L'un était un degré de luminosité, information ascendante (BU pour "*bottom-up*"), ciblant le réseau de saillance par le biais de la voie visuelle dorsale. L'autre était un indice d'orientation de ligne, information descendante (TD pour "*top-down*"), ciblant le réseau de catégorisation basé sur la connaissance par le biais de la voie visuelle ventrale. Nous avons effectué des enregistrements dans la région d'atteinte pariétale (PRR) et le cortex pré-moteur dorsal (PMd) du singe, dont les activités neuronales ont été précédemment impliquées comme étant modulées par des attributs BU et TD similaires. Dans la plupart des essais, les deux attributs étaient congruents – tous les deux favorisant la même cible. Cependant, un sous-ensemble d'essais avait des cibles avec la même valeur de récompense totale, mais où les deux attributs étaient en conflit (les caractéristiques BU et TD favorisant des cibles opposées). Le modèle de l'EC prédit que dans ce cas, l'activité neuronale la plus précoce doit apparaître dans une région exécutive et que les

régions sensorimotrices doivent recevoir la diffusion de cette décision. Ainsi, ce modèle prédit que la différence du temps de réaction entre le PRR et le PMd sera constante, quelle que soit la manière dont la décision est prise. En revanche, le modèle CD prédit que l'intervalle de décision doit refléter le rôle d'une région dans la décision en cours. Plus précisément, si PRR et PMd font tous deux parties du réseau de décision distribué et jouent un rôle dans l'évaluation des attributs BU et TD, un choix en faveur de l'attribut BU devrait apparaître d'abord dans le PRR et par la suite dans le PMd, tandis qu'un choix en faveur de l'attribut TD devrait apparaître dans l'ordre inverse.

Notre étude démontre que le temps de réaction des participants humains était plus rapide dans les essais congruents et lors de l'utilisation de l'information BU par rapport à l'utilisation de l'information TD. La distribution ne reflétait pas linéairement la complexité de l'attribut et semblait plutôt suggérer une intégration incomplète des informations disponibles. Ainsi, le résultat n'était pas entièrement explicable par un modèle d'EC pur. Le temps de réaction des participants était également plus rapide lorsqu'ils choisissaient entre deux options de grande valeur par rapport aux options de faible valeur, ce qui suggère que la loi de Weber ne s'applique pas aux attributs visuels indiquant des informations de valeur. La distribution du temps de réaction de notre premier singe était similaire à celle des participants humains. Sur le plan neuronal, l'intervalle de décision du PMd était presque toujours plus rapide que celle du PRR et le PRR ne précédait jamais le PMd; aussi, la différence de l'intervalle de décision entre ces régions n'était pas constante. Le PMd a montré un biais de base pré-stimulus dans les essais de choix libre, alors que ce n'était pas le cas pour le PRR. La distribution de l'intervalle de décision dans le PMd variait également en fonction des conditions d'essai, tandis que celle du PRR ne distinguait que les cibles uniques des cibles multiples. Une tendance similaire a été observée dans les analyses préliminaires des potentiels de champ locaux (LFP). Enfin, les résultats préliminaires suggèrent des effets plus cohérents de la micro-stimulation dans le PMd que dans le PRR.

Nos résultats soutiennent le rôle causal du PMd, mais pas celui du PRR. Nos résultats sont cohérents avec les rapports précédents sur l'activité neuronale liée au choix dans les régions pariétales, car l'activité du PRR reflétait le choix du singe dans notre tâche. Nos résultats sont également cohérents avec d'autres études montrant l'absence de preuves du rôle causal des régions pariétales dans la prise de décision, car l'ordre relatif de l'activité prédictive du choix dans le PRR et le PMd ne variait pas entre les différentes conditions. À la lumière de ces deux modèles, nos

résultats suggèrent une troisième alternative, qui inclut potentiellement le PMd en tant que partie du réseau de décision, mais pas le PRR.

Mots-clés : prise de décision, multi-attribut, sélection d'action, caractéristique visuelle, libre choix, valeur relative, valeur absolue, conflit, cortex pré-moteur, cortex pariétal postérieur, région pariétale d'atteinte, PMd, PPC, PRR, électrophysiologie, singe, humain.

ABSTRACT

This thesis examines two alternative models of action decisions through human behavioural and monkey electrophysiological data obtained during a multi-attribute decision task.

Classic psychological theories suggest that decision-making is a function of the Central Executive (CE). In line with this, many studies showed neural correlates of decision variables in the prefrontal cortex (PFC), strengthening the notion that decisions are made at an abstract level in the brain's central executive: PFC. However, such neural correlates are also found in sensorimotor areas, which were traditionally considered outside the CE. This has led to an alternative model to the decision making in a CE, involving multiple brain areas including both executive and sensorimotor areas. This second model suggests that a decision is made when competitions within and across brain areas come to a resolution, thus a Distributed Consensus (DC) is achieved.

The main objective of this thesis is to test the predictions made by these two models. To do so, we designed a multi-attribute value-based reaching task, and created a situation in which the two models made distinct neural predictions. In this task, two independent visual attributes indicated the amount of reward associated with each reach target. One was a "bottom-up" (BU) brightness, targeting the saliency network through the dorsal visual pathway. The other was a "top-down" (TD) line orientation cue, targeting the knowledge-based categorization network through the ventral visual pathway. We recorded from monkey parietal reach region (PRR) and dorsal premotor cortex (PMd), whose activities have previously been implied to be modulated by similar BU and TD attributes. In most trials, the two attributes were congruent – both favoring the same target. However, a subset of trials consisted of a conflict between the two attributes (BU and TD features favoring opposite targets), but the targets had the same total reward values. Here, the CE model predicted that the earliest choice-predictive activity should appear in an executive region, and sensorimotor regions were expected to be receiving this decision broadcast. Thus, the model predicted the latency difference between PRR and PMd to be constant, regardless of how the decision is made. In contrast, the DC model predicted choice latency should reflect a region's role in the ongoing decision. Specifically, if both PRR and PMd are part of the distributed decision network and play a role in evaluating the BU and TD attributes, a choice in favor of the BU attribute should appear first in PRR and then in PMd, whereas a choice in favor of the TD attribute should appear in the opposite order.

We report that human participants' reaction time (RT) was faster in congruent trials and when using the BU information compared to when using the TD information. The RT distribution did not linearly reflect the attribute complexity, and instead suggested an incomplete integration of available information. Thus, the result was not fully explainable with a pure CE model. Their RT was also faster when choosing between two high-valued options compared to low-valued options, suggesting that Weber-Fechner law does not apply to visual attributes that indicate value. Our first monkey's RT distribution was similar to that of human participants. Neurally, choice latency of PMd was almost always faster than that of PRR and PRR never preceded PMd, and the latency difference between these regions was not consistent. PMd showed a pre-stimulus baseline bias in free-choice trials, whereas PRR did not. The distribution of choice latency in PMd also varied with trial conditions, whereas that of PRR only discriminated single versus multiple targets. A similar trend was seen in preliminary analyses of local field potentials. Finally, preliminary results suggest more consistent effects of microstimulation in PMd than in PRR.

Our results support the causal role of PMd, but do not support that of PRR. This is consistent with previous reports of choice-related neural activity in the parietal regions, as PRR activity did reflect the monkey's choice in our task. Our results are also consistent with other studies showing the absence of evidence for parietal regions' causal role in decision-making, as the relative order of choice-predictive activity in PRR and PMd did not vary between different conditions. In light of the two models, our results suggest a third alternative, which potentially includes PMd, but not PRR, as part of the decision network.

Keywords: decision making, multi-attribute, action selection, visual features, free choice, relative value, absolute value, conflict, premotor cortex, posterior parietal cortex, parietal reach region, PMd, PPC, PRR, electrophysiology, monkey, human.

LAY ABSTRACT

"Why did I do that?" This thesis is an attempt to understand how our brain chooses between different actions.

According to classic theories, we make decisions by converting all available information into a single measure of desirability and compare it among different options. This allows us to make difficult decisions, such as choosing between a boring job with a high salary versus an exciting job with a low salary. This notion has been supported by neurological and neurophysiological studies, suggesting that decision-making is an executive function governed by the frontal lobe.

However, the neural patterns used to imply the frontal lobe's role as a decision-maker have also been reported in other brain regions. This includes sensorimotor regions, which are traditionally believed to control movement. Does this mean these areas are also involved in making decisions?

To address this question, we designed a multi-attribute choice task, and analysed behavioural and neural data from human participants and two monkeys. Our results support the causal role of one of the two sensorimotor areas, dorsal premotor cortex, but not the other: the parietal reach region. We suggest that action decisions can be influenced by activity in a sensorimotor area, and propose that the brain's decision network reaches beyond the traditional executive regions.

TABLE OF CONTENTS

RÉSUMÉ ..... **C**

ABSTRACT ..... **F**

LAY ABSTRACT ..... **H**

TABLE OF CONTENTS ..... **I**

LIST OF TABLES ..... **N**

LIST OF FIGURES ..... **O**

LIST OF ABBREVIATIONS ..... **R**

DEDICATION ..... **U**

ACKNOWLEDGEMENT ..... **V**

CHAPTER 1 INTRODUCTION **1**

Background 3

The Origin of the Central Executive 4

Isolating Cognition 7

Sense-Think-Act framework in Goods Space 9

Affordance Competition Hypothesis in Action Space 12

Central Executive and Distributed Consensus 15

Global Research Question 17

Neural Latency as a Causality Measure 17

Bottom-up and Top-down Flow of Information 19

Regions of Interest 21

Fronto-parietal Circuit 21
Macaque Monkeys as the Model of the Human Brain 27
Why monkeys? 28
Comparing Humans and Monkeys 29
Summary 31
CHAPTER 2 OVERVIEW 33
Objective 33
Specific Research Questions 33
Hypotheses 33
Specific Predictions 34
CHAPTER 3 HUMAN BEHAVIOUR 38
Scope 38
Graphical Abstract 39
Abstract 40
Keywords 40
New & Noteworthy 41
Introduction 41
Materials & Methods 44
Participants 44
Experimental setup 45
Trial Conditions 46
Behavioural Analysis 49
Statistical Tests 50

Results 50
Accuracy and reaction times varied across conditions. 50
Errors in conflict trials had shorter reaction times when choosing a BU-favored target. 59
Participants made faster choices when choosing between two high-valued targets. 60
Changes of mind were mostly a switch from the BU-favored to the TD-favored target. 63
Discussion 65
Acknowledgements 70
CHAPTER 4 MONKEY BEHAVIOUR AND ELECTROPHYSIOLOGY 71
Introduction 71
Materials and Methods 72
Subjects and Project Timeline 72
Task Apparatus 74
Dual Feature Task 75
Training Timeline 77
Directional Bias 79
Neural Recording 79
Neural Data Analysis 83
Microstimulation 86
Results – Behaviour 87
Monkey RT varied with trial types, but the difference disappeared over time. 87
Monkey RT was similar to human RT 88
Results – Electrophysiology 89
Recorded Neurons 89

Example neuron from PMd 91
Population Latency Analysis 95
Microstimulation 105
Neural Space Analysis 107
Local Field Potential (LFP) Analysis 110
Conclusion 111
CHAPTER 5 GENERAL DISCUSSION 115
Summary 115
On “premotor, but not parietal” 119
Interpreting the Pre-stimulus baseline bias 120
Latency and causality 122
Between a Central Executive and a Distributed Consensus 123
Limitations 127
Sample Sizes 127
The premise and corresponding predictions assumed extreme cases 128
Limited Attributes 129
Overtraining 130
Future Directions 131
Reversible Inactivation 131
Additional Attributes 131
Closing the Loop 132
The Rich Club 132
Conclusion 132

REFERENCES..... 134

LIST OF TABLES

Table 1. Number of recorded neurons from each brain region. 90

Table 2. Summary of Population Tuning Latency 101

Table 3. Microstimulation effect details 107

LIST OF FIGURES

Chapter 1

Figure 1. Three components of the working memory hypothesis 4

Figure 2. The brain as a black box 8

Figure 3. Saccade Network 22

Figure 4. Reach Network 24

Chapter 2

Figure 5. Predictions of the Central Executive model 36

Figure 6. Predictions of the Distributed Consensus model 36

Chapter 3

Figure 0. Graphical abstract 39

Figure 1. Dual Feature Task 48

Figure 2. Effect of target value difference on the (A) accuracy and (B) z-scored log RT 51

Figure 3. Cumulative distributions of RTs 53

Figure 4. Cumulative distributions of z-scored log RTs of all participants. 56

Figure 5. Scatter plot of mean RT across trial conditions 58

Figure 6. Z-scored log RT distributions of correct and error trials during Conflict trials with unequal targets (ConD) 60

Figure 7. Mean RTs grouped by offered reward magnitude. 62

Figure 8. Change of Mind (CoM) trials 65

Chapter 4

Figure 1. Task Setup 74

Figure 2. Dual Feature Task Timeline 75

Figure 3. Target Features, Points and Trial Conditions 76

Figure 4. Monkey Y's performance while he learned the BU and TD features 78

Figure 5. GrayMatter drive electrode placements on Monkey Y 80

Figure 6. Neural Data Collection Flow 82

Figure 7. Example neuron recorded over 5 sessions 83

Figure 8. Microstimulation schematic 86

Figure 9. Cumulative histograms of RT distribution of Monkey Y 87

Figure 10. Scatter plot of mean RT across trial conditions, primates 88

Figure 11. Example neuron during 1T trials 91

Figure 12. Example neuron during Easy trials 92

Figure 13. Example neuron during Twin trials 93

Figure 14. Example neuron during Conflict trials 94

Figure 15. PMd population activity during 1T and Easy trials 96

Figure 16. PMd population activity during Twin, ConS and ConM trials 97

Figure 17. Activity of PMd Population without early cells during 1T and ConS trials 98

Figure 18. PRR Population activity during 1T, Easy-BU, Easy-TD and Twin trials 99

Figure 19. PRR Population activity during Twin, ConS and ConM trials 100

Figure 20. Cumulative Choice Latency 103

Figure 21. Cumulative Choice Latency by conditions 104

Figure 22. Microstimulation location 105

Figure 23. Example microstimulation effects 106

Figure 24. Principal Components of Neural Space Analysis, all neurons 108

Figure 25. Neural Space Analysis, Monkey Y 109

Chapter 5

Figure 1. Schematics of the predictions of the two theories during conflict trials 117

Figure 2. Schematics of the three theories 124

LIST OF ABBREVIATIONS

1T	single target trial
46d	dorsal area 46
46v	ventral area 46
8b	area 8 subdivision b
9d	dorsal area 9
ACC	anterior cingulate cortex
AIP	anterior intraparietal
AS	arcuate sulcus
BU	bottom-up
CE	central executive
CoM	change of mind
ConD	Conflict-Different (non-equivalued targets with incongruent attributes)
ConD-BU	ConD trial, better target indicated by the BU attribute
ConD-TD	ConD trial, better target indicated by the TD attribute
ConM	Conflict-Mirror (equivalued targets with incongruent attributes, one target's BU value equals the other target's TD value)
ConM-BU	ConM trial, chosen target favoured by the BU attribute
ConM-TD	ConM trial, chosen target favoured by the TD attribute
ConS	Conflict-Same (equivalued targets with incongruent attributes, one target's BU value does not equal the other target's TD value)
ConS-BU	ConS trial, chosen target favoured by the BU attribute
ConS-TD	ConS trial, chosen target favoured by the TD attribute
cPMd	dorsal premotor cortex, caudal area
cPMv	ventral premotor cortex, caudal area
CS	central sulcus
dACC	dorsal anterior cingulate cortex
DC	distributed consensus
dlPFC	dorsolateral prefrontal cortex
dmPFC	dorsomedial prefrontal cortex
FEF	frontal eye field
Hz	Hertz (cycle per second)
IPS	Intraparietal sulcus

LFP	local field potential
LIP	lateral intraparietal area
LU	lunate
lPFC	lateral prefrontal cortex
M1	primary motor cortex
MIP	medial intraparietal area
MT	middle temporal visual area
OFC	orbitofrontal cortex
OT	opposite target
PC	principle component
PCA	principle component analysis
PCD	precentral dimple
PE	parietal cortex subdivision E
PEc	parietal cortex subdivision E, caudal area
PEip	parietal cortex subdivision E, medial bank of intraparietal sulcus
PFC	prefrontal cortex
PMd	dorsal premotor cortex
PPC	posterior parietal cortex
PRR	parietal reach region
PS	principle sulcus
PT	preferred target
rPMd	dorsal premotor cortex, rostral area
rPMv	ventral premotor cortex, rostral area
SC	superior colliculus
SEF	supplementary eye field
SF	Sylvian fissure
SMA	supplementary motor area
STS	superior temporal sulcus
TD	top-down
V6A	anterior visual area 6
VIP	ventral intraparietal area
vmPFC	ventromedial prefrontal cortex

"Simplicity is the foundation of complexity."

Slick Dogg at GUTTA ZONE, 2019

DEDICATION

To Matt, who showed me both the beauty and brutality of life

and

for everyone who is like me,

ACKNOWLEDGEMENT

I did not make this happen alone. Many people helped me.

First and foremost, I would like to thank my supervisor Dr. Paul Cisek, for his unconditional support and inspiration, and trusting me to undertake this project. Second, I would like to acknowledge Yoda and Kona, for without them this thesis would not have existed. To the indispensable technician of the Cisek Lab, Marie-Claude Labonté, thank you for being such a great colleague, plus pulling me into the world of running. To my committee members, Dr. John Kalaska and Dr. Aarlenne Khan, thank you for keeping me on track, especially during the toughest times. To my lab mates, I always appreciate your presence and having conversations, both casual and scientific. 知李さん、カナさん、父さん、そしておばあちゃん、いつも応援してくれてありがとう。 And Matt, for taking me to the start line, Mark and Natalia, for being there throughout the journey, Fabi, for being there when things got rough, and René, for supporting me until this finish line. Thank you, gracias, Дякую, merci. I would also like to acknowledge the funding sources, particularly the GRSNC and the FRQNT. Finally, I would like to thank Montreal Krump Alliance for saving my sanity and keeping me grounded.

CHAPTER 1 INTRODUCTION

One of the most crucial survival abilities for an organism is to make the right decisions, especially about actions. For simple organisms in a harsh environment, a wrong move could easily lead to death; for more complex species, suboptimal behavioural responses can result in a loss of feeding or mating opportunities; and for humans, one wrong action could eliminate a path to the dream career or result in developing pathological conditions such as addiction (Borutaite, 2010; Nestler, 2005; Wong & Candolin, 2015). Importantly, while in the modern world many of our most significant decisions are abstract and with long-term consequences, the most significant kind of decisions for which our brains have evolved are those dealing with the concrete needs of survival and immediate actions (Cisek, 2019). Understanding how such decisions emerge in the brain will provide deeper insights into how and why we tend to make certain decisions, and what can be done to help ameliorate certain maladaptive behaviour.

Classically, behaviour is described as a serial process that consists of three separate subcomponents: *perception, cognition,* and *action*. In this view, 1) *perception* processes the sensory input, 2) *cognition* creates the mental representations of the available options which will be used to make a decision, and then 3) *action* is planned and executed to realise the decision (Hurley, 2001). Therefore, decision-making is considered as a part of the *cognition* component, processing the abstract information in isolation from the perception and the action components. In line with this view, numerous neurophysiological studies have reported neural activities reflecting the variables relevant to each component. For example, sensory input such as the visual (Jones & Palmer, 1987; Ringach, 2004; Supèr et al., 2001), auditory (Mesgarani et al., 2014; Pasley et al., 2012; Schnupp et al., 2010) and tactile information (Hernández et al., 2000; Shoham & Grinvald, 2001) is readily decodable from respective sensory cortices in mammals, suggesting neural

substrates for the *perception* component. A plethora of decision-relevant variables, ranging from task rules (Goodwin et al., 2012), stimulus information (Constantinidis et al., 2001), current state (Critchley & Rolls, 1996), desirability of the available options (Hikosaka & Watanabe, 2000; Hosokawa et al., 2007; Padoa-Schioppa, 2009), and the subjective preference (Wallis & Miller, 2003) modulate the neural activity in the subregions of the frontal cortex, which is believed to govern *cognition*. Once a decision is made, the information is sent to sensorimotor regions such as primary motor cortex (C.-S. R. Li et al., 2001; Vargas-Irwin et al., 2010) and superior colliculus (Lee et al., 1988; McPeek & Keller, 2002; Munoz & Wurtz, 1993), where the abstract decision is converted into *actions*, allowing the agent to realise the decision in the world. This hypothesis on decision making will be referred to as the Central Executive model, emphasizing the idea that decision processes are a comparison between abstract representations in the frontal, executive region in the brain.

Intriguingly, the neural correlates relevant to each component are not exclusive to the putative subcomponent regions, but appear to be distributed across various brain regions. A number of studies in monkeys have shown that neural activity in orbitofrontal (OFC) (Padoa-Schioppa, 2009; Wallis, 2007; Wallis & Miller, 2003), dorsolateral prefrontal (dlPFC) (Constantinidis et al., 2001), ventromedial prefrontal (vmPFC) (Delgado et al., 2016; Kahnt et al., 2011) and anterior cingulate (ACC) cortices (Amiez et al., 2006; Hadland, 2002) can be used to predict a subject's choice before the execution of an overt response. Concurrently, such choice-predictive neural modulation is also reported in sensorimotor regions, such as superior colliculus (SC) (Basso & Wurtz, 1998), lateral intraparietal area (LIP) (Colby et al., 1996; Cui & Andersen, 2007; Louie & Glimcher, 2010), parietal reach region (PRR) (Gail & Andersen, 2006; Klaes et al., 2011) and primary motor and premotor cortices (Pastor-Bernier & Cisek, 2011; Thura & Cisek, 2014). Traditionally, these

regions are believed to be involved in the movement planning and execution, and thus considered to be an *action* component of the Central Executive model (Hurley, 2001; Vargas-Irwin et al., 2010). If the decision is a *cognitive* process that happens in an executive region, why should the choice variables affect neural activities in the *action* regions? This has led to an alternative hypothesis that, at least when choosing between actions, decisions are not made in a unified central executive area, but rather emerge as a distributed consensus across multiple brain regions (Cisek, 2012). Accordingly, the observed choice-relevant neural modulation in the sensorimotor regions is not a mere efflux from the central executive area, but potentially contributes to the ongoing decision process. This hypothesis will be referred to as the Distributed Consensus model, emphasizing the notion that decision processes are widely distributed across different brain regions, and the behavioural response results from the consensus among a pertinent decision network.

The goal of this thesis is to dissociate the two aforementioned models to understand how value-based action decisions evolve in the primate brain. Because these models make similar behavioural and neural predictions in most situations, we designed a task to create an experimental condition in which they make distinct predictions about activity of different brain regions. The outcome of this thesis will address whether decisions are always made at the level of abstract representations in the central executive, or whether they can be made at different levels in multiple regions simultaneously (Baddeley, 2003; Barsalou et al., 2018; Cai & Padoa-Schioppa, 2019; Cisek, 2012; Gibson, 1979; Levy & Glimcher, 2012).

BACKGROUND

This thesis focuses on two alternative models about action decisions: one that proposes that all decisions are made in a Central Executive of the brain, and the other that proposes that decisions

about actions are made when a Distributed Consensus is achieved among multiple brain regions that comprise a distributed decision network. A brief history of the two models is described below.

The Origin of the Central Executive

The concept of the central executive comes from the working memory hypothesis, which was developed to explain how humans perform complex behaviour by temporarily storing and manipulating information (Baddeley, 1992; Baddeley & Hitch, 1974). The original working memory hypothesis consists of three components: the phonological loop, the visuospatial sketch pad, and the central executive, illustrated in Figure 1 (Baddeley, 1992). The first two components are considered the slave systems, whose roles are to hold and process the sound- and language- related information and the visuospatial manipulations, respectively (Baddeley, 2003). The central executive overlooks these slave systems and manages cognitive resources.

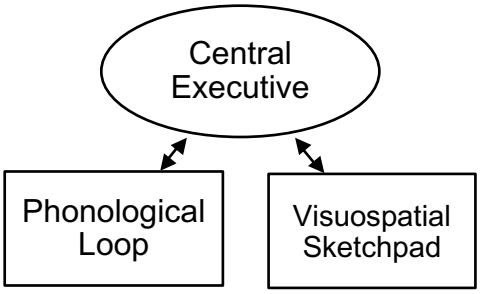

Figure 1. Three components of the working memory hypothesis

The central executive controls cognitive resources, while the phonological loop and the visuospatial sketchpad store language and arithmetic information and process visuospatial information, respectively.

The distinction between the three components is supported by results from the dual-task paradigm, in which human participants are required to perform two tasks simultaneously. It was shown that if the two tasks recruit the same slave systems (e.g., the word span task and the articulation inhibition, both utilising the phonological loop), the performance was greatly affected compared to when the two tasks recruit different slave systems (e.g., the word span task utilising the phonological loop and the tracking task utilising the visuospatial sketch pad) (Baddeley, 1992; Baddeley et al., 1997). Thus, it was suggested that, in a healthy brain, the two slave systems function separately from one another. The role of the central executive and its distinction comes

from the same task performed by a clinical population. Patients with frontal lobe lesion and Alzheimer's disease, who often show impaired executive functions, display reduced performance in the dual-task paradigm compared to their nonclinical counterparts, even though the two tasks differ in their characteristics and should therefore recruit different slave systems (Baddeley et al., 1997; Kaufman et al., 2012). Importantly, their slave systems appear to be intact, because they are able to perform individual tasks well in isolation (Baddeley, 1992). Thus, it was proposed that frontal lesions and Alzheimer's disease affect the central executive functions, resulting in an observed decline in the dual-task performance (Baddeley, 1992). Other studies also suggested the role of the central executive in selective attention, resonating with the notion that the role of the central executive is to manage limited resources (Della Sala et al., 1995; Desimone & Duncan, 1995; Hitch et al., 2018).

Originally, the working memory hypothesis was proposed as a conceptual framework and explicitly admitted its lack of anatomical substrates (Baddeley, 1996). Nonetheless, with the subsequent studies in lesion patients and the recent progress in the imaging and electrophysiological techniques, there has been a progressive accumulation of evidence suggesting the neural substrates for each subcomponent (Baddeley, 2003; de Schotten et al., 2011; Papagno et al., 2017). For example, in human imaging studies, it has been shown that spatial memory tasks activate the right hemisphere, whereas verbal memory tasks activate the left hemisphere, suggesting that the visuospatial sketchpad and the phonological loop reside in separate hemispheres (E. E. Smith & Jonides, 1997). Furthermore, retrieval of different elements within the phonological loop appears to recruit different brain regions, such that the item retrieval in the digit span task was more dependent upon Broca's area, whereas the order retrieval of the same task was more dependent on the supramarginal gyrus (Papagno et al., 2017). Other studies of visuospatial

memory suggest similar neuroanatomical segregation based on different types of visual- and spatial information (de Schotten et al., 2011; E. E. Smith & Jonides, 1997; Suchan et al., 2002). These results strongly supported the argument for the distinction between the two slave systems, while also suggesting the within-system fractionation based on more detailed properties of the task. In contrast to the slave systems, in which the functional dissociation has been more tractable, the central executive has always been a rather loose concept (Baddeley, 2003). Nevertheless, there has been an abundance of studies suggesting that the central executive resides in the frontal lobe in humans (Curtis & D'Esposito, 2003; Delgado et al., 2016; Hitch et al., 2018; Kaufman et al., 2012; Tanji & Hoshi, 2008), monkeys (Goodwin et al., 2012; Tanji & Hoshi, 2008) and rodents (Delgado et al., 2016), supporting the initial premise. In fact, the apparent link between the executive function and the frontal lobe was dominant enough that some researchers inverted the direction, studying the function of the frontal lobe as a means to understand the role of the central executive (Desimone & Duncan, 1995; Shallice, 1982; Shallice & Burgess, 1991). Initially, the author who proposed the working memory hypothesis was hesitant to draw such strong connections between the frontal lobe and the central executive (Baddeley, 1992, 1998; Baddeley et al., 1997). However, in a later article, he accepted this notion of the frontal lobe as the putative neural substrate for the central executive, agreeing with the notion of the frontal lobe as the executive region (Baddeley, 2003).

Throughout the history of the working memory hypothesis, the frontal lobe has always been suggested as a candidate brain area for the central executive (Baddeley, 1996, 2003; Hitch et al., 2018; Tanji & Hoshi, 2008). The central executive was proposed as a resource-managing system which, in a broad sense, can be interpreted as various higher-order cognitive functions that are disturbed upon a frontal lobe injury. Backed by the growing body of neurophysiological and

imaging findings, what was once a fuzzy concept became a category that describes the less tangible "higher-order" processes controlled by the frontal lobe (Baddeley, 2003).

Isolating Cognition

Much of the progress in understanding working memory was made by subdividing the systems based on the properties of the task and exploring the corresponding neural substrates. Undoubtedly, early cognitive psychology and neuroscience tremendously benefited from such a fractionation method and the bottom-up approach. That is, if there is a complex phenomenon to be investigated, researchers deconstruct the phenomenon into simpler elements and attempt to manipulate them in a controlled laboratory setting. The collection of such observations is then used to rebuild and explain the whole phenomenon. For example, a study of speech may start by subdividing it into comprehension and production, and further deconstructing them into sentences to clauses, to words, to phonemes, and so on (Harris, 1970). Once we understand how we perceive and produce certain phonemes, we can then proceed to investigate what happens when they are put together to form words, and then sentences, incrementally adding complexity to finally understand how we carry a conversation. The working memory hypothesis utilises this method and dissociates the function of the phonological loop and the visuospatial sketch pad, which were then combined to demonstrate the function of the higher-order system: the central executive (Baddeley, 1992). The view was further strengthened when the neural substrates for the theorised elements were found, providing the anatomical support that such elements could exist in the brain. In addition, it also provided a convenient framework for explaining the black box nature of brain and behaviour. For example, to study how humans process phonemes, researchers can run experiments that utilise auditory stimuli with a variety of phonetic manipulations and record the behavioural responses of the participants. If the obtained results display a pattern, then it may be used to infer which phonetic

characteristics the brain uses to distinguish one phoneme from the other. In other words, because the input (sensory information) and the output (behavioural response) are tractable and measurable, we only need to come up with some sort of an explanation for what happens in between.

Conceptually, the beauty of such a fractionation approach lies in its ability to strip away the outer layers of a phenomenon to study the core elements without interference from other elements. After all, the majority of scientific investigations are designed based on the philosophy of *ceteris paribus* – "all other things being equal" (Schiffer, 1991). To measure the effects of the variable of interest, one manipulates the variable while keeping everything else the same. Hence, it is unsurprising that a large body of studies about cognition focused on the concept of cognition itself, while other disciplines such as *perception* and *action* were developed and investigated as separate entities. Conveniently, this approach also fits the analogy of the brain as a computer. It allows the intuitive conceptualisation of the tangible hardware as our body, consisting of input and output devices, and the more intricate, indecipherable software as our brain (Piccinini & Bahar, 2013). Thus, if our brain works in the similar manner, perhaps an accumulation of rigorous experimental data shall one day reveal how the brain is programmed to respond to different inputs (Piccinini & Bahar, 2013). (But see also (Jonas & Kording, 2017) for the major caveat of this approach). Studying *cognition*, therefore, is comparable to manipulating the input and the output devices and looking for changes in neural activity, treating the brain as a

Figure 2. The brain as a black box

In a laboratory, researchers can manipulate the target sensory stimulus with high precision, and the behavioural responses can be recorded with high resolution. In other words, we know exactly what the input and the output parameters are. So, all we need to know is what kind of processes happen in the brain that converts the stimulus into the observed responses.

black box (Figure 2). The underlying assumption here is that *cognition* is analogous to computation, which was later elaborated into the philosophy of computationalism (Piccinini & Bahar, 2013). Accordingly, if our brain works like a computer, we should be able to isolate the computation part from the other "peripheral" elements and study them independently (Engel et al., 2013).

Sense-Think-Act framework in Goods Space

The concepts of *input, computation,* and *output* of computationalism is realised as a serial algorithm consisting of *sense, think*, and *act* in robotics (Hurley, 2001). A robot that executes this algorithm will first *sense* the environment through its input devices, then *think* by computing the relevant information based on the preinstalled rules, and finally *act* to achieve a programmed goal using its output devices. Thus, a robot vacuum cleans a room by detecting debris, applying the rules to decide that it is to be removed, and approaches the debris while engaging its sweeping brushes. This linear model also provides a fitting framework for our behaviour: when we see something on the floor (*sense*), we may decide that it is a coffee spill and thus needs to be cleaned (*think*), and grab a mop to get to the spillage (*act*). In both cases, the rule is simple: remove the waste. Therefore, what is decided during the *think* phase is also simple: whether the detected object is a waste or not. This Sense-Think-Act framework is also capable of deconstructing a more elaborate scenario, such as a career choice. If you are deciding between different career options, you will probably first gather the relevant information (*sense*). Then, you will compare the different aspects of the options, such as the duty, salary and benefits, commute distance, and future outlook (*think*). Finally, you will choose one of the offers by signing the contract and declining the others (*act*). In this example, the information at the *sense* phase likely comes from multiple sensory organs such as the eyes and the ears, which is converted into neural signals and processed at respective brain regions, such as the visual and auditory cortices (Ferstl et al., 2008; Nassi &

Callaway, 2009; Saur et al., 2010). These signals are then fed to the brain area whose role is to *think*, wherein the choice-relevant information is converted into a unified common currency. As a result, factors such as the duty, salary, commute distance and future outlook become single values representing their respective desirability, and the sum of these values can be used to represent the overall desirability of different options (Levy & Glimcher, 2012; Padoa-Schioppa, 2011). The comparison between these options happens at an abstract level, also referred to as the *goods space*, and the option with the highest desirability is generally chosen. Finally, once a choice is made, the corresponding action plan is generated and executed in the sensorimotor regions, resulting in the behaviour of signing a contract. Importantly, the main computation of such economic decision happens as the comparison between the abstract common currency in goods space, independently from and undisturbed by the sensorimotor information seen in the *sense* and *act* components (Padoa-Schioppa, 2011; Shizgal, 1997).

Supporting the above notion, a number of studies have reported neural correlates of the economic-decision variables. For example, A seminal study by Schultz et al. showed that activity in the monkey orbitofrontal cortex (OFC) discriminated expected versus unexpected reward, as well as the absence of reward despite the monkey's expectation, and showed that such activity was strongly linked to the dopaminergic cells in the striatum (Schultz et al., 2000). Subsequent studies showed that monkey OFC activity reflects the expected and the actual outcomes of reward, punishment, and the absence of reward (Hosokawa et al., 2007; Schultz et al., 2000; Wallis & Miller, 2003), as well as the subjective preference of different reward types (Hikosaka & Watanabe, 2000; Padoa-Schioppa & Assad, 2006, 2008). In rats and monkeys, studies suggest the role of OFC in satiety-induced devaluation (Critchley & Rolls, 1996; Gallagher et al., 1999; Pritchard et al., 2008). Damage in OFC results in an inability to update the behavioural response when the reward

rule changes, such that macaque monkeys, marmosets and human patients with OFC lesions continue to choose the stimulus that was previously, but is no-longer, rewarded (Clarke et al., 2007; Dias et al., 1996; Rolls et al., 1994). Similarly, lesion studies in rats and macaque monkeys showed that the anterior cingulate cortex (ACC) plays a role in action-reward contingency learning (Kennerley et al., 2006; Schweimer & Hauber, 2005), but not in stimulus-reward contingency learning (Rudebeck et al., 2008; Walton et al., 2003). In addition, a monkey electrophysiology study showed that neurons in the ACC respond to a visual stimulus only when it predicts upcoming reward, suggesting their role in reflecting the monkeys' reward expectancy (Shidara & Richmond, 2002). In line with this, a case study showed that ACC lesion leads to deficits in manual but not verbal response during attentionally demanding tasks (Turken & Swick, 1999). In ventromedial prefrontal cortex (vmPFC), studies showed that neural activity is modulated by the overall value of stimulus options in humans (Kahnt et al., 2011; Philiastides et al., 2010). A careful electrophysiology study in monkey vmPFC revealed regionally distinct neuronal responses to appetitive and aversive stimuli, suggesting that different subregions play distinct roles in processing stimulus-outcome contingency (Monosov & Hikosaka, 2012). Other studies suggest that activity in monkey dorsolateral prefrontal cortex (dlPFC) is modulated by upcoming reward and planned actions (Wallis & Miller, 2003), types of reward (Watanabe, 1996), and working memory-like processes (Funahashi et al., 1989; Iba & Sawaguchi, 2003; Miller et al., 1996). Human studies suggest that dlPFC is involved in processing the sensory parameters of the visual stimuli, the reward predictability of different stimulus attributes (Kahnt et al., 2011), top-down information processes (Yan et al., 2016), and suppressing unwanted reflexive responses (Pierrot-Deseilligny et al., 2005; Pierrot-Deseilligny et al., 2003). Notably, during these sensory and economic decision tasks, decision-related variables are found mainly in the frontal regions.

Together with the notion of the central executive and the Sense-Think-Act framework, it was therefore proposed that decision-making is one of the executive functions governed by the frontal lobe – the central executive, and that decisions are made as abstract comparisons in goods space, separate from the *sense*- and *act*-related processes (Cai & Padoa-Schioppa, 2019; Levy & Glimcher, 2012; Sugrue et al., 2005).

Affordance Competition Hypothesis in Action Space

Considering the amount of results showing neural correlates of decision-making, the frontal regions undoubtedly contribute to the economic decisions. However, a growing number of monkey electrophysiological studies report that other "non-executive" regions, such as sensorimotor cortices and the subcortical regions, contain neural activities that reflect decision variables. For instance, during a saccade task, neural activity in superior colliculus reflects not just the eventual saccade to be executed, but also the other potential saccades and their likelihood of execution (Basso & Wurtz, 1998; Glimcher & Sparks, 1992; Lee et al., 1988; Munoz & Wurtz, 1993; Sparks, 1978). In case of lateral intraparietal area and supplementary eye field, neural activity is modulated by the expected reward size upon a given saccade (Coe et al., 2002; Colby et al., 1996; Louie & Glimcher, 2010; Platt & Glimcher, 1999; Sugrue et al., 2004). In tasks involving arm movements, parietal reach region, dorsal premotor (PMd) and primary motor (M1) cortices have been shown to contain neurons representing multiple aspects associated with the potential arm movements, including the likelihood of executing a given movement and the expected outcome (Caminiti et al., 1996; Cisek & Kalaska, 2005; Pastor-Bernier & Cisek, 2011; Snyder et al., 2000; Stoet & Snyder, 2004; Thura & Cisek, 2014). In the Sense-Think-Act framework discussed above, these regions fall into the *act* category, whose role is to receive the final decision from the central executive and formulate the movement plans accordingly. Such lack of functional specificity in neural

representations is not unique to the sensorimotor regions; studies have shown that neural activity in the putative central executive region is modulated by sensory variables irrelevant to making the right decision (Constantinidis et al., 2001). Strictly speaking, these results are incompatible with the Sense-Think-Act framework, which treats each category as a distinct process that is separate and independent from one another. In other words, if the role of a central executive is to *think*, it only needs to care about the choice variables and not the action to be followed; and if the role of a sensorimotor region is to *act*, its activity should only reflect the final response. Why should their activity be modulated by seemingly irrelevant variables?

One way to approach this question is by taking a step back to think of a more fundamental situation: survival decisions. When the ongoing decision is directly linked to one's survival, the competing options often involve different actions. For example, a squirrel being chased by a cat has a few options. It can continue running on the ground until the cat is exhausted. It can run into a bush so that the cat may lose it. It can run up a tree so that it may outrun the cat. Or, it can turn around and bite the cat's face. The likelihood of each option leading to the squirrel's successful escape changes continuously based on the relative location of the animals, the bushes, the trees and how much energy each animal is willing to spend on the chase. Humans living in an industrialised society are less likely to be chased by a predator. However, in our daily lives, we still engage in action decisions, such as maneuvering against a stream of people to get to a train, veering right or left in contact sports, and choosing to steer the wheel and/or step on the brake when facing oncoming traffic.

According to the Sense-Think-Act framework, decisions in the example situations above can be described as serial processes. In case of the squirrel, the cost of each action may be computed and represented in ACC, whereas the likelihood of successful escape may be represented in dlPFC.

These variables may be combined to represent the value of each escaping option in a common currency, compared in goods space in OFC, and the winning option executed through premotor and primary motor cortices, resulting in the squirrel climbing up the tree (Cai & Padoa-Schioppa, 2019). In other words, one would expect to see a cascade of the final decision flowing from the frontal, central executive regions to the sensorimotor cortices, followed by the squirrel placing its paw on the tree. In this view, what may appear as decision-relevant neural modulation in the sensorimotor areas are considered irrelevant to the actual decision processes, as decisions are always made at an abstract level, in goods space in the central executive regions (Cai & Padoa-Schioppa, 2019).

An alternative way of looking at this situation proposes that, rather than creating abstract representations of different options for a comparison, the choice between different actions can be made in action space in the sensorimotor regions. In this view, the locations such as the bush and the tree are perceived as "affordances" by the squirrel, providing a potential shelter from the cat (Cisek, 1999; Gibson, 1979). Instead of following the serial order of the Sense-Think-Act framework, it proposes that when choosing between actions, the decision process occurs as a competition between the affordances (e.g., bush/jump/shelter VS tree/climb/shelter VS cat/bite/defense), specified by the sensory information. The advantage of this affordance competition hypothesis is in its responsiveness; as the squirrel runs around, the sensory information such as the relative distance between the animals and the shelters changes, which is reflected in real time as changes in the affordance representations in the squirrel's sensorimotor regions. Once the competition between these affordances is resolved (i.e., a choice is made), the corresponding action can be immediately executed, as the candidate actions are already represented in the sensorimotor regions and are essentially ready-to-go. This is in contrast to the

decisions made in a central executive, which assumes an agent to create abstract representations of the available options every time a decision is to be made. This extra step of decision process results in an inevitable and suboptimal lag between the arrival of new information (e.g., change in the immediate landscape due to the ongoing chase), and the planning and execution of an action. The affordance competition hypothesis suggests that the decision-relevant neural modulations in the sensorimotor regions are causally involved in the ongoing decision processes (Cisek, 2007). In other words, the reason the squirrel climbed up the tree is because it afforded more escapable shelter than other options and with the least distance and energy expenditure at that moment, which was based on the activity in the sensorimotor areas. The total desirability of the same option may have exceeded that of others in the abstract representation in other, non-sensorimotor areas, but that is not always the sole reason of the decision.

Central Executive and Distributed Consensus

So far, I have discussed two possible theories – the Sense-Think-Act framework and the Affordance Competition hypothesis – in which decisions about actions can be made. These two theories provide foundations for the following two decision-making models, whose predictions will be tested in this thesis.

The first model proposes that decisions are always made at an abstract level in a Central Executive. Following the linearity of the Sense-Think-Act framework, this Central Executive model depicts the decision-making processes as a comparison of option representations, which happens in the central executive region, presumably the frontal areas (Baddeley, 2003; Hurley, 2001; Padoa-Schioppa, 2011). This is preceded by the preprocessing of the sensory information and followed by the generation and execution of the corresponding action. The advantage of the Central Executive model is its versatility. As long as the options can be converted into representations of

common currency, virtually anything can join the race, allowing a multi-faceted comparison of different options. It is therefore capable of converting any comparisons into economic decisions, from a complex decision about life partners to a simple choice of grabbing big versus small apples. Furthermore, most classical psychology studies are done in controlled laboratory settings, in which participants are asked to react to a certain stimulus through a simple response such as a button press. In such cases, details of the available action options are limited, and thus should be ignored to increase the efficiency of the current task. The Central Executive model is a straight-forward, one-size-fits-all model of decision-making, which generally separates the decision processes from the other, sensorimotor processes.

The second model proposes that a decision is made through a Distributed Consensus (DC). The Distributed Consensus model is based on the affordance competition hypothesis, in which multiple action options are simultaneously represented in the sensorimotor regions. Note that this model does not oppose the presence of the abstract, goods space; rather, it is treated as one of the many aspects that influence the affordances of each option. During deliberation, different aspects of the available options compete against each other in the respective regions, influencing the competition between the candidate actions in the sensorimotor regions. For example, a group of sensorimotor neurons representing one action may receive a boost from ACC based on its low action cost (Walton et al., 2003), whereas another group of neurons representing a different action may receive a boost from vmPFC based on the trial history (Delgado et al., 2016; Juechems et al., 2017). As one or more of these within-region competition is resolved, it begins to influence the other regions' competition to "tip the scale" in favour of one option over the other. Once the whole brain comes to an agreement through reciprocal connections and the winner-take-all dynamics, a distributed consensus is achieved, and the winning action is executed (Cisek, 2012). Importantly, the

Distributed Consensus model does not assume that all decisions are made in the sensorimotor regions. For example, if the choice is between two job opportunities, the main competition likely occurs in regions that represent the economic variables rather than the sensorimotor cortices. By contrast, when choosing between different actions, the decision processes could occur as a competition between the representations of potential actions in the sensorimotor regions, rather than between abstract representations in isolation of sensorimotor information (Cisek, 2012).

GLOBAL RESEARCH QUESTION

The global research question of this thesis is the following: *Are value-based action decisions made in a central executive or through a distributed consensus?* In other words, is there a single central executive region that broadcasts its final decision to the rest of the brain, or do decisions evolve in multiple brain regions simultaneously? To date, a number of studies have shown neural correlates of decision variables across brain regions (Basso & Wurtz, 1998; Cai & Padoa-Schioppa, 2019; Chang et al., 2013; Chang & Snyder, 2012; Cisek & Kalaska, 2005; Gail & Andersen, 2006; Gold & Shadlen, 2007; Hosokawa et al., 2007; Klaes et al., 2011; Pastor-Bernier & Cisek, 2011; Platt & Glimcher, 1999; Thura & Cisek, 2014; Wallis & Miller, 2003). To gain further insight into the neural mechanisms of decision-making, the next logical step is to verify the causal role of such neural activities.

Neural Latency as a Causality Measure

In order to determine whether a given decision-related neural modulation is causally involved in the ongoing decision, the neural latency of decision variables will be explored. Previous studies reported that, in monkey sensorimotor regions, decision-related neural modulation occurs somewhere between 74 ms and 150 ms after stimulus onset (Cisek & Kalaska, 2005; Ledberg et al., 2007; Pastor-Bernier & Cisek, 2011; Siegel et al., 2015; Thura & Cisek, 2014). Due to the

physiological constraints of the cells in the retina and the brain, there exists a delay between the stimulus onset and the time neural activities reflect the effect of the stimulus (J. H. R. Maunsell et al., 1999; Schmolesky et al., 1998). In addition, activities that are too close to the stimulus onset (e.g., within 50 ms) may only reflect the sensory input rather than decision-related variables, while activities that are further away (e.g., >300 ms) likely contain information pertinent to the motor preparation, especially if the task does not involve a delay period and the subject is allowed to respond at their will (Thura & Cisek, 2014). Therefore, this thesis focuses on the activities observed between 50 ms to 250 ms from the stimulus onset, treating it as a tentative decision time window.

Once the time window is defined, the time course of decision-related population activities can be compared across different brain regions. The logic is as follows: if a region is causally involved in the ongoing decision process, its activity should reflect the subject's choice earlier than regions that are not causally involved. Accordingly, the Central Executive model predicts that a central executive region will always reflect the subject's choice first, and the latency in which other regions receive decision-related modulations will be consistent regardless of the chosen option. In contrast, the Distributed Consensus model predicts that the latency in which a given region reflects the subject choice will depend on whether that region was the tipping point of a given decision. This means, for example, when the decision is made based on one aspect of an option, such as colour, a region that is sensitive to colour will reflect the subject choice before other regions, whereas if the decision was based on another aspect, such as spatial remapping, the space-sensitive region will reflect the choice before the colour-sensitive region (Westendorff et al., 2010).

Bottom-up and Top-down Flow of Information

One of the major inspirations of this thesis was the results reported by Buschman and Miller (Buschman & Miller, 2007). In their study, monkeys performed a match-to-sample task, and reported the target stimulus by making saccadic eye movements. In a given trial, the distractor stimuli were manipulated in such a way that sometimes the target stimulus was a visual "pop-out," while in other times the monkey needed to engage in a serial search. They reported that during the pop-out trials, activities in LIP predicted monkeys' choice substantially earlier than lateral PFC (lPFC) and frontal eye field (FEF). Conversely, lPFC and FEF preceded LIP when the monkeys performed a serial search (Buschman & Miller, 2007). Thus, they concluded that information based on bottom-up attention such as salience flows in the direction of posterior to anterior, whereas information based on top-down attention such as a serial search flows in the opposite direction.

Their conclusion that different types of attentional information are processed along different directions is in line with the theory of two visual pathways (Goodale & Milner, 1992). According to this theory, information about locations and potential actions ("where" and "how") is derived from visual input and takes a dorsal pathway to be processed in the parietal regions, while information about the identity ("what") takes a ventral pathway, through the temporal lobe and is processed in the frontal regions (Goodale & Milner, 1992). It is logical to assume that, due to the salience of the target stimulus, the information during the pop-out trials took the dorsal pathway. Likewise, the serial search trials likely recruited more memory-related circuits for stimulus comparisons, thus the information took the ventral pathway.

Although attentional information is an important player of many decision-making processes, it should not be considered equal to deciding factors. In the task discussed above, it is likely that the

pop-out target triggered the LIP activity for its saliency. However, it is also possible that the actual decision to choose that salient target was made after the first sweep of saliency-driven flow of information. In other words, what Buschman and Miller reported in the LIP activity could be interpreted as sensory information reflecting pure salience, and the decision information reflecting a saccadic eye movement may have occurred afterwards. Similarly, the lack of LIP activation during the serial search may simply reflect the absence of an attention-grabbing stimulus, independent from the decision processes that follow.

The observation of the first sweep of sensory-driven information is compatible with both the Central Executive and Distributed Consensus models. The difference lies in how the correct target is chosen. From the perspective of the Central Executive model, the decision to look at the correct target is made in a CE, presumably in the frontal regions, and the saliency-driven activity in LIP is not a part of the decision processes. From the perspective of the Distributed Consensus model, however, LIP could play a causal role in the decision processes. As the competition between different saccadic eye movements evolves, the saliency-sensitive LIP can boost the choice for the pop-out target, resulting in looking at the salient target. However, it is equally likely that the other regions that are sensitive to the visual feature (e.g., colour, orientation, whether it matches the sample stimulus) or the value (i.e., one is rewarded whereas the others are not) of the target also voted for the same target, making it impossible to decipher where the tipping point was. Therefore, the paradigm by Buschman and Miller demonstrates the different directionality of two types of information flow, but their results do not allow dissociation of the Central Executive and Distributed Consensus models. One approach to dissociate these models is to present subjects with a conflict situation, in which there is no correct answer, forcing different regions to "vote" for different choices and observing how the conflict is resolved.

REGIONS OF INTEREST

Fronto-parietal Circuit

In this thesis, the fronto-parietal circuit was chosen as a candidate circuit whose activity pattern may allow us to dissociate the two models. The fronto-parietal circuit is generally considered as one of the primary neural networks involved in producing eye and arm movements (Borra & Luppino, 2017; Chang & Snyder, 2012; Snyder et al., 1997). From the perspective of serial processing (e.g., Sense-Think-Act framework), the connection from the parietal to the frontal regions allow the integration of the multisensory and motor information, and the frontal to parietal connection provides a route for the transformation from cognitive to motor decisions, which is executed as behaviour (Borra & Luppino, 2017; Hurley, 2001). From the perspective of parallel processing (e.g., affordance competition hypothesis), the interconnectivity allows bidirectional communication between different lobules, providing neural substrates for the inter-regional interactions (Cisek, 2007). Furthermore, by including the temporal lobe into the frame, the temporo-parieto-frontal circuit provides a neural basis for the ventral and dorsal visual pathways, which is supported by rigorous anatomical studies (Markov et al., 2014; Schmahmann et al., 2007). These notions appear valid in both the saccade and reaching movement selections, two of the main behavioural repertoires the circuit is known for. The functional and anatomical details are discussed below.

Saccade Network

The fronto-parietal oculomotor network consists of lateral intraparietal area (LIP), frontal eye field (FEF), and a subset of caudal prefrontal regions adjacent to the FEF, shown in Figure 3 (Borra & Luppino, 2017). LIP resides laterally in the posterior part of the intraparietal sulcus, adjacent to but cytoarchitectonically distinct from the neighbouring regions such as anterior intraparietal area (AIP), medial intraparietal area (MIP) and ventral intraparietal area (VIP) (Borra & Luppino, 2017; Pandya & Seltzer, 1982; Rizzolatti et al., 1998; Swaminathan et al., 2013). LIP is interconnected with FEF and the superior colliculus (SC), receives input from extrastriate areas in the occipital cortex, and projects to dlPFC (Andersen, Asanuma, et al., 1990; Johnson et al., 1996; Lewis & Van Essen, 2000). Along with SC and FEF, LIP neurons are strongly

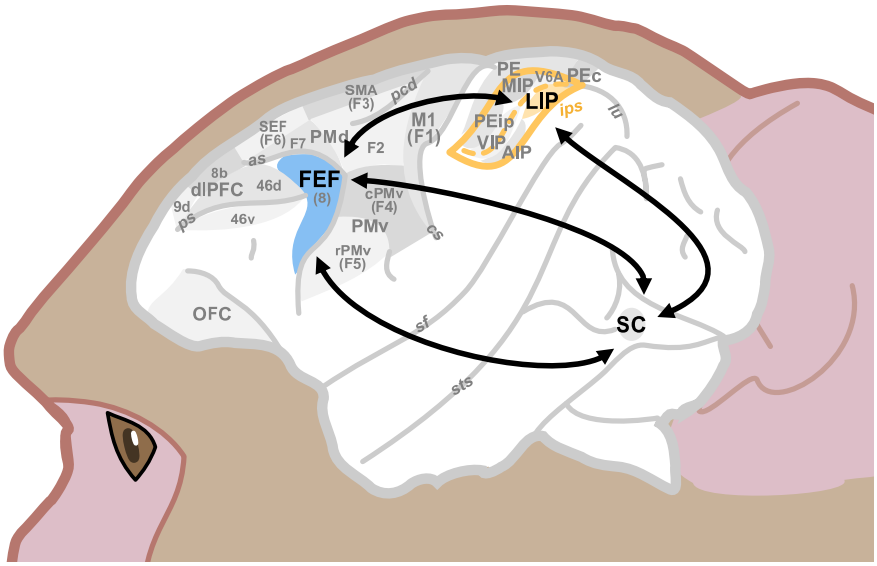

Figure 3. Saccade Network

A schematic of projections between the main areas of saccade network in a monkey brain. FEF and LIP are interconnected, and both areas receive input from SC (dark arrows). Solid and dotted yellow lines indicate the opening and the bottom of the intraparietal sulcus to show the areas inside. AIP, anterior intraparietal; as, arcuate sulcus; CS, central sulcus; dlPFC, dorsolateral prefrontal cortex; FEF, frontal eye field; ips, intraparietal sulcus; LIP, lateral intraparietal area; lu, lunate; M1, primary motor cortex; MIP, medial intraparietal; OFC, orbitofrontal cortex; pcd, precentral dimple; PE, dorsal parietal; PEc, dorsal parietal, caudal area; PEip, dorsal parietal, intraparietal sulcus; ps, principle sulcus; PMd, dorsal premotor cortex, SC, superior colliculus; sf, Sylvian fissure; SEF, supplementary eye field; SMA, supplementary motor area; sts, superior temporal sulcus; VIP, ventral intraparietal area. 8d, 9d, 46d and 46v are subdivisions of PFC. V6A is a subdivision of posterior parietal area. Area definition is based on Rizzolatti et al. (1998), which is an agglomeration of Matelli et al. (1985) and Pandya & Seltzer (1982).

modulated by saccade-related properties, and thus known for their implication in controlling eye movements (Andersen, Asanuma, et al., 1990; Andersen et al., 1998; Basso & Wurtz, 1998; Borra & Luppino, 2017; Caminiti et al., 1996; Colby et al., 1996; Glimcher & Sparks, 1992; Platt & Glimcher, 1999; Sugrue et al., 2004) (but see also (Katz et al., 2016)). In addition, based on its multisensory integrative nature, LIP has been referred to as part of the "association" cortex, suggesting its role as a bridge between sensory, cognitive and motor information (Gottlieb, 2007). It has also been shown that LIP neurons represent space in a body-centered reference frame (Andersen et al., 1998). FEF is located medially in the precentral gyrus, anterior to the premotor cortex and posterior to the Brodmann area 8 (Borra & Luppino, 2017; Matelli et al., 1985; Rizzolatti et al., 1998). It receives input from extrastriate areas in the occipital cortex, and is interconnected with LIP and dlPFC (Andersen, Asanuma, et al., 1990; Markov et al., 2014). FEF is also interconnected with SC with their respective topography preserved, such that the lateral FEF neurons project to the anterolateral SC and medial FEF neurons project to the posteromedial SC (Komatsu & Suzuki, 1985). Similar to SC and LIP, FEF has been strongly implicated in the production of voluntary eye movements (Bruce et al., 1985; Hanes & Schall, 1996; Schall & Thompson, 1999).

Reach Network

The fronto-parietal reach network consists of two of the agranular frontal regions – dorsal premotor cortex (PMd) and primary motor cortex (M1) – and the parietal reach region (PRR), which includes area 5 (also known as PE) of posterior parietal cortex (PPC), V6A in the parietal-occipital area, and medial intraparietal area (MIP) in the intraparietal sulcus, shown in Figure 4 (Andersen et al., 1998; Johnson et al., 1996). PMd is located just posterior to the arcuate sulcus and ventrolateral to the supplementary motor cortex (SMA) and pre-SMA, corresponding to Brodmann area 6 (Matelli

et al., 1985; Rizzolatti & Luppino, 2001). Histological studies suggests a topographic organization of PMd, dividing it into rostral (rPMd or F7) and caudal (cPMd or F2) subregions and are shown to have representations of different body parts (Rizzolatti & Luppino, 2001). rPMd is interconnected with cPMd, M1, area 5, dlPFC, OFC and ACC, whereas cPMd is interconnected with rPMd, M1, area 5, OFC and ACC, and projects to, but does not receive input from dlPFC (Borra & Luppino, 2017; Markov et al., 2014; Rizzolatti & Luppino, 2001; Tanné-Gariépy et al., 2002). Given this connectivity, it has been proposed that the rPMd activity may be prefrontal-dependent, while that of cPMd, due to its high interconnectivity with the area 5, may be parietal-dependent (Luppino & Rizzolatti, 2000). M1, also known as Brodmann area 4 or F1, occupies the area anterior to the central sulcus (Borra & Luppino, 2017; Rizzolatti et al., 1998). M1 is interconnected to cPMd, rPMd and area 5, and its strong projection to the spinal cord is

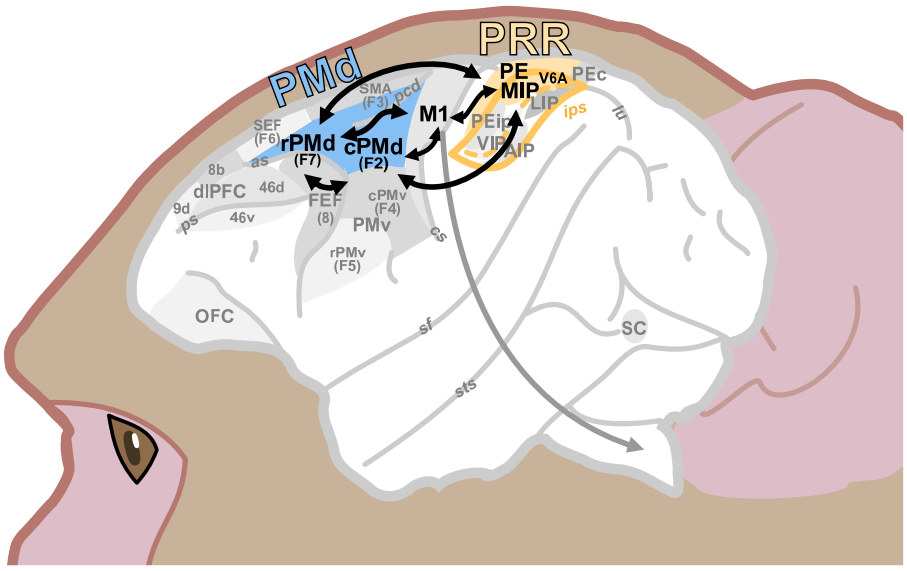

Figure 4. Reach Network

A schematic of projections between the main areas of reach network in a monkey brain. PMd can be subdivided into a rostral (rPMd) and caudal (cPMd) areas, which are interconnected with each other but have slightly different connectivity with areas outside of the reach network (not shown). Solid and dotted yellow lines indicate the opening and the bottom of the intraparietal sulcus to show the areas inside. Dark arrows indicate reciprocal connections. A gray arrow from M1 indicates spinal projection. Abbreviations are the same as Figure 3. cPMd, dorsal premotor cortex, caudal area; ips, Intraparietal sulcus; M1, primary motor cortex; MIP, medial intraparietal sulcus; PMd, premotor cortex; PRR, parietal reach region; rPMd, dorsal premotor cortex, rostral area. V6A is a subdivision of posterior parietal cortex. Area definition is based on Rizzolatti et al., 1998, which is an agglomeration of Matelli et al., 1985 and Pandya & Seltzer (1982).

considered the foundation for its primary role in movement execution (Dum & Strick, 2002; He et al., 1993; Markov et al., 2014; Schmahmann et al., 2007). It also projects weakly to dlPFC, while dlPFC does not project back to M1 (Markov et al., 2014). Area 5, also known as PE of the superior parietal lobule, is the dorsal cortical surface adjacent to the intraparietal sulcus (IPS) (Pandya & Seltzer, 1982). The area 5 is interconnected with cPMd, rPMd and M1, and receives input from, but does not project to, dlPFC (Markov et al., 2014). Area V6A is in the posterior edge of the IPS under the caudal subregion of area PE and anterior to the occipitoparietal area (PO). V6A receives input from prestriate and extrastriate areas, premotor cortex as well as subcortical areas such as pulvinar, caudate nucleus and superior colliculus (Shipp et al., 1998). The MIP resides inside the IPS, posterior to the anterior intraparietal (AIP) and medial to the lateral intraparietal (LIP) area (Pandya & Seltzer, 1982; Seltzer & Pandya, 1986). MIP projects to dlPFC and cPMd, but not to rPMd (Johnson et al., 1996; Markov et al., 2014).

As part of the reach network, PMd, M1, and area 5 and MIP are implied to play distinct roles in planning and executing reaching movements. For example, during an instructed delay period, activity in PMd and M1 has been reported to reflect parameters of upcoming movement such as reaching type, direction, amplitude, speed, the number of targets, and the likelihood that a given action may be rewarded (Churchland et al., 2006; Messier & Kalaska, 2000; Pastor-Bernier & Cisek, 2011; Song & McPeek, 2010; Thura & Cisek, 2014; Vargas-Irwin et al., 2010). In case of area 5 and MIP, studies have shown their role in visuomotor transformation, representing information with respect to action-relevant variables such as the current location of hand, head and eye (Borra & Luppino, 2017; Buneo et al., 2002; Colby & Goldberg, 1999; Fogassi et al., 2005; Gail & Andersen, 2006).

The connectivity characteristics and the functional segregations within the reach network are compatible with both the Central Executive and Distributed Consensus models. From the perspective of the Central Executive model, the non-uniform interconnectivity between the aforementioned regions supports the concept of a linear information flow, from the central executive regions to the action regions, following the fronto-parietal projection. In contrast, the Distributed Consensus model would interpret the distribution of varying projections as the neural basis for the within- and between-region competition. Specifically, the fact that the sensorimotor regions are interconnected, while different prefrontal regions project to some, but not all, of these regions provides an ideal network architecture for a feature-specific biased competition.

Dorsolateral Prefrontal Cortex

Dorsolateral prefrontal cortex (dlPFC) includes Brodmann areas 9 and 46d, located dorsally adjacent to the principal sulcus (Borra & Luppino, 2017; MacDonald et al., 2000). The more dorsal area 9 of dlPFC is interconnected with the more lateral area 46d, rPMd, cPMd, OFC and ACC, and receives input from M1 and area 5 (Markov et al., 2014). Area 46d is interconnected with area 9, rPMd, OFC and ACC, and projects to the area 5 and receives input from M1 and cPMd (Markov et al., 2014).

Along with the OFC, vmPFC and ACC, for which a number of studies propose a role in decision-making processes, the dlPFC has been suggested to be of particular importance, reflecting variability of value prediction, task difficulty, target selection, and sensory information and reward size of available options (Delgado et al., 2016; Iba & Sawaguchi, 2003; Kahnt et al., 2011; Kim & Shadlen, 1999; Levy & Glimcher, 2012; Rushworth et al., 2012; Wallis & Miller, 2003). In particular, Wallis and Miller reported that the dlPFC activity reflected both the decision variables

and the subject choice, as opposed to the OFC activity which only reflected decision variables (Wallis & Miller, 2003), making dlPFC a candidate region in which decision processes may occur.

According to the Distributed Consensus model, dlPFC is one of the many regions where the competitions occur, and its role may be more strongly implied when the ongoing decision involves abstract thinking. In contrast, according to the Central Executive model, dlPFC is one of the candidates of central executive regions, in which the options are converted into abstract representations and decisions are made. However, it has also been reported that during different decision tasks, different prefrontal regions are activated, suggesting the possibility that the central executive may not be a single entity (Baker et al., 1996; Rushworth et al., 2012).

MACAQUE MONKEYS AS THE MODEL OF THE HUMAN BRAIN

So far, I discussed the two possible theories that can explain how our brain makes decisions, focusing mostly on studies with humans and non-human primates. This is not to dismiss studying other animals, such as rodents, birds, fish and invertebrates. In fact, depending on the research questions, non-primate animal models are more suitable. For example, if the experimental design requires precise manipulation of a specific neuronal population, animal models with established optogenetic techniques, such as rodents and fish, should be chosen (Bliss-Moreau et al., 2022; Boyden et al., 2005; Del Bene & Wyart, 2012). Likewise, if the research question explores certain behavioural traits that are converging across different species, such as vocal learning and tool use, it makes sense to study animals that are evolutionarily further from humans (Falótico, 2022; I. Jacobs & Osvath, 2023; Janik, 2014; Jarvis, 2007; Pal & Sinha, 2022). Depending on the research question, one can also conduct human experiments in a purely non-invasive manner using imaging techniques. However, current technology such as functional magnetic resonance imaging, electroencephalography, positron emission tomography and near-infrared spectroscopy are still

limited in spatial or temporal resolution, resulting in the experimental outcome with compromised precision. Thus, if one seeks to understand how a human brain works, the best way to date is to design a behavioural paradigm that can be performed by both human participants and the animal model, draw behavioural parallels, and measure the neurophysiological correlates in the animal model. My project took this very approach; human participants and two macaque monkeys (*macaca mulatta*) performed the same task, their behavioural data were compared to ensure there were similarities between the species, and the neural correlates in the monkey brains were investigated.

Why monkeys?

The biggest advantage of macaque monkeys as the animal model for human cognition is that they are genetically as well as phenotypically closer to us compared to other laboratory animals. Macaque monkeys and humans diverged about 30 million years ago, and have front-facing eyes and opposable thumbs. In contrast, rodents, which are the most widely used laboratory animals, diverged from us 90 million years ago, whose eyes are laterally placed and lacks opposable thumbs. Certain physiological and behavioural characteristics are preserved at the level of the mammalian class or even at the vertebrate subphylum, whereas other traits are observed in only a subset of species. For example, trichromatic vision is found in humans, great apes, macaque monkeys, cats, and toads (Dacey, 2000; Gesemann & Neuhauss, 2023; Kondrashev, 2023; Tan & Li, 1999), but not in dogs, most rodents, and our ancestry vertebrate relative: lampreys (Abballe & Asari, 2022; Collin et al., 2003; G. H. Jacobs et al., 1993; Neitz et al., 1989; Neitz & Jacobs, 1986). In addition, there are often important differences in the fundamental behavioural traits reflecting the animals' adaptation to their physical and social environment. Mice and monkeys are both capable of reaching and grasping objects, but they differ in the way they use their digits. When holding onto

objects, humans and macaque monkeys grip by placing their opposable thumb facing the remaining digits (Yan et al., 2022). Rats do not possess opposable thumbs, and they do not appear to have a systematic placement of digits when grasping (Blackwell et al., 2018; Gharbawie et al., 2005; Metz & Whishaw, 2000). Such behaviour stems from morphological differences between primate hands and rodent front paws, reflecting the niche these species evolved to fulfill. Therefore, if one wants to understand neural mechanisms of a specific behaviour, it is important to pay attention to what the model species evolved to do.

Comparing Humans and Monkeys

This thesis investigates neural correlates of value-based action decisions using human participants and macaque monkeys. The baseline assumption is that these two primate species share common neural substrates giving rise to similar behavioural responses during action decisions. Below, I briefly summarise the similarities and differences in the behaviour and brain of humans and macaque monkeys.

Reaction Time of Humans and Macaque Monkeys

Humans and macaque monkeys exhibit comparable reaction time distributions in simple tasks such as perceptual detection. On average, humans make saccadic eye movements as a response to a visual stimulus onset 140-250 ms, excluding express saccades (Kingstone & Klein, 1993; Kunita & Fujiwara, 2022; Rayner, 1998; Yep et al., 2022), and macaque monkeys do so at 90-250ms (Chen et al., 2021; Khan et al., 2016). When they are required to respond by a forelimb reaching movement, human average reaction time is 200-300 ms (Contemori et al., 2022) and that of trained macaque monkeys ranges between 170 to 220 ms (Cecala et al., 2023). In more complex tasks, both humans and monkeys increase their reaction times compared to a simple stimulus-response task, suggesting that they are both affected by task demand (Caselli & Chelazzi, 2011).

Brains of Humans and Macaque Monkeys

On average, a human brain weighs 1.3 kg or 2.3 % of the body weight, which is larger than an average rhesus macaque brain which weighs 94g and occupies 1.4 % of the body weight (Marino, 1998). In terms of the number of neurons , an average human brain is estimated to contain approximately 86 billion neurons (Azevedo et al., 2009). An average macaque monkey brain contains approximately 6.4 billion neurons (Herculano-Houzel et al., 2007). When matched for the body size, a human brain is slightly larger, and contains only 7% more neurons than an estimated primate brain (Azevedo et al., 2009). The ratio of the cerebral cortex to the rest of the brain is also comparable: approximately 75 to 82% in an human brain (Rilling, 2006), and 86 to 88% in rhesus macaques (Scott et al., 2016). Looking into more detailed anatomical structures, studies have mapped the homologous brain areas between humans and macaque monkeys. Some features in a human brain are believed to be lacking in that of a macaque brain (e.g., von Economo cells (Allman et al., 2011) but see also (Evrard et al., 2012), right and left hemisphere asymmetry (Croxson et al., 2018)). However, cytoarchitectonic, electrophysiological, and imaging studies showed that many sensory and motor areas, as well as areas that are known to play a role in higher cognitive processes such as frontal areas, are found in anatomically similar locations along with the sulcus patterns (Croxson et al., 2005; Hackett et al., 2001; Orban et al., 2004; Petrides et al., 2012; Petrides & Pandya, 2009; Ramnani et al., 2006; Zilles et al., 1995). This includes the target areas of this thesis: PMd and PRR. The combination of tracing studies and DTI techniques also showed similarities in the connectivity of these regions between humans and monkeys (Barrett et al., 2020; L. Li et al., 2013; Markov et al., 2014; Thiebaut de Schotten et al., 2012).

Implication to decision-making

A number of studies provide support that in simple as well as complex tasks, macaque monkeys and humans respond similarly, and the underlying neural substrates are also similar. While there may be differences in response patterns, certain differences diminish when the key component of the task is carefully matched (Evans & Hawkins, 2019). For the purpose of this thesis, I focused on the choice and reaction time of humans and macaques, as their distributions are comparable between humans and macaque monkeys. Two target areas in the fronto-parietal circuit, namely PMd and PRR, also share cytoarchitectonic, connectivity and functional patterns between species. Thus, it is assumed that when the two species are faced with a situation that are designed to activate these brain areas, and produce similar behavioural responses, the underlying neural processes are also similar. In other words, I expect that if monkeys and humans behave similarly during the value-based action decision task, the activity of PMd and PRR will be similar between the two species, allowing us to generalise conclusions from electrophysiological data from the monkeys to the human brain.

SUMMARY

How do we choose what to do? The Central Executive model suggests that decision making is a serial process. It postulates a sequential activation of different brain regions in accordance with the sense-think-act framework, where all decisions are made in a central executive area at an abstract level. In contrast, the Distributed Consensus model suggests that decision making is a parallel process involving multiple brain areas, including sensorimotor regions. In this view, certain decisions may be made in an executive region at an abstract level, whereas others may be made in sensorimotor regions at a stimulus feature or an action level. To investigate the validity of these models, we need an experimental situation in which the models make distinct neural predictions,

such that the candidate regions' causal role can be examined. This thesis aims to realise this objective by analysing human and monkey behaviour and monkey electrophysiological data collected during a multi-attribute decision task, in which different stimulus attributes favor different choices and thus offer a situation of conflict.

CHAPTER 2 OVERVIEW

OBJECTIVE

The objective of this thesis is to test two candidate models of value-based decisions. A major part of the project aims to investigate whether decision-related neural modulation in the sensorimotor regions has a causal role in the ongoing decision processes. To do so, we attempted to dissociate choice-predictive neural activity that merely correlates with choices from activity with causal effects. We designed a decision task in which two independent visual attributes indicated the reward outcome for a given reaching movement. The attributes were chosen such that they are likely to be processed by distinct neural pathways. We performed electrophysiological recordings from two candidate brain areas in monkeys to compare the characteristics and timing of choice-predictive activity.

SPECIFIC RESEARCH QUESTIONS

Q1. Do humans always fully integrate information from all sources prior to making action decisions?

Q2. Of the brain areas that show choice-predictive activity, which are causally involved in action decisions?

HYPOTHESES

This thesis aims to test two contrasting models of action decisions.

The first hypothesis is that decisions are always made in a Central Executive, where all aspects of available options are converted into an abstract representation, such as utility and economic value. According to this hypothesis, decisions are made at this abstract level, and the resulting commands

are sent to the sensorimotor regions to realise the chosen action. Therefore, decision-related neural modulation in the sensorimotor regions is merely a "spill over" from the executive regions, and does not contribute to the ongoing decision processes.

The alternative hypothesis is that when choosing between actions, multiple brain regions, including sensorimotor regions, compete for different action options based on different aspects of the options (e.g., salience, reward, or action cost). When one or more regions resolve this competition, this resolution propagates to other brain regions, affecting their competition. As a result, the whole brain achieves a Distributed Consensus when a decision is made. This hypothesis suggests that the decision-related neural modulation in the sensorimotor regions may be causally involved in the ongoing decision processes, as much as those in the traditional executive regions, at least during decisions about concrete actions.

SPECIFIC PREDICTIONS

Our premise is as follows: If a given region is causally involved in the decision, the neural latency reflecting the choice will appear earlier than regions that contribute less to the choice. Alternatively, if a given region is merely receiving the decision input, the neural choice latency will always be later than the regions that are causally involved in the decision processes. However, a decision task with a "correct" answer would be inadequate to evaluate these predictions, because the stimulus-driven neural activity may be inherently confounded with the choice-predictive activity. Thus, we designed a reach decision task in which the stimulus-driven and choice-predictive activity can be separated. We used two independent visual attributes to indicate the reward outcome for each reaching choice, which were aimed at activating distinct brain regions at different neural latencies. One attribute was based on salience, aimed at activating the "bottom-up" attention network through a dorsal occipital-to-parietal pathway. The other was based on an arbitrary mapping of

visual cues, aimed at activating the more deliberate, memory-based categorisation in the "top-down" areas through a ventral temporal-to-prefrontal pathway. In some trials, the correct choice is indicated by "bottom-up" information, and in other trials, by the "top-down" cues. In still other trials, these attributes are in conflict but both options are equally valued, so there is no "correct" choice. It is these conflict cases where the two hypotheses make the most contrasting predictions.

One prediction is purely behavioral, and concerns the distributions of reaction times in different kinds of trials. Because "bottom-up" processing is presumably fast, choices based on that information should be quicker than those based on "top-down" cues. However, what happens in conflict trials? The Central Executive suggests that both attributes have to be integrated before any choice can be made, predicting similar reaction times for choices where conflict was resolved in favor of "bottom-up" information and those where it was resolved in favor of "top-down" information. In contrast, a Distributed Consensus suggests that sometimes decisions can be made before both kinds of information have been processed, predicting the mean reaction time to be shorter when the conflict is resolved in favor of "bottom-up" information as compared to when it is resolved in favor of "top-down" cues. These predictions were tested in a study with human subjects (Chapter 3).

To truly distinguish the hypotheses at the level of brain circuits, we need to turn to neural recordings. Here (Chapter 4), we focused on recordings in the arm region of dorsal premotor cortex (PMd) and the parietal reach region (PRR), and examined the latency with which these regions predicted the monkey's choice in the same task studied in humans.

In particular, if decisions are always made in a Central Executive region upon a full integration of all information, then the transmission delay between the Central Executive region and non-deciding regions will be constant, regardless of the attribute used to pick the final choice.

Consequently, choice-predictive activity in the sensorimotor areas should always appear at the same relative latency. For example, if both PMd and PRR lie outside of the Central Executive, then choice-predictive activity may arrive in PRR after X ms, and in PMd after Y ms, but the *difference* between X and Y should always be constant, even when comparing across different situations in which decisions take more or less time (Figure 5). Note that activity reflecting purely sensory information (e.g., stimulus onset) will likely appear in sensorimotor areas, which we attempt to dissociate from the choice-predictive activity using the conflict trials.

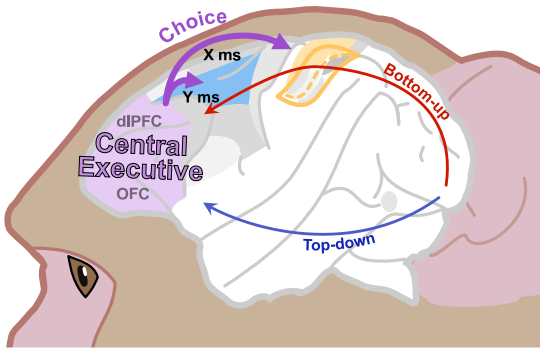

Figure 5. Predictions of the Central Executive model

Bottom-up and top-down information (thin arrows) go to the Central Executive, where a choice is made, and broadcast to the rest of the brain (thick purple arrows).

In contrast, if decision processes consist of multiple competitions involving multiple brain regions, and the final choice is a result of the whole brain achieving a Distributed Consensus, the latency of choice-predictive activity is expected to reveal the causality of a given region. For example, suppose that both PMd and PRR take part in the Distributed Consensus, and PRR is the first to receive "bottom-up" information while PMd is the first to receive "top-down" information. If so, then when conflict is resolved in favor of the "bottom-up" information, PRR should exhibit faster choice-predictive activity than PMd, but the

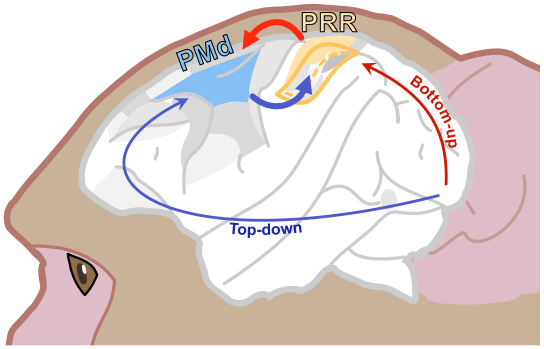

Figure 6. Predictions of the Distributed Consensus model

Bottom-up information goes to PRR and top-down information goes to PMd, and the choice is made when an inter-areal consensus is achieved.

opposite should be true when the conflict is resolved in favor of the "top-down" information (Figure 6).

It should be admitted that these predictions are based on rather extreme renderings of the two models – a *single* Central Executive versus a *whole brain* Distributed Consensus. In reality, different types of decision-making processes may fall on a gradient between these extremes. For example, it is possible that decisions are made by a Central Executive that does not always integrate all sources of information before making a choice. It is also possible that decisions involve a Distributed Consensus that does not include activity in PMd or PRR, or both. The present work is intended to help narrow down among these options as a step toward understanding decision-making in the brain.

CHAPTER 3 HUMAN BEHAVIOUR

SCOPE

As a first step to examine the two decision theories, we collected behavioural data from human participants performing the same multi-attribute decision task performed by the monkeys. This human project had two main objectives. First, we wanted to know how our monkey behavioural data compare against that of humans. This is discussed in Monkey Behaviour and Electrophysiology. In short, their behavioural patterns were comparable, at least prior to the inevitable overtraining that comes with electrophysiological experiments. Second, we wanted to investigate whether human participants always decide after integrating information from all attributes, or if decisions can be made based only on a subset of attributes, and sometimes subsequently corrected, resulting in a change of mind. An additional analysis was performed to examine whether the Weber-Fechner law, which postulates that perceptual decision difficulty is a function of stimulus strength, holds when the stimulus strength is coupled with reward magnitude (Fechner, 1948). The following manuscript was published in the Journal of Neurophysiology (Nakahashi & Cisek, 2023).

Parallel processing of value-related information during multi-attribute decisions

GRAPHICAL ABSTRACT

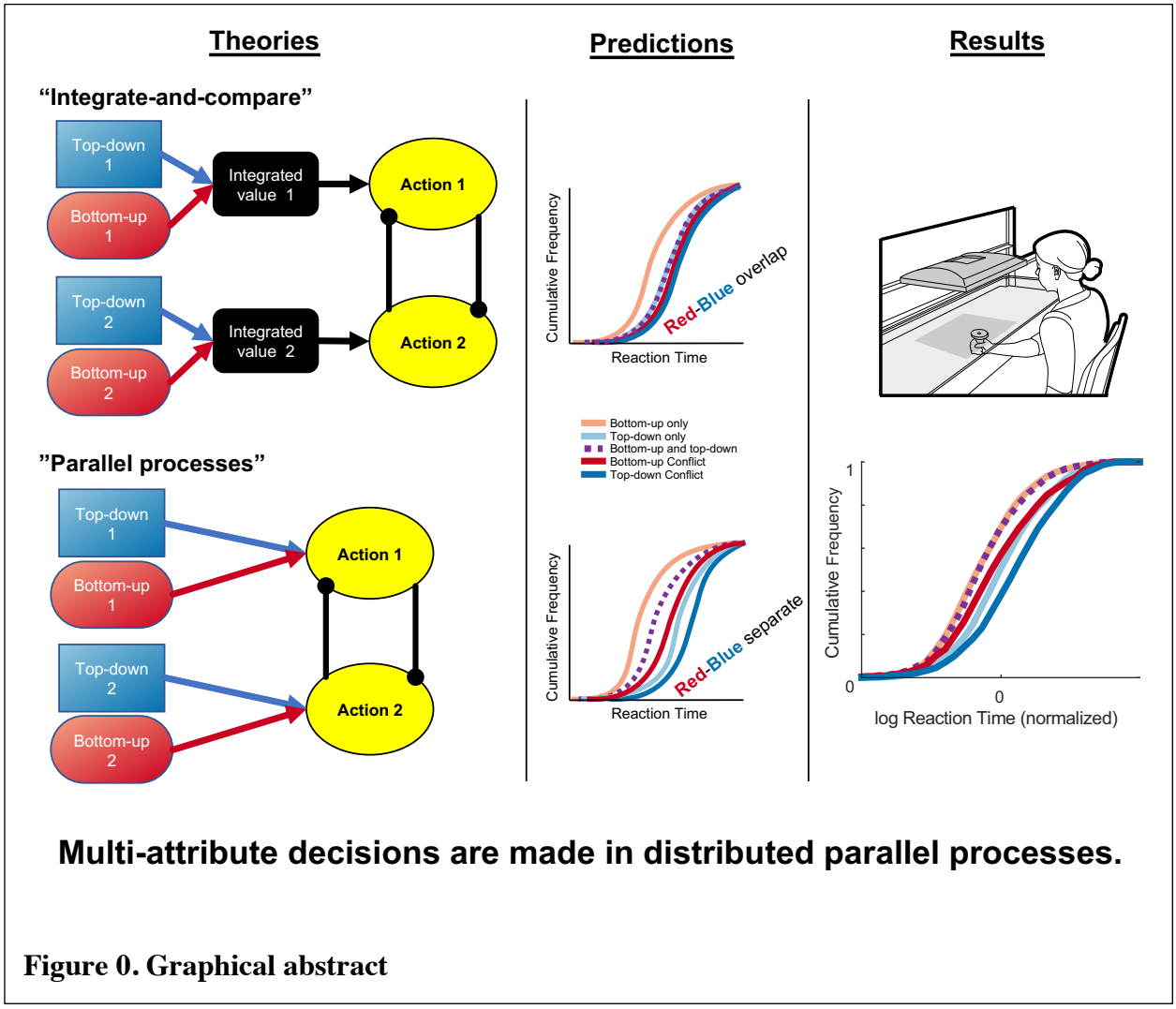

Figure 0. Graphical abstract

ABSTRACT

When choosing between options with multiple attributes, do we integrate all attributes into a unified measure for comparison, or does the comparison also occur at the level of each attribute, involving parallel processes that can dynamically influence each other? What happens when independent sensory features all carry information about the same decision factor, such as reward value? To investigate these questions, we asked human participants to perform a two-alternative forced choice reaching task in which the reward value of a target was indicated by two visual attributes – its brightness ("bottom-up" feature) and its orientation ("top-down" feature). If decisions always occur after integration of both features, there should be no difference in the reaction time (RT) regardless of the attribute combinations that drove the choice. Counter to that prediction, RT distributions depended on the attribute combinations of given targets and the choices made by participants. RTs were shortest when both attributes were congruent or when the choice was based on the bottom-up feature, and longer when the attributes were in conflict (favoring opposite options). In conflict trials, nearly two-thirds of participants made faster decisions when choosing the option favored by the bottom-up feature than when choosing the top-down-favored option. We also observed mid-reach changes-of-mind in a subset of conflict trials, mostly changing from the bottom-up to the top-down-favored target. These data suggest that multi-attribute value-based decisions are better explained by a distributed process including competition among different features than by a competition based on a single, integrated estimate of value.

KEYWORDS

Decision-making, multi-attribute, response conflict, change of mind, human

NEW & NOTEWORTHY

We show that during value-based decisions, humans do not always use all reward-related information to make their choice, but instead can "jump the gun" using partial information. In particular, when different sources of information were in conflict, early decisions were mostly based on fast bottom-up information, and sometimes followed by corrective changes-of-mind based on slower top-down information. This supports parallel decision processes among different information sources, as opposed to a single integrated "common currency".

INTRODUCTION

Many of our decisions are based on multiple sources of information about a wide variety of factors. For example, when choosing a house to buy, we consider its cost and size, the property and environment, as well as its location relative to workplaces, good schools, public transportation, etc. Such multi-attribute decisions also occur in the wild, when for instance, animals need to weigh the value of seeking food against the effort required to obtain it and the potential exposure to danger. One plausible model suggests that the multiple factors pertinent to each option are integrated together into a central representation of subjective value that reflects them all, and each factor is weighted by the degree to which it matters for the deciding agent (Cai & Padoa-Schioppa, 2019; Kable & Glimcher, 2009; Levy & Glimcher, 2012; Padoa-Schioppa, 2011; Shizgal, 1997). This permits comparison between options that may differ in every way, such as when choosing between a small apartment that is close to work versus a large house that will require a longer daily commute, and permits a rational decision process that optimizes some general measure of global utility. At a mechanistic level, such "integrated competition" models predict that only a single comparison is made in the brain – a comparison between the integrated values of the options under consideration.

Alternatively, "distributed competition" models of multi-attribute decision-making suggest that the individual factors can themselves compete against each other prior to integration, and even that the weights of the factors can vary over time due to fluctuations in covert or overt attention (Busemeyer & Townsend, 1993; Diederich, 2003; Hunt et al., 2014; Krajbich & Rangel, 2011; Roe et al., 2001; Trueblood et al., 2014; X. Yang & Krajbich, 2022). For example, Hunt and colleagues suggested that during multi-attribute decision-making tasks, human behavior is best explained by a hierarchical scheme in which the higher-level competition between choices is biased by information from multiple lower-level competitions that each compare the options in terms of a given attribute, and that the weighting of each attribute is itself subject to a competition based on its relevance and discriminatory efficacy (Hunt et al., 2014). Such models predict that even when the total value should favor choice A over B, subjects may sometimes choose B if one of its attributes is particularly outstanding. Another prediction of such models is that when decisions are made quickly, commitment can be reached even before all of the factors have been considered (Diederich, 2003), explaining preference reversals as a function of deliberation time.

Here, we ask whether the competition can be distributed even among different sources of sensory information about a single factor, such as reward value. In particular, we ask how different visual features, both of which carry information about value, are integrated into the decision process. Importantly, certain kinds of "bottom-up" visual signals are processed very quickly, including information about spatial location of stimuli and simple features like brightness. This is believed to implicate the dorsal visual stream from occipital cortex to the posterior parietal lobe (Galletti & Fattori, 2018; Goodale & Milner, 1992; Mishkin & Ungerleider, 1982; Treisman & Gelade, 1980), throughout which sensory responses have been reported in as little as 50ms (Ledberg et al., 2007; Schmolesky et al., 1998). Other kinds of visual information require more sophisticated and slower

"top-down" processing, including categorization of arbitrary shapes according to task-dependent rules, which involves the ventral visual stream and prefrontal cortical regions (DiCarlo et al., 2012; Freedman et al., 2002; Goodale & Milner, 1992; Kravitz et al., 2013).

In this study, we presented human participants with a two-alternative forced choice task in which the reward value associated with each choice was determined by two different visual features – a bottom-up brightness cue and a top-down orientation rule – and asked whether the timing of their responses revealed how these features interact. Of particular interest were situations in which the two features were in conflict, such that the total reward value of each choice was identical, so it did not matter which was chosen but a choice still had to be made. In those trials, was the choice random or did it depend on the relative timing with which each feature was processed with respect to the time of commitment? Importantly, these trials were interleaved among a variety of other trials in which one choice was clearly better than the other. Consequently, because value could only be evaluated after both features were processed, participants were motivated to take the time to integrate both kinds of information prior to committing to either choice, especially since there was no time pressure to respond quickly. Therefore, "integrated competition" models would predict that participants should always take the time to evaluate the options fully, so decision timing should be similar across all choices, whether or not they are easy (both features favor the same target) or ambiguous (different features favor different targets). By contrast, "distributed competition" models would predict preference changes as a function of time, with initial choices more biased by bottom-up stimulus features and later ones increasingly based on top-down information.

The design of our task also allowed us to examine whether the effect of reward size on reaction times and choice accuracy follow predictions from the Weber-Fechner law, which states that the

"just noticeable difference" (JND) between stimuli increases with stimulus amplitude (Fechner, 1948) [see also the more general Stevens' law (Stevens, 1957)]. The prediction is that participants will take longer to make decisions and will commit more errors when the JND is small as compared to when it is large. Indeed, discrimination of physical properties such as size, length, weight, as well as more subjective properties such as value, are reported to become slower and more inconsistent when the scale of the discriminated property is increased but the difference is held constant (Busemeyer et al., 2019; Killeen et al., 1993; Marks & Algom, 1998). At the neural level, divisive normalization between neurons has been proposed as a plausible mechanism that can explain such behavioral and neuronal responses to different stimulus strengths (Carandini & Heeger, 2012). However, it has also been shown that certain stimulus properties do not follow the Weber-Fechner law. For example, properties that lack an absolute zero, such as estimates of positions in space, have been reported to show a lack of increase in the deviation as the size of the target object increases (Ganel et al., 2008; Smeets & Brenner, 2008) but see also (Utz et al., 2015). Other studies showed that human reaction time decreased as the overall value of choice options increased (Shevlin et al., 2022). This is the opposite of what one would predict if increasing values made their differences less salient, and thus harder to distinguish. In our task, participants made binary choices based on two independent visual attributes, allowing us to investigate whether the response varied as a function of the range of the offered value and attribute types.

MATERIALS & METHODS

Participants

Fourteen participants (13 right-handed, 6 females, mean age: 27; range 20-35) participated in the study. Participants 1-3 were colleagues of the authors who volunteered during the pilot study and were not offered monetary compensation. They were aware of the project design but uninformed

of the specific predictions. Participants 4-14 signed a consent form prior to the study, and were offered monetary compensation of $20 plus an additional $5-9 based on their final score. All participants had no known neurological conditions and had normal or corrected to normal vision. At the beginning of the session, participants were given verbal instructions describing the task and performed a practice session to familiarize themselves with the task. The practice session lasted until they made 10 consecutive correct choices (i.e., choosing the target with a higher score), and verbally reported that they felt ready. The experimental paradigm was approved by the Comité d'éthique de la recherche en santé of the Université de Montréal.

Experimental setup

Participants 1-2 performed the task using a standard computer mouse to control a cursor on a screen. The remaining participants performed the task as follows: They were comfortably seated at a planar digitizing tablet (CalComp Drawing Board IV) on which they performed horizontal arm movements by moving a vertically oriented cylindrical handle with their right hand (Figure 1A). The handle contained a wireless digitizing stylus which sent its location to the tablet at 125 Hz. An LCD computer monitor was suspended above the tablet and half-way between them, a semi-silvered mirror that reflected the stimuli displayed on the monitor. The handle with the stylus was placed between the mirror and a digitizing tablet. The monitor, the mirror and the digitizing tablet were equally spaced, creating an illusion that the visual stimuli on the monitor floated at the height of the tablet. During the task, a cross cursor was displayed over the handle to provide continuous feedback about its location.

At the beginning of each trial, a circular target (3 cm diameter) appeared in the center of the workspace (Figure 1B). Participants initiated a trial by moving the cursor into this center circle. After a variable delay (600±200 ms, uniform distribution), two circular targets appeared at 0- and

240-degree positions with respect to the center circle, 7.5 cm away, center to center. This choice of targets was used in order to reduce the difference in the biomechanical costs of the associated reaching movements (Cos et al., 2011; Hogan, 1985). Participants then moved the cursor into their target of choice, earning the value of that target toward their total score for the session. The value of each target was indicated by two visual features (Figure 1C). The bottom-up (BU) feature consisted of three possible levels of brightness, such that the brightest target was worth 5 points, a dim target was worth 3 points, and the darkest target was worth 1 point. The top-down (TD) feature consisted of three possible orientations of an overlaid line, such that a line pointing at eight o'clock was worth 5 points, twelve o'clock was worth 3 points, and four o'clock was worth 1 point. The sum of the BU and TD points was earned upon a successful reach to a given target, which was converted into a monetary amount at the end of the session. Once the cursor hit one of the targets, the non-reached target disappeared as feedback confirming the choice. At the end of each trial, the points obtained from the chosen target were added to the total points accumulated, and displayed for 700 ms. The maximum reaction time allowed was 2000 ms, and the maximum movement time was 1000 ms. The inter-trial interval was 800 ms. On average, participants completed 913 trials over the course of 60.4 minutes (range: 684-1085 trials, 41.8-85.5 minutes).

At the end of the session, participants 4-14 received $20 for their participation, plus an additional $5-9 based on the points earned (mean $27.27). The additional amount was determined based on the deviation from the estimated average score, such that the first tercile above the estimated average score would yield an additional $7.00, and the second tercile $8, etc.

Trial Conditions

Each trial was classified as one of 9 conditions based on the features of each target and the participant's choice (Figure 1D). When the targets varied in brightness (i.e., BU feature) but not

in their line orientation, the trial was labelled **Easy-BU**, because the choice was easy (one target is better than the other) and the better target was indicated by the BU feature. When the targets varied in line orientation (i.e., TD feature) but not in their brightness, the trial was labelled **Easy-TD**, as the better target was indicated by the TD feature. When the targets varied in both BU and TD features and both favored the same target, the trial was labelled **Easy-Both**. When the targets were identical, the trial was labelled **Twin**. When the targets varied in both features, but the features favored opposite targets (i.e., one target had better BU feature while the other target had better TD feature), the trial was considered a Conflict trial. These were further categorized as follows: In Conflict-Mirror (**ConM**) trials, the targets' total scores were equal and the distribution of the feature scores were inverted (e.g., one target had 3 BU points and 1 TD point, while the other had 1 BU point and 3 TD points). In Conflict-Same (**ConS**) trials, the targets' scores were equal and the distribution of the feature scores were not inverted (e.g., one target had 5 BU points and 1 TD point, while the other had 3 BU points and 3 TD points). In Conflict-Different (**ConD**) trials, the features were in conflict but the target scores were *not* equal. Furthermore, we subcategorized the Conflict trials based on the choice made: if the participant chose the target with the better BU feature, the trial was marked with the suffix BU (i.e., **ConM-BU, ConS-BU, ConD-BU)**, and if the target with the better TD feature was chosen, it was marked with the suffix TD (i.e., **ConM-TD, ConS-TD, ConD-TD)**. As explained below, this was motivated by interest in comparing the timing of choices driven by BU versus TD features.

An average session consisted of 15.7% EasyBU, 15.8% EasyTD, 15.6% EasyBoth, 8% Twin, 14.9% ConM, 10.1% ConS, and 20% ConD trials, all randomly interleaved.

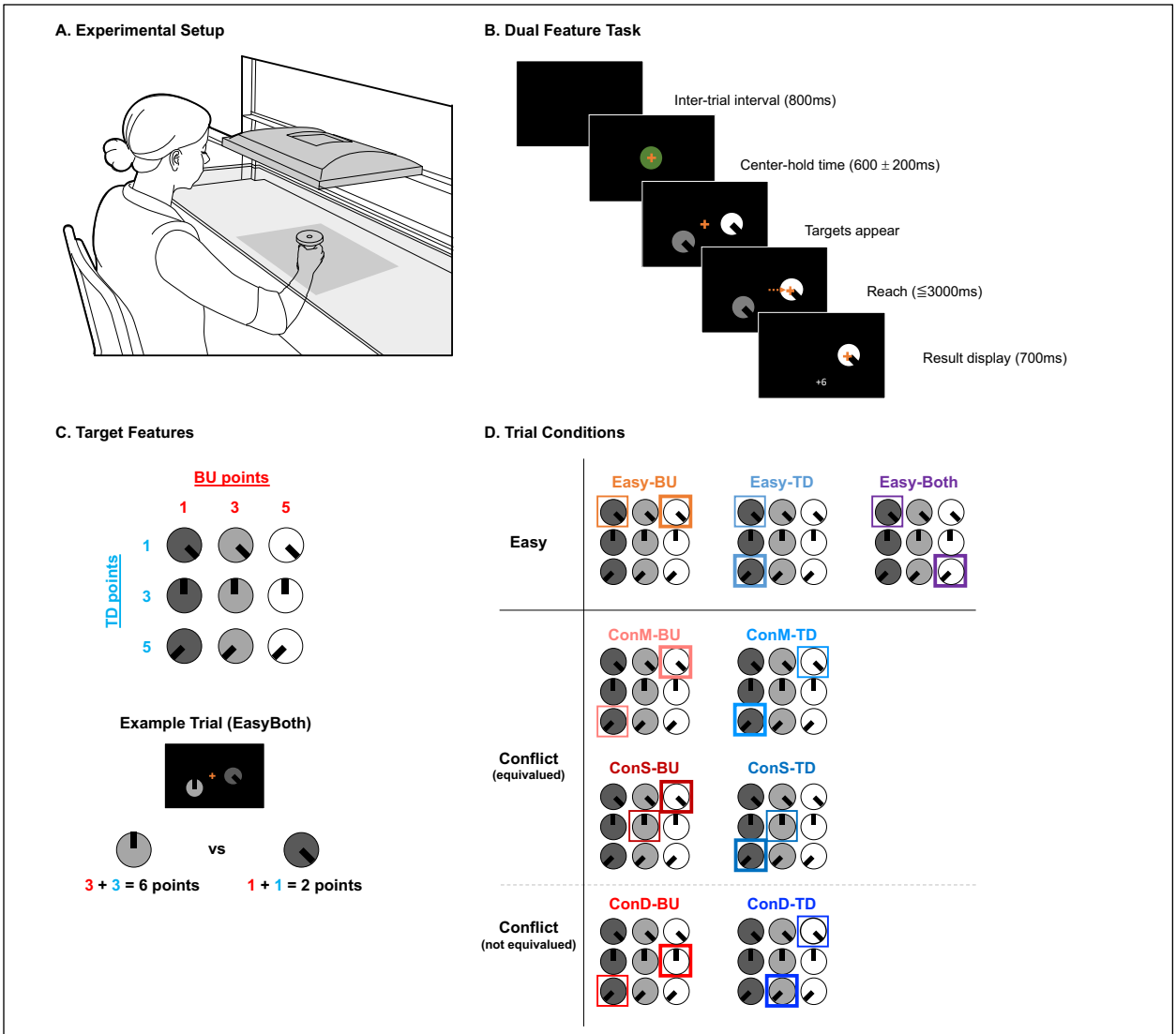

Figure 1. Dual Feature Task

(A) Experimental setup, with the participant sitting at the tablet and holding the cursor. **(B)** Progression of the task. After an inter-trial interval, a trial was initiated by moving the cursor (orange cross) into the center target in the middle of the screen. After a variable delay, one or two targets appeared on the right and left bottom of the screen and the center target disappeared. Once the participant chose a target by moving the cursor into it, the unchosen target disappeared and the obtained points were displayed. **(C)** Target Features. The bottom-up (BU) feature was based on three levels of brightness of the target. Targets were given 1, 3 or 5 points if they were dim, medium-bright and bright, respectively. The top-down (TD) feature was based on the orientation of an overlaid line. Targets were given 1, 3 or 5 points if the line was at 4:00, 12:00 and 8:00, respectively. **(D)** Trial conditions and example target combinations. Boxes with a thicker line indicate the chosen target. Top, from left to right. Easy-BU (example in orange): targets vary only in BU features. Easy-TD (example in cyan): targets vary only in TD features. Easy-Both (example in violet): targets vary in both features, and both features favor the same target. Bottom, from left to right. Conflict: targets vary in both features, but the BU and TD features favor opposite targets. Two of the conflict conditions, ConM and ConS, consisted of equivalued targets, while ConD consisted of targets with different values. In all conflict conditions, trials were subdivided with a suffix of -BU and -TD based on which feature of the target chosen by the participant had the higher score (these are indicated by a colored frame). ConM (Conflict-Mirror, examples in salmon and pale blue): Conflict trials in which one target's BU point is the same as the other target's TD point and vice versa. ConS (Conflict-Same, examples in dark red and dark blue): Conflict trials in which the targets are equivalued, but the BU and TD points did not mirror each other. ConD (Conflict-Different, examples in vivid red and vivid blue): Conflict trials in which the targets had different values. Twin: two identical targets (not shown).

Behavioural Analysis

Reaction time (RT) was defined as the duration between the stimulus onset and the movement onset. Raw movement velocity was filtered using a 6th order Butterworth low-pass filter with a cut-off frequency at 10 Hz. Movement onset was detected when the filtered velocity exceeded 1.5 cm/second and reached the velocity peak of the trial. Based on the reaching trajectory, each trial was assigned an "Initial Choice" and a "Final Choice". The Initial Choice was assigned to a target when the cursor moved toward it during the first 100 ms after leaving the center and the linear trajectory estimate fell within 0.6 cm from that target. When a trial did not meet these criteria, the experimenter assigned the Initial Choice via visual inspection. The Final Choice was assigned based on the target which the cursor eventually reached. In a subset of trials, there was a clear change in the reaching trajectory, indicating that the participants changed their mind mid-reach. Such "Change-of-Mind" (**CoM**) trials were assigned a secondary RT (CoM RT), either at the time when the filtered velocity fell below half of the peak velocity of the initial movement, or when the velocity was at its lowest value before it started to increase again as the participant started reaching toward the final target.

Trials were considered outliers when the RT was more than 3 standard deviations away from the median and were excluded from further analysis. For most analyses, only trials in which participants chose the target with a higher score were included, resulting in an exclusion of 1449 or 11.5% of trials (mean per participant: 11.9%, range: 5.2-25%). The excluded trials mainly consisted of ConD trials (61%), followed by Easy-TD trials (21.9%), Easy-BU trials (9.2%) and Easy-Both trials (6.4%). Error trials were analysed separately, and focused primarily on the ConD trials.

Statistical Tests

To analyze the difference in the reaction time (RT) distributions across conditions at the individual level, we performed one-way ANOVAs with condition and target positions as factors. Because our task contained free-choice trials (e.g., Twin and Conflict), the number of trials per condition varied across participants. To account for this, we fitted a linear mixed-effects model prior to ANOVA. Target position was included to verify if participants had any directional bias. To analyze the effects of condition at the population level, we took the logarithm of each RT (since RTs tend to follow a lognormal distribution) and converted it into a z-score by subtracting each participant's mean log RT across all conditions and dividing by the standard deviation across all conditions. This allowed us to combine data from participants with different mean RTs to analyse the order in which different conditions were completed, as we were interested in the relative rather than the absolute values of the RTs across conditions. We then averaged the z-scored log RTs across participants to obtain a single mean log RT per condition and performed univariate repeated measures ANOVA using a custom MATLAB function (Caplette, 2023). The *p*-values were adjusted with Greenhouse-Geisser to account for the distortion due to the violation of sphericity (Mauchly's test $\chi^2(9) = 40.05$, $p < .001$). For planned comparisons between specific conditions (e.g. Easy-BU vs. Easy-TD), we ran post hoc pairwise t-tests. Results were considered significant at $p < 0.05$. All data were processed in MATLAB R2014b.

RESULTS

Accuracy and reaction times varied across conditions.

First, we examined how accuracy and reaction time varied as a function of the difference in the evidence favoring each target, as in previous work on perceptual (Gold & Shadlen, 2007) and value-based decisions (Krajbich & Rangel, 2011; Milosavljevic et al., 2010). Figure 2A shows that

participants almost never chose the lower-valued target when the difference was large, but they made more errors as the value difference decreased, especially when the features were in conflict (ConD trials). Figure 2B shows that reaction times were shorter when the value difference was large and increased when it was small (e.g. zero in Twin, ConM and ConS trials). These results are congruent with previous studies, but also show that beyond the effects of the difference of total evidence, there are large effects of trial types: RTs were in general shorter in Easy than Conflict trials, and in trials in which the choice was driven by the BU as opposed to the TD feature. Below, we examine these effects in detail at both the level of individual participants as well as at the level of group data.

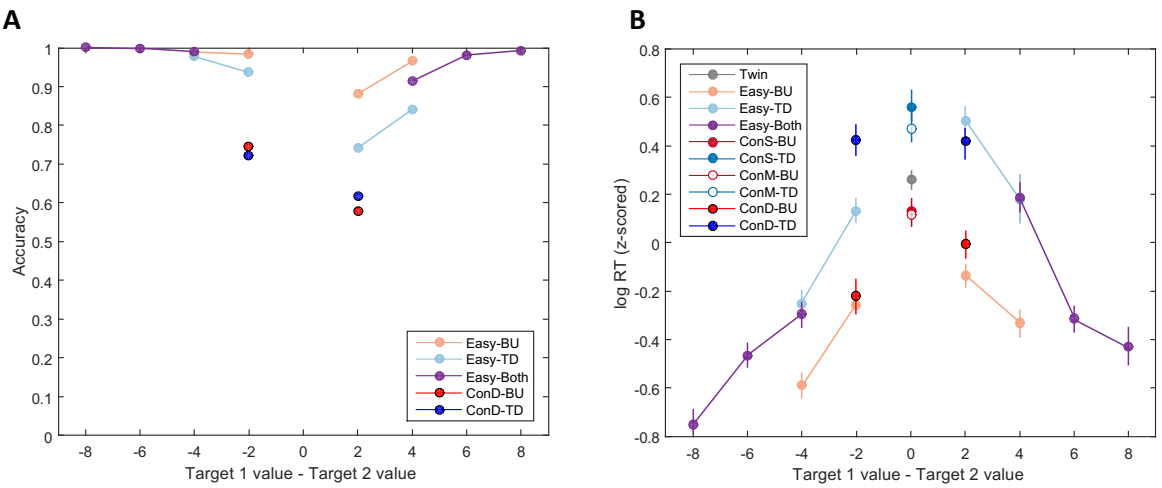

Figure 2. Effect of target value difference on the (A) accuracy and (B) z-scored log RT

Different colors indicate different trial conditions. Vertical lines indicate standard error of the mean. Twin, ConS and ConM trials do not appear in the accuracy plot because in those trials there is no error choice. Target 1 appeared at 0° and target 2 appeared at 240°.

First, we show the within-participant effects by focusing on three example participants whose RTs were short (median RT<500 ms), medium (median RT between 500 and 1000 ms), and long (median RT>1000 ms). To analyze the effects of conditions and target positions on the individual

participants' RT distributions, we fitted a linear mixed-effect model and performed a one-way ANOVA with condition and target position as factors. The example participant with short RTs (participant 1, median RT: 316 ms, (Figure 3A) had different RTs for different trial conditions ($F(9, 560) = 3.27$, $p < .001$). There was also an effect of target position ($F(1, 560) = 8.32$, $p = .004$). There was no interaction between the condition and position ($F(9, 560) = 0.72$, $p = .69$). The example participant with medium RTs (participant 14, median RT: 663 ms, Figure 3B) had different RTs for different trial conditions ($F(9, 913) = 10.51$, $p < .001$). There was no effect of position ($F(1, 913) = 0.04$, $p = .85$) nor interaction between condition and position ($F(9, 913) = 1.59$, $p = .11$). The effect of condition was observed in all other participants with medium RTs. The example participant with long RTs (participant 5, median RT: 1257 ms, Figure 3C) had different RTs for different conditions ($F(9, 889) = 20.80$, $p < .001$). There was no effect of position ($F(1, 889) = 2.84$, $p = .09$), but there was an interaction between condition and position ($F(9, 889) = 5.16$, $p < .001$). This participant was the only one whose RTs were longer than 1000 ms. Three participants were excluded from within-subject analysis due to the lack of trials in certain conditions (participant 8 made no rightward choices in ConS-TD, participant 9 made no leftward ConS-TD choices, and participant 12 made no ConS-BU choices). In summary, 10 out of 11 participants showed an effect of condition and 3 out of 11 participants showed an effect of position (data not shown).

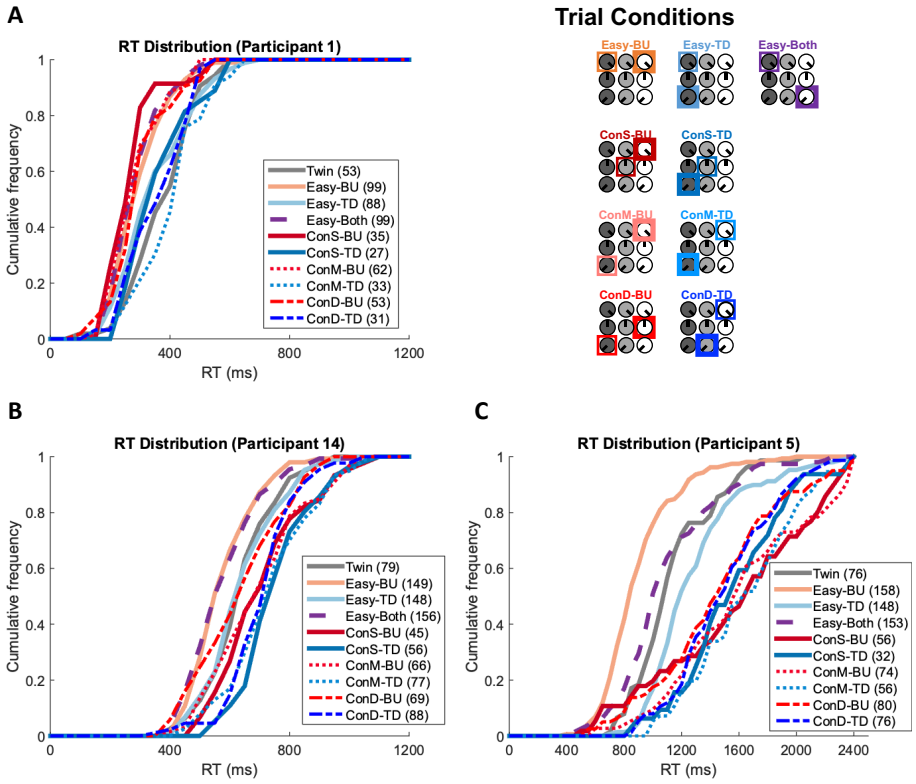

Figure 3. Cumulative distributions of RTs

(A) Example participant whose median RTs were short (<500 ms). **(B)** Example participant whose median RTs were medium (between 500 and 1000 ms). **(C)** Example participant whose median RTs were long (>1000 ms). Line colors indicate different conditions. The number of trials of each condition is indicated in parentheses. Each time bin is 50 ms.

To analyze the effects at the population level, we z-scored individual participant's RTs after taking the logarithm and calculated one mean log RT per condition per participant (see cumulative distributions in Figure 4A). To simplify the comparisons, we collapsed equivalued Conflict trials based on the chosen attributes. As a result, Conflict-BU condition consisted of ConS-BU and ConM-BU conditions, and Conflict-TD condition consisted of ConS-TD and ConM-TD conditions. Our planned comparisons focused on the attribute-based combinations (i.e., Easy-BU vs Easy-TD, Conflict-BU vs Conflict-TD) and the presence of a conflict (i.e., Easy-BU vs Conflict-BU, Easy-TD vs Conflict-TD), and comparisons against Easy-Both condition (e.g., Easy-

Both vs Easy-BU, Easy-Both vs Easy-TD and so on). A univariate repeated measures ANOVA showed an effect of condition ($F(4, 52) = 15.30$, $p < .001$). Post hoc pairwise t-tests on planned comparisons (see Statistical Tests for details) revealed a significant difference between Easy-BU (z-scored mean $M = -0.296$, $SD = 0.281$) and Easy-TD ($M = 0.144$, $SD = 0.214$) conditions ($p < .001$), and Conflict-BU ($M = 0.118$, $SD = 0.396$) and Conflict-TD ($M = 0.5$, $SD = 0.331$) conditions ($p = .036$); Easy-BU and Conflict-BU conditions ($p = .022$); Easy-TD and Conflict-TD conditions ($p < .001$); Easy-Both ($M = -0.29$, $SD = 0.164$) and Easy-TD conditions ($p < .001$); Easy-Both and Conflict-BU conditions ($p < .001$); and Easy-Both and Conflict-TD conditions ($p < .001$). There was no difference between Easy-Both and Easy-BU conditions ($p = .907$) In summary, at the population level there were significant RT differences between BU- and TD-based decisions within Easy trials and within Conflict trials, as well as between Easy and Conflict conditions that were based on the same attributes.

Not all participants exhibited the same trends as the average shown in Figure 4A. In particular, eight participants' RTs were significantly shorter for ConS-BU compared to ConS-TD trials (Wilcoxon rank sum test, $p < 0.05$), but this difference was not significant for five others. We thus subdivided the participants into two groups. For the first group (Figure 4B), a univariate repeated measures ANOVA showed an effect of condition ($F(4, 28) = 21.2$, $p < .001$). Post hoc pairwise t-tests on planned comparisons revealed a significant difference between Easy-BU ($M = -0.309$, $SD = 0.22$) and Easy-TD ($M = 0.226$, $SD = 0.251$) conditions ($p = .002$); Conflict-BU ($M = -0.107$, $SD = 0.229$) and Conflict-TD ($M = 0.673$, $SD = 0.289$) conditions ($p < .001$); Easy-TD and Conflict-TD conditions ($p = .002$); Easy-Both ($M = -0.29$, $SD = 0.179$) and Easy-TD conditions ($p < .001$); and Easy-Both and Conflict-TD conditions ($p < .001$). There was no difference between Easy-BU and Conflict-BU conditions ($p = .227$); Easy-Both and Easy-BU conditions ($p = .833$);

and Easy-Both and Conflict-BU conditions (p = .233). In summary, this subgroup exhibited significant differences similar to the trends observed in the overall population. For the group that did not show RT differences between ConS-BU and ConS-TD trials (Figure 4C), a univariate repeated measures ANOVA also showed an effect of condition (F(4, 16) = 5.75, p = .005). Post hoc pairwise t-tests on planned comparisons revealed significant difference between Easy-TD (M = 0.037, SD = 0.061) and Conflict-TD (M = 0.321, SD = 0.211) conditions (p = .04); Easy-Both (M = -0.301, SD = 0.144) and Conflict-BU (M = 0.425, SD = 0.407) conditions (p = .019); and Easy-Both and Conflict-TD conditions (p = .016). There was no difference between Easy-BU (M = -0.336, SD = 0.352) and Easy-TD conditions (p = .1); Conflict-BU and Conflict-TD conditions (p = .66); Easy-BU and Conflict-BU conditions (p = .091); and Easy-Both and Easy-BU conditions (p = .846). This subgroup did not exhibit the same trend as the overall population.

In conclusion, when participants had shorter RTs for ConS-BU than ConS-TD, their RT distributions varied across different conditions, suggesting that they were processing BU and TD features with different latencies. In contrast, participants with similar RTs for ConS-BU and ConS-TD conditions completed most of the conflict conditions with a similar latency, which was nevertheless significantly longer than during the Easy-Both trials. Figure 4D-F show the normalized RT distributions of BU- and TD-favored choices during equivalued Conflict trials as a function of z-scored log RTs. The histograms show how on average, the early (i.e., left tail) choices were dominated by BU-favored choices (red), while later choices become more balanced. This effect was not seen for the second group of participants (Figure 4F)

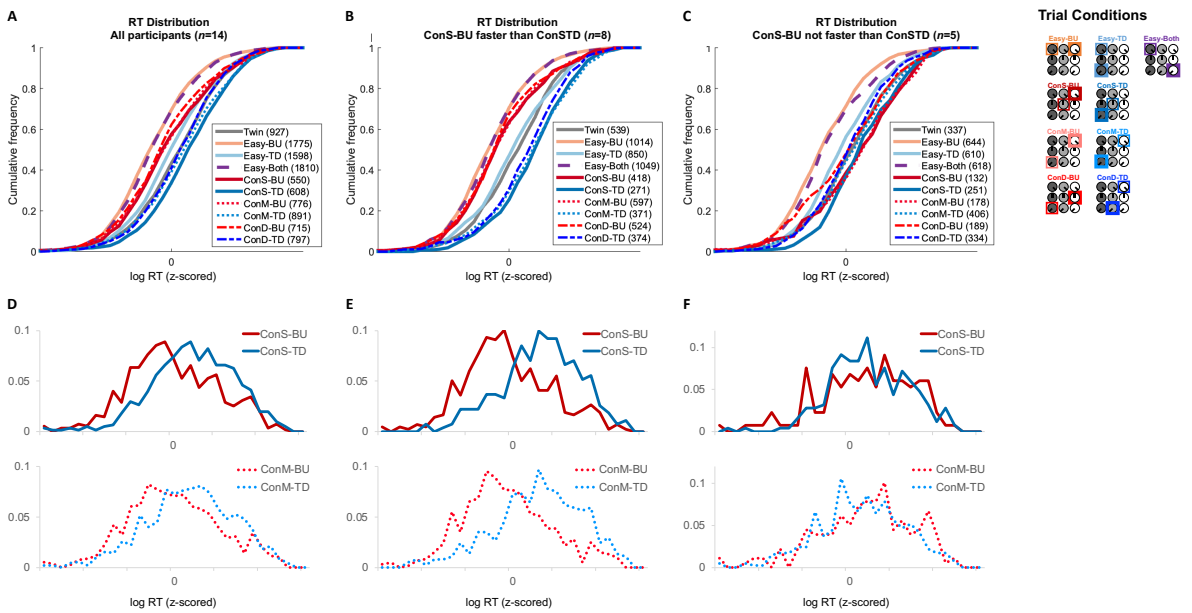

Figure 4. Cumulative distributions of z-scored log RTs of all participants.

(A) Z-scored average log RTs of all participants. **(B)** Z-scored average log RTs of participants whose RT for ConS-BU was shorter than that of ConS-TD (N=8). **(C)** Z-scored log RTs of participants whose RT for ConS-BU was equal or longer than that of ConS-TD (N=5). In all groups, Easy-BU (orange) and Easy-Both (dashed purple) had the shortest RT. **(D-F)** Normalized frequency of BU and TD choices during ConS (top) and ConM (bottom) trials, plotted as a function of z-scored log RT. Participant subgroups are the same as in plots A-C.

To compare the effect of the attributes and the total integrated value on the overall RT, we ran a three-way ANOVA with the BU and TD attributes and the target value as independent variables. There was a statistically significant effect of the BU attribute ($F(1, 9489) = 83.87$, $p < .001$), the TD attribute ($F(1, 9489) = 11.73$, $p < .001$), and the target value ($F(4, 9489) = 43.8$, $p < .001$). There was also a significant interaction of TD attribute and value ($F(2, 9484) = 3.29$, $p = .037$).

Finally, to visualize the global trend, we generated a scatterplot of each participant's mean RT in different trial conditions (Figure 5). Within Easy trials, 10/14 participants were faster in Easy-BU than Easy-TD (two sample t-test at $p < .05$, Figure 5A). During ConS trials, 6/13 participants were significantly faster when choosing BU-favored targets while 1/13 was faster when choosing TD-

favored targets (Figure 5B). This comparison could not be performed for participant #12 because that person never chose the BU target in ConS trials. During ConM trials, 5/14 participants were faster when choosing BU-favored targets while 1/14 was faster when choosing TD-favored targets (Figure 5C). During ConD trials, 8/14 were faster when choosing BU-favored targets, while 1/14 was faster when choosing TD-favored targets (Figure 5D). When all Easy trials and all equivalued Conflict trials are collapsed together, 8/14 participants were faster in Easy trials (Figure 5E). Similarly, 12/14 participants were faster in Easy trials than Twin trials (Figure 5I). Between Twin and all equivalued Conflict trials, 3/14 participants were faster in Twin whereas 6/14 were faster in Conflict trials (Figure 5J). There was no systematic clustering observed in the RT distributions.

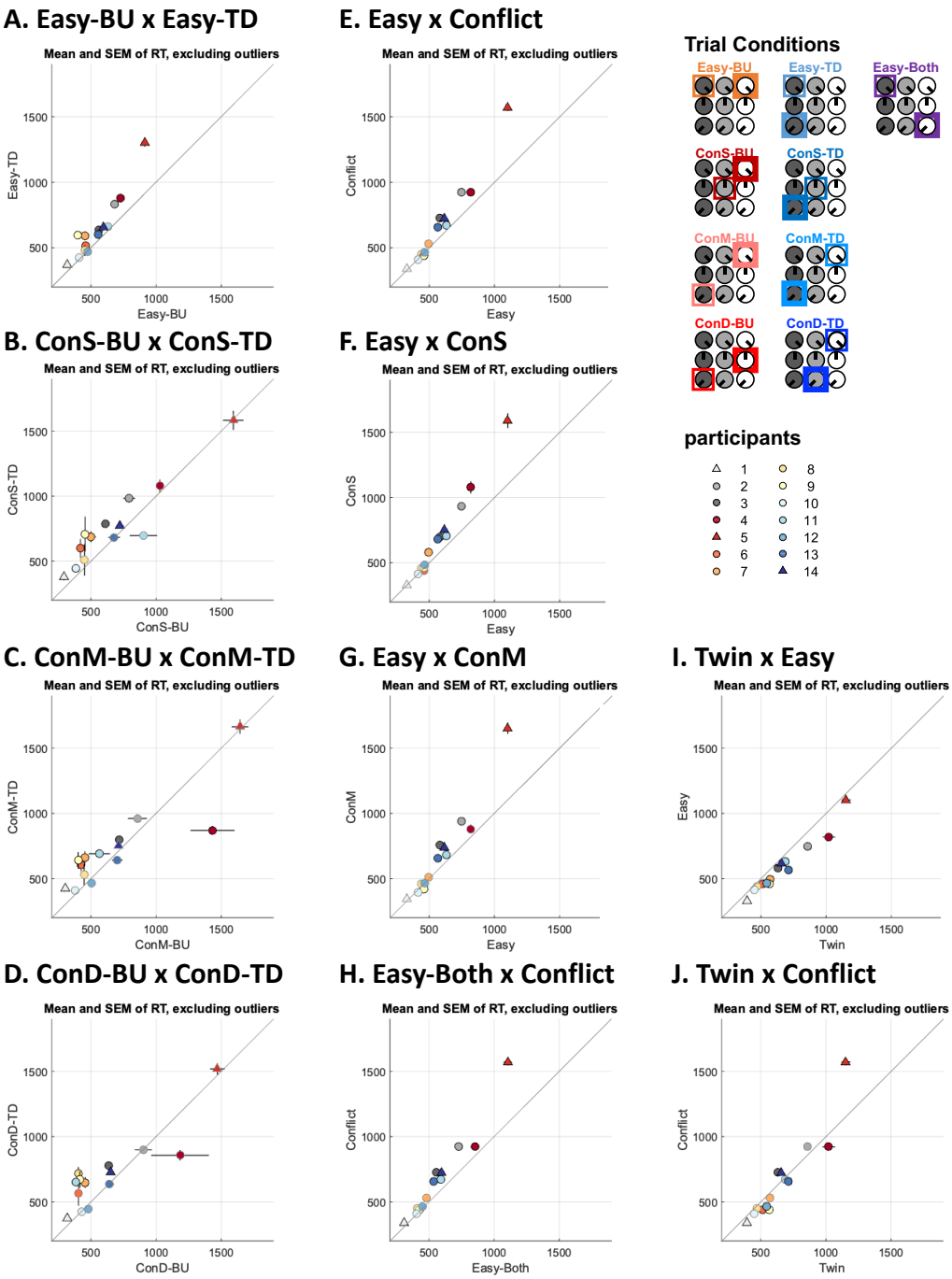

Figure 5. Scatter plot of mean RT across trial conditions

Circles and triangles indicate the mean reaction time of each participant (identified as shown in the legend at bottom right). The standard error of the mean is indicated by the overlaid lines along the respective dimensions. **(A-D)** Comparison of RT between BU and TD features for Easy, ConS, ConM and ConD trials. **(E-H)** Comparison of Easy and Conflict trials. **(I-J)** Comparison of Twin trials against Easy and Conflict trials. Triangles indicate the participants whose data are further described on Figure 3. Symbol edge color indicate the result of Wilcoxon rank sum test between the plotted conditions (black: $p < .05$, gray: $p > .05$).

Errors in conflict trials had shorter reaction times when choosing a BU-favored target.

In ConD trials, one target is less valuable than the other, so choosing it can be considered an error. Of 1072 ConD-BU trials, 715 were correct and 357 were error trials, in which the participant chose the BU-favored target even though its total value was lower than the other target. Thus the accuracy was 66.7% (Figure 6A, top). Of 1205 ConD-TD trials, 783 were correct and 422 were error trials, thus the accuracy was 65% (Figure 6A, bottom). We predicted that error trials favoring the BU attribute would have shorter RTs than error trials favoring the TD attribute. Confirming this prediction, a two-sample t-test on the z-scored log RT revealed a significant difference between ConD-BU (z-scored log RT mean M = -0.155, SD = 1.015) and ConD-TD (M = 0.119, SD = .913) error trials ($t(777) = -3.96$, $p < .001$). We focused on ConD conditions because Easy-BU, Easy-TD and Easy-Both conditions all had very few error trials (data not shown).

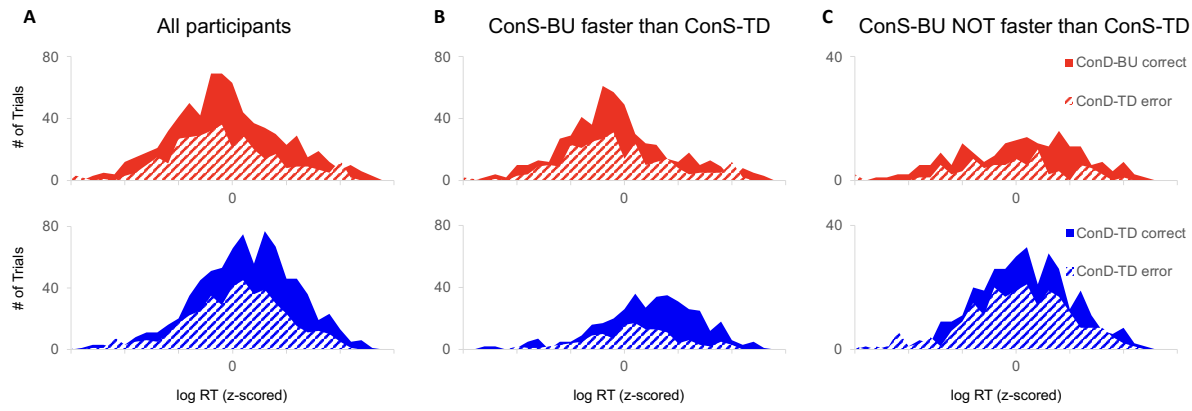

Figure 6. Z-scored log RT distributions of correct and error trials during Conflict trials with unequal targets (ConD)

of (**A**) all participants, (**B**) participants whose RT for ConS-BU was shorter than that of ConS-TD, and (**C**) participants whose RT for ConS-BU was not significantly different from that of ConS-TD. Filled areas represent correct trials. Striped areas represent error trials.

Participants made faster choices when choosing between two high-valued targets.

The Dual Feature task was designed as a value-based decision task. However, due to the nature of the stimuli we used, one could also treat it as a perceptual discrimination task. Importantly, while the BU feature has a linear component (dark to bright), the TD feature was more arbitrary, and the discrimination between different line orientations was not comparable to the discrimination between different brightness levels. This allowed us to test whether the Weber-Fechner law, which postulates that perceptual discrimination becomes more difficult (and therefore slower) as the amplitude of the discriminated stimuli increases, applies when the discriminated stimuli are associated with reward magnitude. Specifically, we analyzed the reaction time of choices between two high-valued targets versus two low-valued targets by comparing the reaction times when the choice was based on the attribute whose stimulus strength was linearly correlated with the reward magnitude (i.e., Easy-BU) or not (i.e., Easy-TD).

We compared the RT and choice accuracy of Easy trials that offered two of the highest and two of the lowest possible values (Figure 7). In high reward trials, the choice is between two high-value targets, one worth 10 points (5 BU + 5 TD points) and another worth 8 points (Easy-BU: 5 BU and 3 TD, or Easy-TD: 3 BU and 5 TD). In low reward trials, the choice is between a target worth 4 points (Easy-BU: 3 BU and 1 TD, or Easy-TD: 1 BU and 3 TD) and another worth 2 points (1 BU and 1 TD). In Easy-BU trials, there was no significant difference in RT between low (M = 594.6, SD = 251.3) and high (M = 566.2, SD = 252.1) reward offers (p = .15, two-sample Kolmogorov-Smirnov test). The accuracy was better for low (M = 0.95, SD = 0.09) than high (M = 0.86, SD = 0.11) trials ($t(26)$ = -2.27, p = .031, two-sample t-test) offers. By contrast, in Easy-TD trials, RT was shorter when the offered rewards were higher (M = 777.94, SD = 334.95) than

lower (M = 604.29, SD = 290.09, p < .001). The accuracy was not significantly different between low (M = 0.78, SD = 0.22) and high (M = 0.87, SD = 0.12) offers ($t(26)$ = 1.38, p = .17).

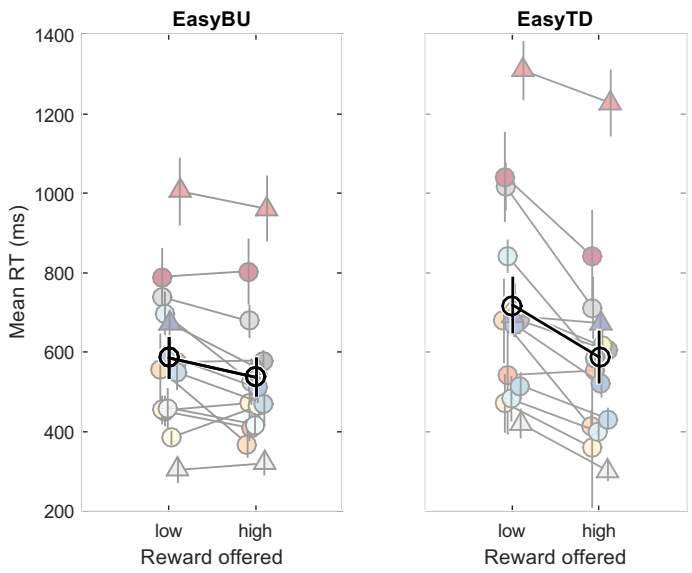

Figure 7. Mean RTs grouped by offered reward magnitude.

RT did not increase when the offered reward was larger. Different colours correspond to different participants. The triangles represent the example participants from Figure 3, whose mean RTs were short (<500 ms, light gray), medium (between 500 and 1000 ms, dark blue) and long (>1000 ms, red). Black open circle with black overlaid lines indicates the mean RT of all participants with standard errors of the mean.

The mean RT of Easy-BU trials did not vary between high and low offers, though participants made more mistakes when the offers were higher. In fact, the accuracy for low offer Easy-BU trials were almost at the ceiling. The mean RT for Easy-TD trials was shorter for higher offers and the accuracy was comparable.

In Easy-BU trials, the observed decrease in the accuracy for high offers may be due to the Weber-Fechner law in brightness discrimination, although there was no difference in the RTs between high and low offers. In Easy-TD trials, the presence of the highest BU features reduced the latency of the TD-based choices, although the accuracy was unaffected. Overall, our results are not

compatible with Weber-Fechner law, which predicts both reduction in the accuracy and increased latency for higher offers. The reduction in the latency in high offer Easy-TD trials is similar to what has been reported in previous studies (Shevlin et al., 2022).

Changes of mind were mostly a switch from the BU-favored to the TD-favored target.

All participants showed some changes-of-mind (CoM), particularly during conflict trials, indicated by an abrupt change in the movement trajectory (see examples in Figure 8A). Participant 12 had no ConS-BU trials because they changed their mind in all of those trials, making them ultimately end up as ConS-TD trials. Out of 3467 equivalued conflict trials, 174 trials (5%) contained a change-of-mind (68 in ConS trials, 106 in ConM trials). In ConS, 57/68 (84%) changes were from the BU-favored to the TD-favored target (Figure 8B, left). In ConM, 83/106 (78%) were from the BU- to the TD-favored target (Figure 8B, right). Thus, most changes of mind happened as a switch from BU to TD.

We tested whether the CoM was a result of participants correcting their premature decisions. If CoM was a corrective maneuver, we predicted that the initial RT prior to the CoM would be shorter than the RT of the same condition without the CoM. We thus compared the RTs of Conflict trials with and without CoM (Figure 8C). The initial RT of BU-to-TD CoM trials (M = 563.66, SD = 327.28) and the RT of non-CoM Conflict-BU trials (M = 588.92, SD = 392.73) were not significantly different ($t(1880) = 0.75$, $p = .4$, two-sample t-test, compare red distributions in the two top rows of Figure 8C). The initial RT of TD-to-BU CoM trials (M = 608, SD = 521.13) was shorter than the RT of non-CoM Conflict-TD trials (M = 744.15, SD = 364.8, $t(1576) = 2.1$, $p = .036$, compare blue distributions in two bottom rows of Figure 8C). There was no statistical difference between the initial RTs of the BU-to-TD and TD-to-BU CoM trials ($t(176) = -0.62$, $p = .54$). As shown in Figure 8D, the timing of the CoM was not constant with respect to target onset,

but instead followed the initial RT by approximately 266 ms (regression slope = 1.04, $R^2 = 0.91$, $p < .001$).

The majority of changes of mind were from the BU-favored to the TD-favored target, and there was no significant difference between the initial RTs of these trials versus non-CoM trials (see above). Changes from TD to BU were much more rare, so while their initial RTs were shorter than in non-CoM trials, it is precarious to make any strong conclusions on this basis. Furthermore, across CoM trials the time between the initial RT and the CoM was almost constant. This does not support the idea that CoM trials result from correcting a premature decision, but instead, suggests they are better interpreted as a real change-of-mind process that occurs with a constant delay following the initial movement onset.

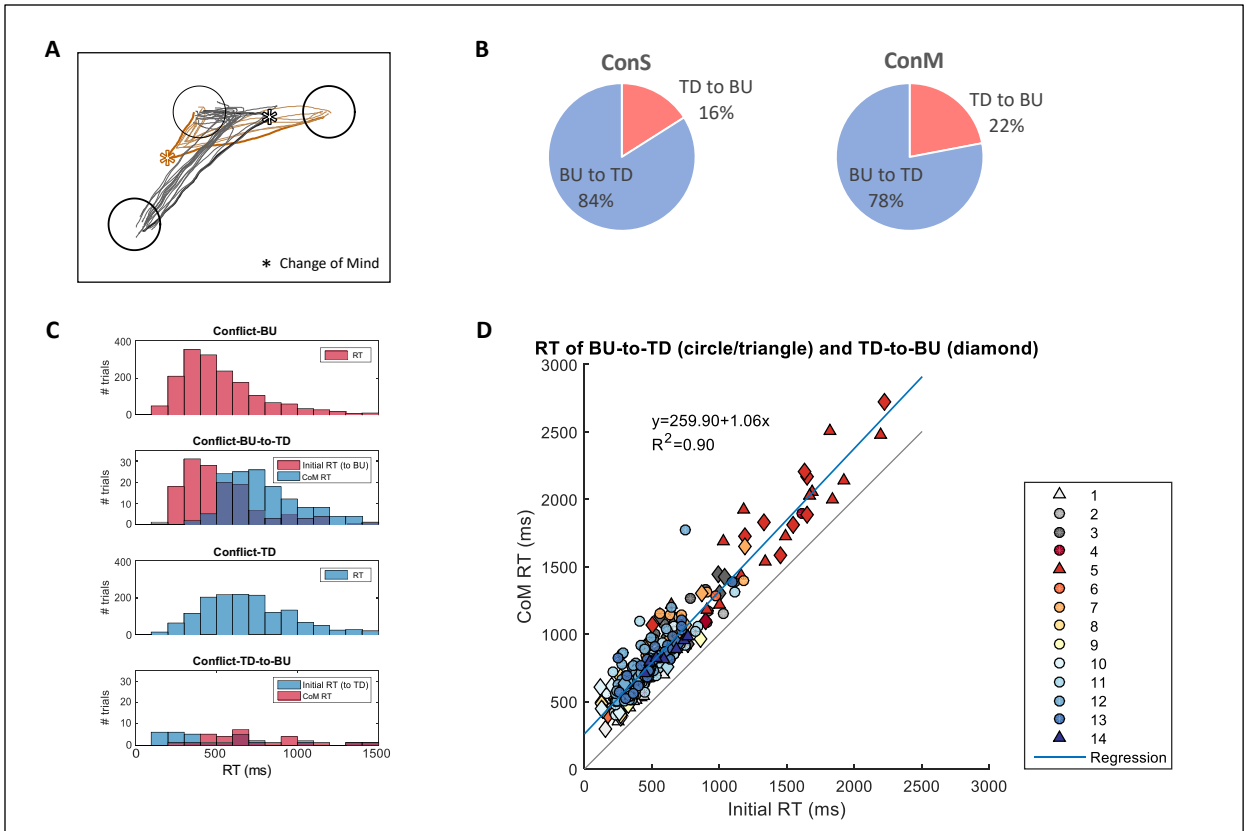

Figure 8. Change of Mind (CoM) trials

(A) Sample trajectories of change-of-mind trials. Black and brown lines are trajectories to bottom left and right targets, respectively. Stars indicate the point in which CoM was assigned for two example trials (thick lines). **(B)** In ConS trials, 84% of CoM were from BU to TD. In ConM trials, 78% of CoM were from BU to TD. **(C)** Reaction time distributions of conflict trials with and without CoM. TOP to BOTTOM: Conflict-BU trials without CoM (i.e., straight trajectory). Conflict trials in which the initial trajectory was toward the BU-favored target (red RT), but finally reached the TD-favored target (blue CoM RT). Conflict-TD trials without CoM. Conflict trials in which the initial trajectory was toward the TD-favored target (blue RT), but finally reached the BU-favored target (red CoM RT). **(D)** Scatter plot of initial and CoM RT of individual trials. Different colors correspond to different participants. Circles and triangles: CoM trials changing from BU to TD. Diamonds: CoM trials changing from TD to BU. Blue line: Linear regression, $p < .001$, $R^2 = 0.91$.

DISCUSSION

We investigated whether humans make value-based decisions by fully integrating all available information into a unified measure of subjective value, or whether such decisions involve a more distributed process whereby separate sources of information can themselves compete. Participants

chose one of two reachable targets whose value was based on two visual attributes, the brightness of the target (a bottom-up cue, BU), and an oriented line overlaid on the target circle (a top-down cue, TD). We predicted that, if the BU and TD attributes in our task are always converted into representation of reward value and decisions are made by comparing the total value of each target, decisions would be faster when only one feature is different (Easy-BU and Easy-TD trials) and slower in more complex conditions where both features differ (Easy-Both and Conflict trials), but there would be no difference between Easy-Both, Conflict-BU, and Conflict-TD trials. Under this "integrated competition" hypothesis, the differences in RTs between different trial conditions would be determined by the time it takes to process both the BU and TD features. If we assume that the comparison process is bypassed when a feature is identical across the targets, then we would predict that RTs in Easy-BU trials would be the shortest, followed by Easy-TD, then followed by Easy-Both and Conflict conditions. In this view, Conflict trials might be expected to be slower than Easy-Both trials, as a decision may require recruiting an additional process that resolves the conflict, but Easy-Both trials should not be faster than Easy-TD. Most importantly, identifying Conflict trials could only be done after both features were processed, so there should be no difference between the RT distribution of Conflict-BU versus Conflict-TD trials.

Alternatively, if the BU and TD attributes in our task are processed in different neural substrates, and the decision could be made prior to a complete integration at the level of total reward value, then differences in the RTs should reflect which attribute was used to decide, especially during trials with equally valued targets. That is, a "distributed competition" hypothesis predicts that decisions based on the BU attribute would be faster than those based on TD attributes in both Easy and Conflict trials, and choices in favor of the BU attribute (Conflict-BU) would be more frequent

in early decisions whereas those in favor of the TD attribute (Conflict-TD) would be more frequent in later decisions.

We found that RTs varied across trial types and that the order of the conditions was not strictly congruent with the complexity of the features. Notably, all participants were fastest in Easy-BU and Easy-Both trials, and slower in Easy-TD trials. This suggests that the BU feature was processed more quickly than the TD feature, as expected. Importantly, if all information was integrated before making the decision, one would expect that the latency for Easy-Both to have been similar to that of Easy-TD, as solving Easy-Both trials should take at least as long as processing the TD feature in Easy-TD trials. In fact, when some participants chose the BU-favored target in ConS and ConM trials, they did so faster on average than in Easy-TD trials. This suggests that during these types of Conflict trials, participants often chose the BU-favored target before taking the TD feature into account. In this group of participants, the slowest condition was ConS-TD and ConM-TD, suggesting that choosing in favor of the TD feature in Conflict trials takes longer than choosing a left or right target when the two targets are identical (Twin trials). For the other group of participants, Easy-TD and Twin were the second fastest conditions, and ConS-BU, ConM-BU, ConS-TD and ConM-TD conditions were all similar and the slowest. In other words, these participants were faster when solving Easy trials and slower when the choice was ambiguous (i.e., the targets were equal-valued), especially when the features were in conflict. This suggests the possibility that Conflict trials potentially involved an additional conflict-resolution process that took more time. However, the overlap between the RT distributions of Easy-Both and Easy-BU trials and the fact these subjects took longer to solve Easy-TD than Easy-Both are incompatible with decision timing being simply determined by trial complexity. Instead, these results are

compatible with the proposal that BU and TD features are processed in parallel by different neural mechanisms and the decision can sometimes be made before both processes are complete.

Furthermore, we saw that changes-of-mind in Conflict trials were mostly from the BU-favored target to the TD-favored target. The timing of the change of mind was not constant with respect to target onset, but instead followed the initial RT by approximately 266 ms. Importantly, changes from the TD-favored to a BU-favored target occurred most often when the initial RT was very short, again suggesting that subjects sometimes make choices before integrating all sources of information about value.

Finally, we investigated whether the BU and TD features in our task follow predictions of the Weber-Fechner Law, a psychophysical theory that posits an increase in the just-noticeable-difference proportional to the magnitude of the stimuli. We subdivided Easy-BU and Easy-TD trials based on the magnitude of offered reward, and compared the RTs to see if deciding between two large offers took longer than deciding between two small offers, as would be expected if the just-noticeable-difference was smaller and thus took longer to discriminate. We found that the magnitude of the reward offered did not influence RT in Easy-BU trials, but higher offers negatively affected choice accuracy. During Easy-TD trials, participants were faster when choosing between two high reward options than when they were choosing between two low reward options, whereas the choice accuracy was similar between the two. This was partially in line with previous results that argued against diminishing value sensitivity in value-based decisions (Shevlin et al., 2022).

Taken together, our results suggest that despite indicating the same type of information (i.e., the reward value of a target), the two visual features used in our task were not simply integrated into a "common currency" before entering into a decision process. Instead, our data are consistent with

the premise that BU and TD features are treated in parallel, possibly by different neural substrates. The finding that a subset of participants had shorter RT in ConS-BU and ConM-BU trials than in Easy-TD trials suggests that the decision processes that favor BU features can sometimes bypass the processing of the TD feature. That is, a decision-making area in the brain that has received information about the BU feature has the capability to trigger the choice without waiting for the complete integration of information about the TD feature. In summary, our results suggest that action decisions can be made before all information is integrated, supporting the proposal that a hierarchy of within- and between-attribute competitions influences the higher-order choice-level competition (Hunt et al., 2014).

There are many possibilities of where in the brain such competitive processes might unfold. For example, based on functional magnetic resonance imaging (fMRI) data in humans performing multi-attribute multi-alternative choice task, Hunt and colleagues suggested that cells in the intraparietal sulcus signal the between-attribute competition, whereas medial prefrontal cortex signals the between-option competition at the 'integrated' value level (Hunt et al., 2014). Other human fMRI studies suggested that the orbitofrontal and ventromedial prefrontal cortex reflect subjective value comparison across categories such as food, money, consumable products and pain (FitzGerald et al., 2009; Kable & Glimcher, 2007; D. V. Smith et al., 2010; Talmi et al., 2009). When tasks require incorporation of negative values such as effort, monetary loss, pain or satiation-induced devaluation, ventromedial prefrontal cortex, anterior cingulate cortex, supplementary motor area, amygdala and nucleus accumbens have been suggested to provide the devaluation signal (Basten et al., 2010; Croxson et al., 2009; Gottfried et al., 2003; Klein-Flügge et al., 2016; Talmi et al., 2009). In a seminal study, Buschman & Miller (Buschman & Miller, 2007) showed that when monkeys perform a visual pop-out task in which the correct target can be

easily discriminated from among distractors in a bottom-up fashion, choice-related activity appears in posterior parietal cortex before frontal regions, but when the task requires a slower serial visual search the opposite pattern of latencies is observed. This suggests that bottom-up decision tasks may be solved by the fast dorsal visual stream (Ledberg et al., 2007; Schmolesky et al., 1998), while more complex tasks require slower processes that combine distinct visual features, implicating the ventral visual stream and its projections to prefrontal regions (Donner et al., 2002; Yan et al., 2016) In our experiment, both of these kinds of processes may be taking place within the context of a single task, even during individual trials. This could make it possible to identify where in the brain the two kinds of relevant cues – bottom-up and top-down – are processed, and whether they compete in a distributed manner or only after being integrated into a unified estimate of subjective value within a single "central executive". Such studies are underway (Nakahashi et al., 2018; Nakahashi & Cisek, 2016, 2020), but their results are beyond the scope of the current paper.

ACKNOWLEDGEMENTS

The authors thank Aarlenne Khan and Lawrence Snyder for helpful comments on an earlier draft of this manuscript.

CHAPTER 4 MONKEY BEHAVIOUR AND ELECTROPHYSIOLOGY

INTRODUCTION

Behavioural data from humans suggest that participants treated two visual attributes differently despite the fact that both attributes provided information about the same thing: the absolute reward magnitude. Furthermore, reaction time distributions suggest that action decisions can occur before all information is considered. During equivalued conflict trials, more than half of the participants made decisions in favour of the *"bottom-up"* feature faster than when their decisions were based on the *"top-down"* feature. Are these features preferentially processed in different brain regions, such that activities in bottom-up and top-down regions can simultaneously and independently reflect subject choice? We drew inspiration from a study by Buschman and Miller, which reported that the order in which activity predicting saccades appeared in different brain regions was dependent on whether the choice involved bottom-up or top-down processes. In their study, monkeys performed a delayed match-to sample task, either with a pop-out target or with a target requiring serial visual search. With a pop-out target, activities in the lateral intraparietal (LIP) area predicted saccadic eye movements faster than those in the frontal eye field (FEF), whereas the order was reversed when the target was not a pop-out and a serial search was necessary (Buschman & Miller, 2007). Our aim was first to replicate these findings in the equivalent regions for arm movements, and second, to investigate the neural activity during a free-choice situation to tease apart the neural latency related to stimulus information from that of choice. We recorded neural activity from two sensorimotor areas related to arm movements, dorsal premotor cortex (PMd) (a frontal arm region, a surrogate to FEF for saccades) and the caudal part of area 5 of posterior parietal cortex (PPC), also known as the parietal reach region (PRR) (an arm region analogous to

LIP), and compared the latency of neural activities that predicted the monkey's choice (Christopoulos et al., 2015). We predicted that, if decisions are always made in a Central Executive that lies outside of these sensorimotor areas, the differences in latency of choice predictive activity in PMd and PRR will not vary as a function of what kind of decision is made (e.g. value-based choice in easy trials versus free choice in conflict trials) or as a function of the feature that drives the choice (e.g. bottom-up versus top-down). If that is the case, the latency difference reported by Buschman and Miller may be interpreted as a representation of stimulus parameters and not of the choice itself. In contrast, if decisions are made through a Distributed Consensus, and both PMd and PRR are part of that process, then we predict that PMd and PRR will predict choice at different latency depending on the specific feature that drives a particular choice. Specifically, if our top-down and bottom-up stimuli are preferentially processed in PMd and PRR, respectively, this would predict that neural correlates of decisions based on our top-down feature would appear earlier in PMd than in PRR, while neural correlates of decisions based on our bottom-up feature would appear earlier in PRR than in PMd.

In the subsequent sections, behavioural and electrophysiological procedures performed on two monkeys will be described, but only the first monkey's data will be presented. At the time of writing, electrophysiological recording with the second monkey is still in progress.

MATERIALS AND METHODS

Subjects and Project Timeline

Two male macaque monkeys (*macaca mulatta*) were used in this project. The electrophysiological recording was performed on monkey Y starting at 5 years of age for 5 years, and on monkey K starting at 9 years of age for 2.5 years. During this time, they weighed approximately 10 kg and

12.5 kg, respectively. After the monkeys learned the features in the Dual Feature task, a titanium head fixation post was implanted on the skull under general anesthesia. The monkeys were then trained on an eye fixation task, followed by combining the eye fixation and the Dual Feature task so that they were performing the reaching movement without moving their eyes. Initially, Monkey Y was implanted with custom chambers over the same regions and neural recording was performed using NAN microdrives (NAN Instruments, Israel) and AlphaLab data acquisition system (AlphaOmega, Israel). During this time, 2-4 microelectrodes (FHC or AlphaOmega) were advanced daily until task-related single units were isolated. At the end of the daily session, electrodes and the microdrives were removed and the chambers were closed with hermetically sealed caps. After 195 sessions of recording, we modified our approach to improve yield. This involved chronically implanting GrayMatter microdrives (Monkey Y: 17.5 mm diameter, Monkey K: 23.37 mm and 17.5 mm diameter) over the dorsal part of the arcuate sulcus and intraparietal sulcus. Microstimulation sessions were conducted after a sufficient number of well isolated neurons were recorded.

All procedures were in accordance with the ethics protocol of the Université de Montréal.

Task Apparatus

Behavioural task and data collection were done with LabVIEW 8.2 on a Windows 10 computer. Reaching kinematics were recorded using a digitizing tablet (CalComp, 120 Hz). Eye movement was recorded at 120 Hz using an infrared oculometer (Applied Science Laboratory), and a hot mirror was placed in front of the monkey's face to reflect the pupil. Visual stimuli were displayed at 144 Hz on a horizontally positioned LCD monitor (EIZO), which was reflected on a mirror placed at equidistance from the monitor and the digitizing tablet. This created a visual illusion that the cursor and the targets were floating at the height of the reaching workspace.

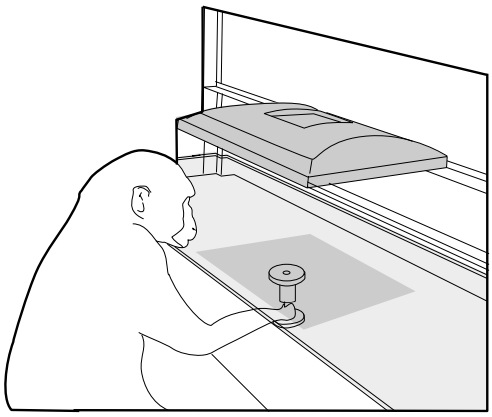

Figure 1. Task Setup

A macaque monkey sitting at the tablet.

To detect the true stimulus onset, we used photocells to record when the LCD monitor displayed the key stimuli (Wang & Nikolic, 2011). Two photocells were placed on the edge of the monitor at the same height as where the targets were drawn, and a small white square was drawn at the same time as the targets. The analog signal from the photocell was recorded via LabVIEW and analyzed in MATLAB, and event onsets were assigned when the signal crossed a threshold.

All data were stored in MSSQL database using custom software.

Dual Feature Task

Each trial was initiated by eye fixation at the small red circle at the center of the workspace. After a variable fixation delay (500 ±400 ms), a circular reach target (1.4cm diameter) appeared in the center of the workspace, and subject had to move the cross cursor (depicted in orange in Figure 2) inside to continue the trial. After a variable center-hold time (700 ±400 ms), two circular reach targets (2.7cm diameter) appeared on the left and right of the center circle, 3.3cm away, center to center. Just like the human version of the task, each target contained two independent visual features, indicating the amount of reward given upon a successful reach. The brightness of the target served as the "bottom-up" (BU) feature, with three different levels of desirability score (dark gray = 1 point, medium gray = 3 points, and white = 5 points). The angle of an overlaid line served as the "top-down" (TD) feature, also with three different levels (4:00 = 1 point, 12:00 = 3 points, 8:00 = 5 points, see Figure 3). The sum of these scores divided by 2 translated into the amount of reward (i.e., the number of water or juice drops), which ranged from 1-5. During the recording, we restricted the range of trial conditions to keep the maximum reward size at 3 to encourage the monkey to complete more trials.

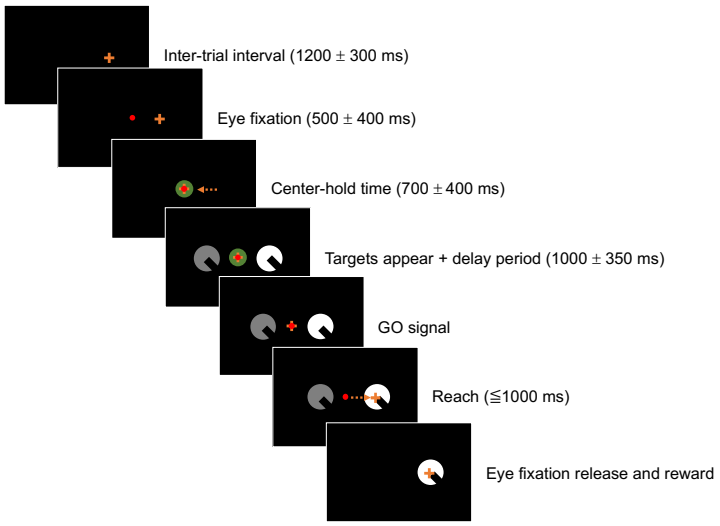

Figure 2. Dual Feature Task Timeline

The cross cursor is depicted in orange for visual clarity, which was light gray during the actual experiment.

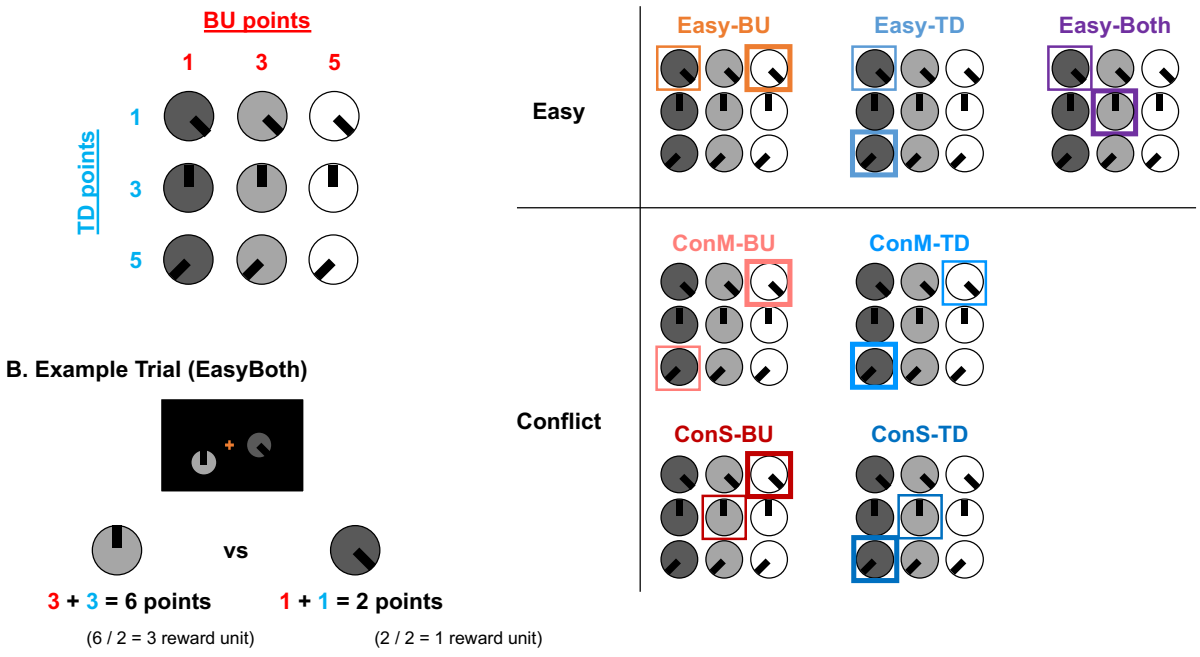

Figure 3. Target Features, Points and Trial Conditions

(A) Target features with three levels of bottom-up (BU) brightness feature and top-down (TD) line orientation feature, **(B)** an example trial showing the combination of BU and TD features that yields an Easy-Both trial, and **(C)** Trial conditions used for the monkey project, which did not contain the ConD trials. Target features were identical to those used in the human project (see chapter 3 Human Behaviour).

There was a variable delay period (1000 ±350 ms) before a GO signal (disappearance of the central circle) was given, at which point the subject can report his choice by moving the cross cursor into one of the two targets. A subset of sessions was a reaction-time version of the same task, in which the reach targets and the GO signal appeared simultaneously and the monkey could start moving towards his choice as soon as he was ready. Subject had to exit the central circle within 700 ms from the GO signal (i.e., maximum Reaction Time (RT) was 700 ms) and enter a target within 1000 ms after exiting the central circle (i.e., maximum Movement Time was 1000 ms). The subject was required to maintain eye fixation until the target was reached, and breaking the fixation caused

the trial to abort. In addition to two-target trials of different types, the experiment also included trials with just one target (1T trials), whose reward value was also determined by the two features according to the same rules. Since we were most interested in ConS trials, which would only occur 10% of the time, we artificially increased the number by randomly inserting ConS trials. As a result, an average session consisted of 15% 1T, 17% Easy-BU, 17% Easy-TD, 4% Easy-Both, 23% ConS, 8% ConM, and 13% Twin trials, all of which were randomly interleaved.

Training Timeline

Both monkeys were trained in steps. First, they were trained in a single-target, center-out reaching task with an instructed delay until they were successfully reaching the target at least 80% of the trials. Second, they were given two identical targets (i.e., Twin trials) until they were successfully reaching to one of two targets in at least 90% of the trials. Then, the BU feature was introduced and performance was observed until it reached a plateau. Subsequently, the TD feature was introduced, and performance was again observed until it reached a plateau. Finally, equivalued Conflict trials (ConS and ConM) were introduced. Non-equivalued Conflict trials (i.e., ConD) were not presented to monkeys in order to maximize the number of equivalued Conflict trials, which was the focus of this project. By the time we performed electrophysiological recordings, monkeys were choosing the “better” target at least 90% of the time during Easy trials.

On the first day when Monkey Y was presented with the BU feature, he chose the brighter target during the first 130 trials (Figure 4A, red arrow). This was followed by some exploration for two days, after which his performance started to stabilize. His performance plateaued 7 days after the introduction of the BU feature. He was then presented with the TD feature while the BU feature was held identical between the two targets. On the first day, he appeared to ignore the TD feature. On the second day, he began exploring, and on the third day, he started choosing the "correct"

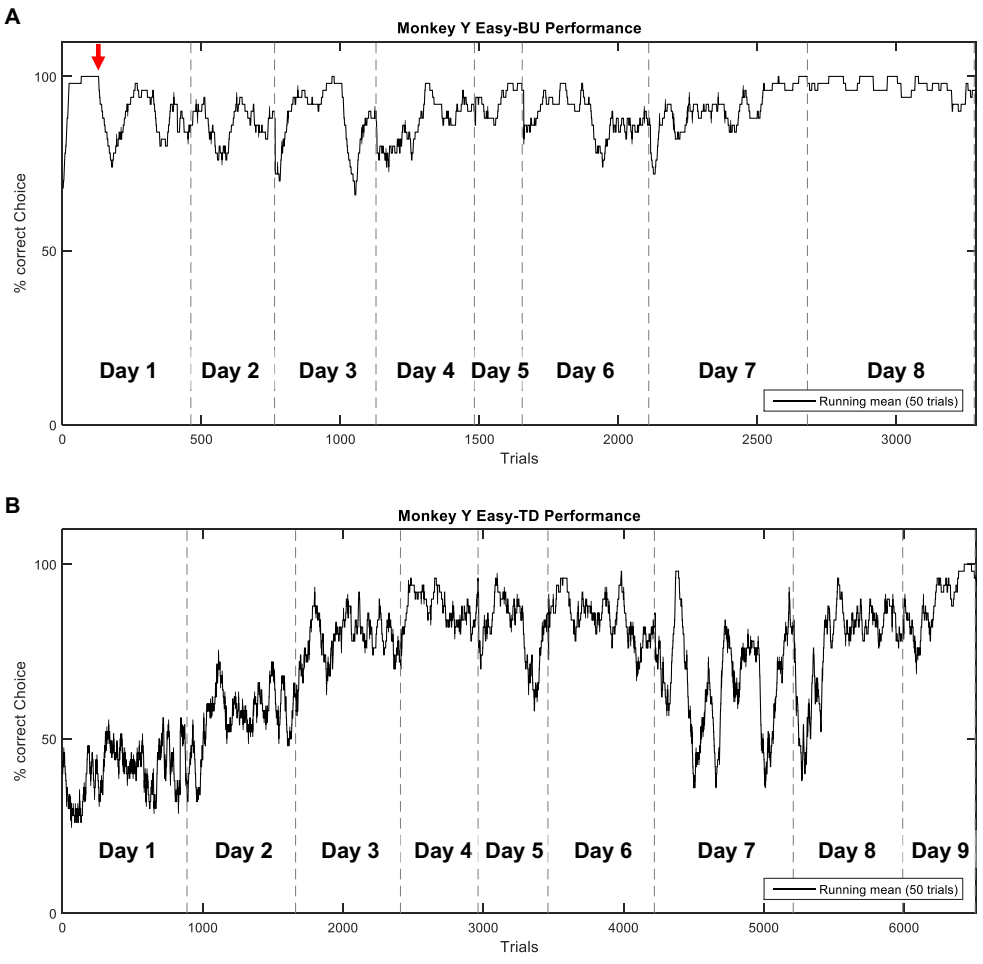

Figure 4. Monkey Y's performance while he learned the BU and TD features

Percentage of correct choices, averaged using a sliding window of 50 trials, during the feature learning period. **(A)** Easy-BU training sessions spanning 8 days until performance plateaued. Red arrow indicates the moment Monkey Y abandoned the initial brightness bias and started exploring. **(B)** Easy-TD training sessions spanning 9 days until performance plateaued. Gray dotted lines indicate separation of different days and the resetting point of the running mean.

target. Despite some variability (e.g., day 7, see Figure 4B), his performance plateaued 9 days after the introduction of the TD feature.

Directional Bias

Monkey Y developed a directional bias during the course of training, and it persisted into the electrophysiological recording period. In most sessions, when presented with equivalued options, he would choose the target on the left almost exclusively. In order to discourage this bias, so that we can obtain a more balanced data both behaviourally and neurally, we introduced a pre-reward delay that increased as a function of the magnitude of the bias. The delay occurred between the time the monkey successfully reached a target and the delivery of reward, only during the trials with equivalued options (i.e., Twin, ConS and ConM trials), starting at 4 consecutive biased choices. The delay started at 133 ms and increased by 133 ms every time the biased target was chosen, up to 1166 ms. When the target on the opposite side was chosen, the reward was delivered without a delay and the bias count was reduced by one. This manipulation successfully discouraged monkey Y's directional bias and provided sufficient trials in which the target on the right was chosen when options were equivalued. We chose the delay instead of manipulating the reward size to avoid altering the meaning of the attributes used to indicate the reward size.

Neural Recording

Using structural MRI data processed with BrainSight (Rogue Research, Montréal, Québec), recording chambers were placed over the arcuate sulcus and the intraparietal sulcus, respectively (Figure 5). A majority of recordings were performed using two chronically implanted microdrives (GrayMatter Research, Bozeman, MT), with data acquisition using Synapse (Tucker-Davis Technologies, Alachua, FL). All data came from the left hemisphere, and the monkeys used their right arm to perform the task.

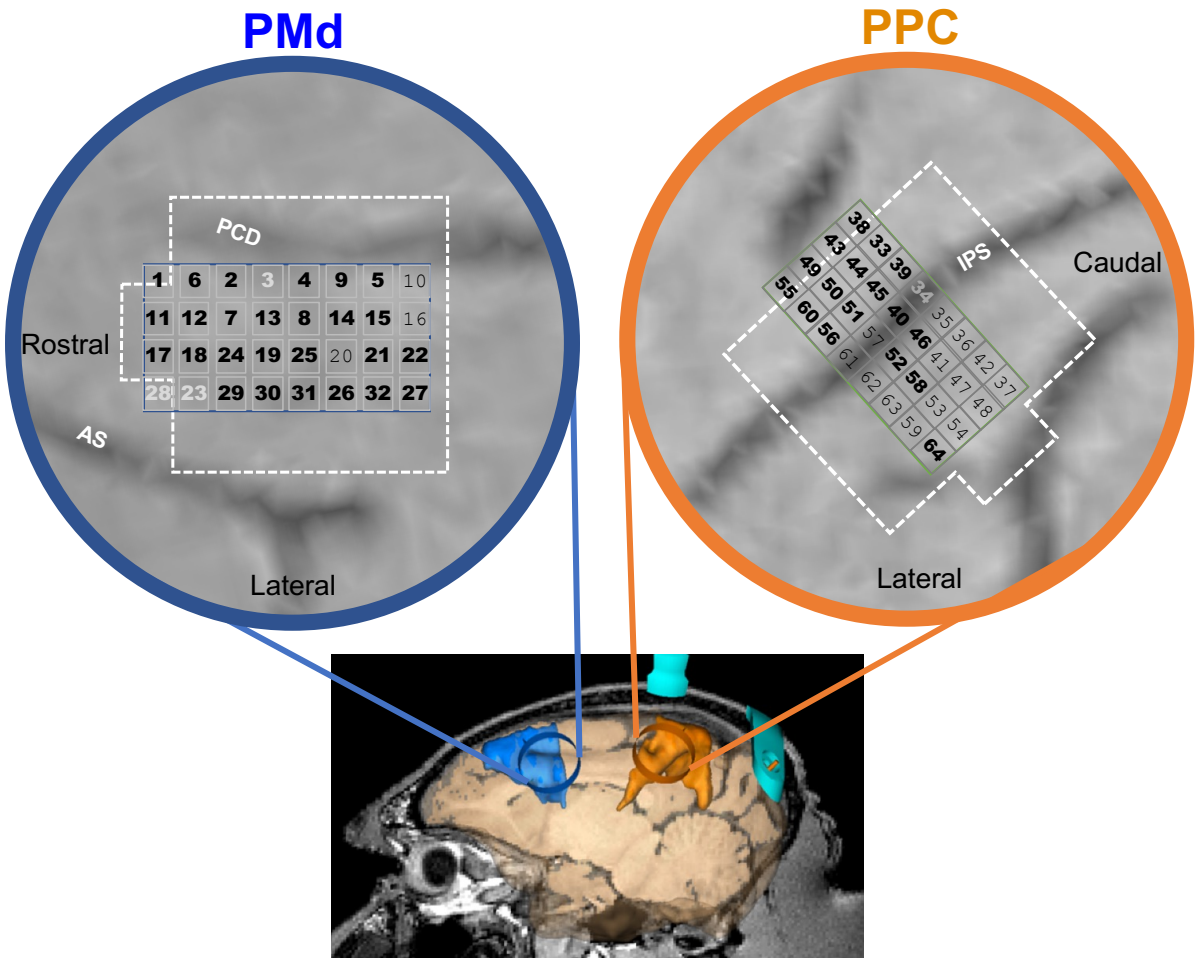

Figure 5. GrayMatter drive electrode placements on Monkey Y

A 4x8 electrode grid was placed between the precentral dimple and arcuate sulcus to aim at PMd **(A)**, and over the intraparietal sulcus to aim at the arm region of PPC **(B)**. Dashed white outlines show the footprint of the Microdrive where it meets the skull. PMd electrodes were 1.2 mm apart medial to lateral (in 4 rows) and 1 mm apart rostral to caudal (in 8 columns). PPC electrodes were 1.0 mm apart in both directions. Electrode numbers in bold were inserted into the brain. Black electrodes remained intact during the recording period, whereas those in gray (3, 23, 28, and 34) broke during descent. Bottom: an MR image of Monkey Y's brain, sagittal view. The blue region indicates a 3D reconstruction of PMd and the orange indicates parietal areas near the intraparietal sulcus. PCD: precentral dimple, AS: arcuate sulcus, IPS: intraparietal sulcus.

The recording microdrives were implanted in two steps under general anesthesia. The initial step was chamber implantation. First, a trephine was made at the placement of the chamber. Second, 12-18 bone screws were securely placed on the skull and anchored with C&B-Metabond (Parkell, Edgewood, NY). Third, durotomy was performed inside the trephine. Fourth, a chamber was

placed over the trephine and the location was verified with BrainSight, and cranioplastic was used to anchor the chamber to the bone screws. Chambers for the 32-channel microdrives were installed with the Silastic membrane insert within at the time of placement. On the second monkey, the chamber for the 96-channel Microdrive was installed with DuraGen (Integra Life, Princeton, NJ) on the surface of the cortex, and then sealed with a dummy plug. The animals then recovered under veterinary monitoring. The second step was the microdrive installation. Upon disinfecting the implant areas, sterile microdrives were inserted in the chambers. Bone wax was applied to the gap between the chamber and the microdrives, and cranioplastic was used to anchor the microdrives.

At the beginning of recordings, a given electrode was descended until it touched the surface of the animal and its impedance dropped. The electrode was then further descended by 0.5 mm. After that, before each session, a subset of electrodes was moved by a maximum of 0.5 mm or until neural action potentials were audibly and visually identified. Once cell activity was observed, we reduced the maximum daily distance of travel to 0.25 mm, or until we observed sufficient change in the signal. In order to reduce the risk of dimpling the brain surface, we avoided moving adjacent electrodes on a given day.

The neural signal was collected at approximately 24 kHz and bandpass filtered at 300-3000 Hz in Synapse software (Tucker-Davis Technologies, FL). Single units were isolated offline either in Plexon Offline Sorter (Plexon, Dallas, TX), or where possible, with Full Binary Pursuit (FBP), an automatic spike sorting algorithm (Hall et al., 2021). Local field potentials (LFPs) were collected at approximately 1017 Hz, bandpass filtered at 3-300 Hz, and stored using custom MATLAB codes provided by Tucker-Davis Technologies. The flow of data acquisition is illustrated in Figure 6.

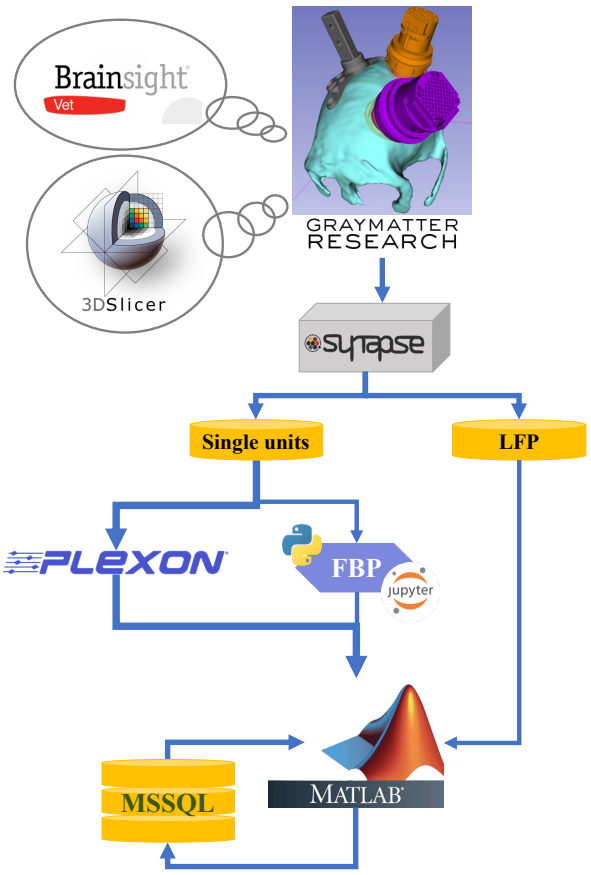

Figure 6. Neural Data Collection Flow

Most neural data were recorded from GrayMatter microdrives implanted over the target areas, which were planned and verified using 3D reconstruction applications (BrainSight and 3DSlicer). Data were preprocessed and stored by Synapse software. Single units were isolated using Plexon Offline Sorter or Full Binary Pursuit (FBP), then stored to MSSQL using custom MATLAB codes. Local field potential (LFP) data were also stored using custom MATLAB codes.

Beyond yielding data from a larger number of neurons simultaneously, this approach had two other advantages. First, because we advanced electrodes prior to running the task and stopped whenever an isolatable neuron was found, our sampling of the neural population was not biased toward obviously task-related neurons like previous approaches, including our own. While it still favors larger neurons that are easier to find and hold, this approach gives us a more unbiased picture of what percentage of those cells are task related and those that are not, all of which are recorded for at least one session. Second, because

the microdrives were chronically implanted and very stable, we could often find the same neuron on the next day of recording (Figure 7). To maximize these cases, each day's strategy for advancing electrodes was based on the data from neurons recorded in the previous session, facilitating the recording of particularly task-related neurons for more than one session.

Neural Data Analysis

To decide whether a given cell should be treated as the same one recorded in a previous session, we compared each pair of potentially identical cells based on the waveforms and their firing pattern. Cells were considered identical when

1) The Pearson's *r* of the cells' normalised waveforms is equal to or above 0.9,
2) the electrode was not moved between the sessions,
3) the experimenter concluded that their firing pattern during different trial types were not visibly different between sessions.

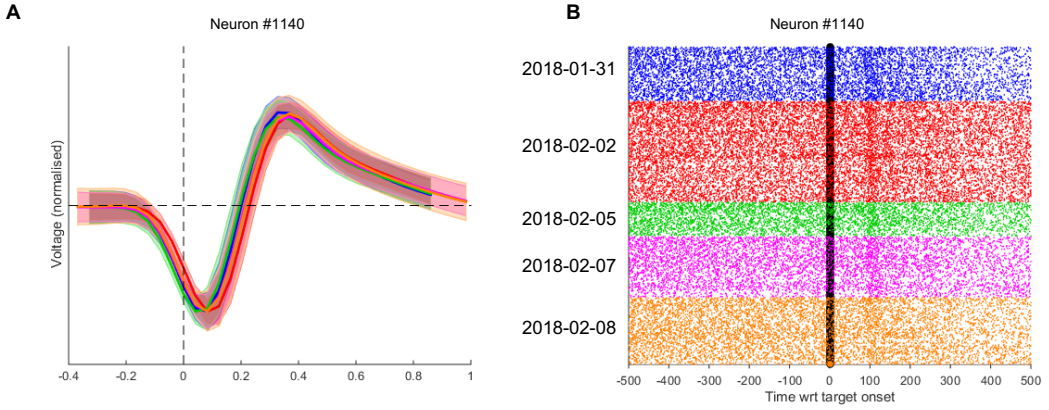

Figure 7. Example neuron recorded over 5 sessions

(A) Normalised waveforms of neuron #1140 showing high overlap of pre-trough, trough, peak and post-peak shapes. Solid line and shading indicate the mean and 95% confidence interval in a given session, each shown in a different color. **(B)** Raster of spiking activity aligned to target onset (black vertical line). The characteristic increase in the firing rate at 100 ms after target onset is visible in all 5 sessions.

Each cell's firing rate was represented as a partial spike interval calculated based on the sum of fractional inter-spike intervals contained during each of the 10 ms time bins (Sergio et al., 2005; Taira et al., 1996).

Population analyses

Distributions of decision latency

To compare the speed with which decisions emerge across the cortical regions we recorded, we performed an analysis of the latency distribution across the different populations. Because this relies primarily on early events, we applied additional criteria for focusing on just the fastest neurons. Thus, for a cell to be included in the population latency analysis, the following criteria needed to be met:

1) During 1T trials, its mean firing rate for left versus right choice became more than 5 standard deviations (SD) apart and remained a minimum difference of 2SD apart for 50 ms within 250 ms from target onset (modified criterion from (T. R. Sato & Schall, 2003)),

2) The neuron's directional preference (e.g., higher firing rate for right than left target) was the same in both TWIN and 1T trials.

This resulted in 292 PMd cells and 71 PRR cells to be included in the population analysis. To account for the difference in the number of cells included from each region, we bootstrapped over individual cells to obtain a resampled population of 100,000 cells, with replacement, per region.

The mean firing rate was calculated using a 10 ms sliding window with a step size of 5 ms. Each area's population average was obtained by first calculating an individual neuron's average firing rate across the session(s) in which it was recorded, before averaging these across the population.

Pre-stimulus baseline bias

A neuron or a group of neurons are considered to display a pre-stimulus baseline bias when the baseline firing rate was predicting the monkey's choice prior to the target onset. The Wilcoxon rank sum test was used to detect the difference in the mean firing rate between preferred target (PT) and opposite target (OT) trials during the 300 ms pre-stimulus time period (Coe et al., 2002).

Neural space analyses

To investigate the dynamical nature of the entire population of neurons, we applied a dimensionality reduction on a hyperspace constructed by each neuron's firing rate (Cunningham & Yu, 2014; Thura et al., 2022). For this analysis, regardless of their response properties, all well-isolated neurons recorded during the delay version of the Dual Feature task were included, which consisted of 776 PMd and 487 PRR neurons. First, each neuron's spiking activity was aligned to the target onset and firing rate was computed using partial spike intervals in 10 ms bins, between 200 ms before and 500 ms after target onset. Second, the firing rate was square root transformed and temporally smoothed using a 10 ms Gaussian kernel. Third, we forced symmetry on the data by creating a population of "anti-neurons", duplicating the original population and inverting the directional tuning of each neuron. This was based on an assumption that for every left-preferring neuron we recorded, there exists a right-preferring neuron with similar properties which we did not record, and vice-versa (Thura et al., 2022). We repeated this procedure to build, for each of 12 conditions of interest (1T, Easy-BU, Easy-TD, Twin, ConS-BU, and ConS-TD, for the leftward and the rightward choices), a 2678-by-51 matrix whose rows consisted of individual neurons (776×2 neurons representing the PMd population and 487×2 neurons representing the PRR population with a forced directional symmetry) and columns consisted of time bins (10 ms bins, 100 ms before to 400 ms after target onset). These matrices were horizontally concatenated to

build a 2678×204 matrix, and the *pca* function (MATLAB 2014b) was applied. This yielded a matrix of loading coefficients between the neurons and principal components (PCs) and the variance explained by each PC.

Microstimulation

In a subset of sessions, electrical microstimulation was performed on one of the electrodes with audible, visible or isolatable neural activity. The stimulation train consisted of 19 biphasic square pulses with 0.2 ms per phase, rising edge first (Figure 8). Each set of pulse was 0.4 ms during the 3.0 ms total duration and delivered at 333 Hz, 70 μA in amplitude. The pulses were configured with 50% temporal jitter, thus half of the pulses were delivered with a randomized timepoint within the 3.0 ms bound. This resulted in a total stimulation train duration of 57 ms. The stimulations were delivered in 50% of trials, either 100 ms or 150 ms after the target onset, detected online based on the photocell signal. Trials without stimulation on the same day were used as a control. We collected a minimum of 2000 trials per stimulation site, which took typically 3 to 4 sessions. During the microstimulation session, the monkey was allowed to report his decision as soon as the reach targets were presented (i.e., there was no instructed delay period). We analyzed the effects of stimulation by comparing the RTs of stimulation and control trials within the same trial conditions. In most cases, microstimulated electrodes continued to have a similar, recognizable neural activity and the impedance remained unaffected.

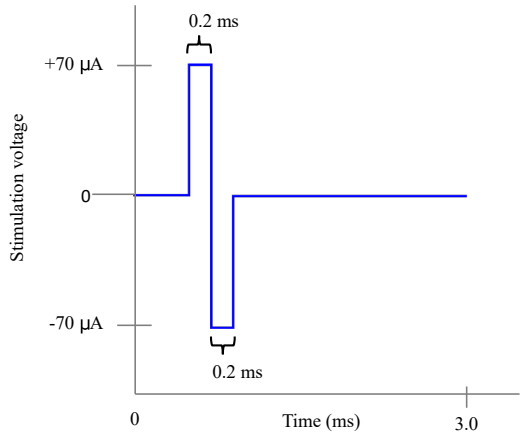

Figure 8. Microstimulation schematic

A train consisted of 19 of this biphasic stimulation, jittered at 50%.

RESULTS – BEHAVIOUR

Monkey RT varied with trial types, but the difference disappeared over time

To visualise whether Monkey Y completed different trial conditions with different reaction times, we plotted the cumulative histogram of his RT. Figure 9 shows the first two days when Y was presented with Conflict trials during the Dual Feature Task without the instructed delay. On the first day (Figure 9A), his RT for ConM-BU (median RT: 391 ms) was faster than all the other conditions (p<0.03 across all comparisons). The longest RT was for ConM-TD (median RT: 431 ms). The rest of the trials had similar RTs (Easy-BU: 415 ms, Easy-TD: 410 ms, Twin: 426 ms, p>0.05 across all comparisons). On the second day, most of these RT differences disappeared as the RT distributions collapsed (Figure 9B). ConM-BU was no longer the fastest (median RT: 434 ms). Most trial types slowed down (Easy-BU: 431 ms, Easy-TD: 435 ms,

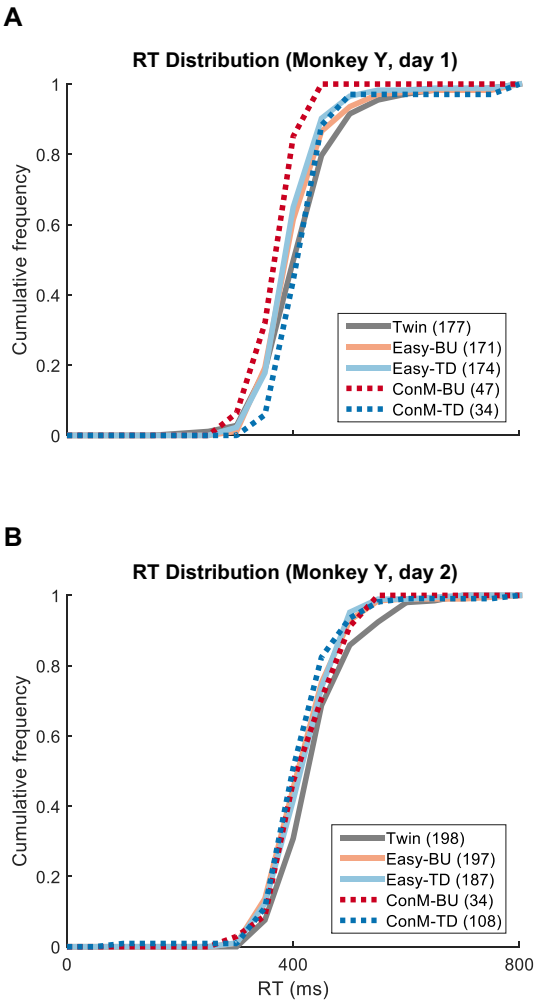

Figure 9. Cumulative histograms of RT distribution of Monkey Y

(A) RT distribution of the first day Y was presented with Conflict trials. ConM-BU is faster than the rest. **(B)** Same plot of the second day after Y was presented with Conflict trials. RTs slowed down in general and most of the differences disappeared. Different colours represent different trial types. The numbers in the parentheses indicate the number of trials per trial type.

Twin: 450 ms), except ConM-TD (median RT: 425 ms), which remained relatively the same as on day 1. Twin trials were slower than most other trial types except for ConM-BU (p<0.03 across comparisons). This trend of Twin trials being slower than other types continued for 6 sessions, and disappeared on the 7th session when all RTs collapsed and the median RT was 437 ms. The analysis of Monkey K's behavioural data during the RT version of the task is currently underway.

When there was a variable delay between the target onset and the GO signal, both monkeys' RT distributions collapsed and there was no difference between trial types.

Monkey RT was similar to human RT

To compare the RT distributions between human participants and Monkey Y, we generated a scatter plot of mean RT in different trial types. In Figure 10, gray circles represent the RT of human participants from Chapter 3 and the red square indicates the RT of Monkey Y on the first day when he was presented with Conflict trials. Monkey Y's RT was shorter than most human subjects, but still fell

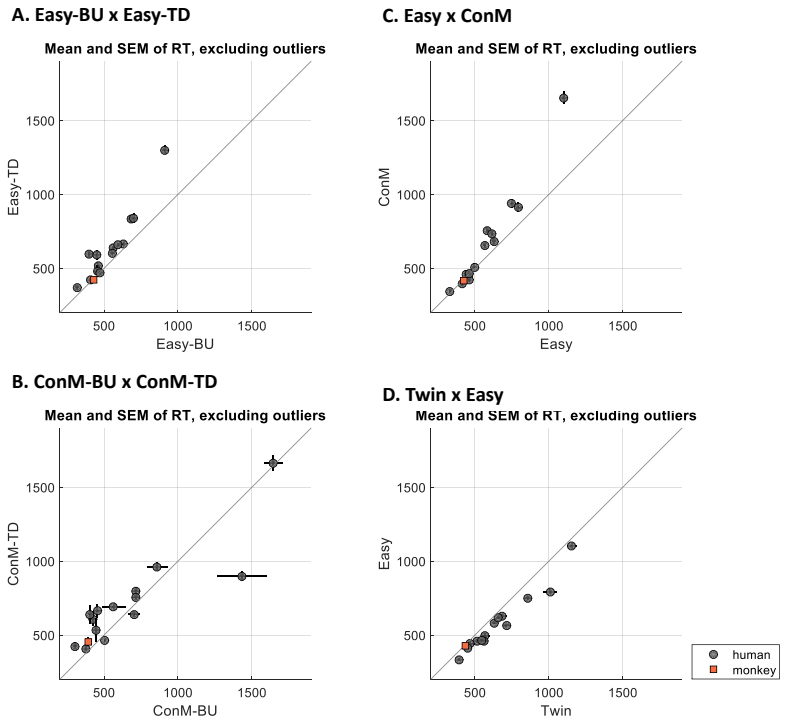

Figure 10. Scatter plot of mean RT across trial conditions, primates

Gray circles represent the mean RT of human participants, and orange squares represent mean RT of Monkey Y on the first day when he was presented with Conflict trials.

within the cluster of distributions in all trial types compared.

RESULTS – ELECTROPHYSIOLOGY

Recorded Neurons

We recorded neural activity of a total of 1207 PMd and 871 PRR neurons from Monkey Y, and so far from 157 PMd and 54 PRR neurons from Monkey K. Table 1 shows the overview of neurons recorded from two monkeys. In Monkey Y, directional tuning was observed in 65% (*N*=780) of PMd and 50% (*N*=438) of PRR neurons during the delay period. Of these, 28% (*N*=332) of PMd and 17% (*N*=148) of PRR neurons were tuned within 250 ms from target onset during Twin trials. In Monkey K, tuning was observed in 60% (*N*=94) of PMd and 74% (*N*=40) of PRR neurons. Of these, 7% (*N*=11) of PMd neurons were tuned within 250 ms during Twin trials. We have not yet recorded PRR cells with early tuning. We also recorded other frontal areas in Monkey K; 39% (*N*=135) of dACC, 34% (*N*=25) of dlPFC (area 46/9) and 50% (*N*=16) of dmPFC (area 8B) neurons displayed directional tuning during the delay period. Of these, 7% (*N*=23) of dACC and 3% (*N*=2) of dlPFC neurons were tuned within 250 ms during Twin trials. Note that because recordings and analysis of data from Monkey K is still ongoing, this thesis primarily reports neural results from Monkey Y.

Area	Category	Monkey Y		Monkey K	
	All neurons	2182		1010	
PMd	All PMd	1207		157	
	Tuned pre-GO	780	65%	94	60%
	Tuned within 500 ms in Twin	458	38%	13	8%
	Tuned within 250 ms in Twin	332	28%	11	7%
	Met population latency analysis criteria	292	24%	7	4%
PRR	All PRR	871		54	
	Tuned pre-GO	438	50%	40	74%
	Tuned within 500 ms in Twin	222	25%	0	0%
	Tuned within 250 ms in Twin	148	17%	0	0%
	Met population latency analysis criteria	71	8%	0	0%
LIP	All LIP	97		109	
	Tuned pre-GO	70	72%	73	67%
	Tuned within 500 ms in Twin	31	32%	3	3%
	Tuned within 250 ms in Twin	22	23%	0	0%
dACC	All dACC	-		350	
	Tuned pre-GO	-		135	39%
	Tuned within 500 ms in Twin	-		33	9%
	Tuned within 250 ms in Twin	-		23	7%
dlPFC	All dlPFC	-		73	
	Tuned pre-GO	-		25	34%
	Tuned within 500 ms in Twin	-		6	8%
	Tuned within 250 ms in Twin	-		2	3%
dmPFC	All dmPFC	-		32	
	Tuned pre-GO	-		16	50%
	Tuned within 500 ms in Twin	-		0	0%
	Tuned within 250 ms in Twin	-		0	0%

Table 1. Number of recorded neurons from each brain region.

A cell was considered tuned when its mean firing rate difference between left and right target choice became 5SD apart and remained at least 2SD apart for a minimum of 15 ms. Cells not clearly assignable to a given region are not included except in the grand total.

Example neuron from PMd

Figure 11 shows a histogram of the mean firing rate and a raster of an example neuron from PMd, aligned to the target onset and movement onset during 1T trials. This neuron's firing rate increased shortly after a target appeared on the left of the center circle (dark line). We describe these trials as having the neurons' preferred target (PT). The same neuron's firing rate decreased when a target appeared on the right of the center circle (broken gray line). These trials are labelled as having the opposite target (OT). This divergence of firing rate for PT vs OT was interpreted as the time in which the neuron discriminated the location of the target, and thus predicted the monkey's decision to reach to the left or the right. In order to determine the time the neuron predicted the monkey's reach direction, we looked for the first moment when the difference in the firing rates exceeded 5 standard deviations of the baseline period (300 to 0 ms prior to the stimulus onset) and remained 2SD apart for a minimum of 50 ms (T. R. Sato & Schall, 2003). During 1T trials, this neuron predicted the monkey's choice 80 ms after target onset. The separation in the firing rate for PT and OT trials persisted during the delay period. Towards the movement onset, the firing rate for PT decreased while that for OT gradually

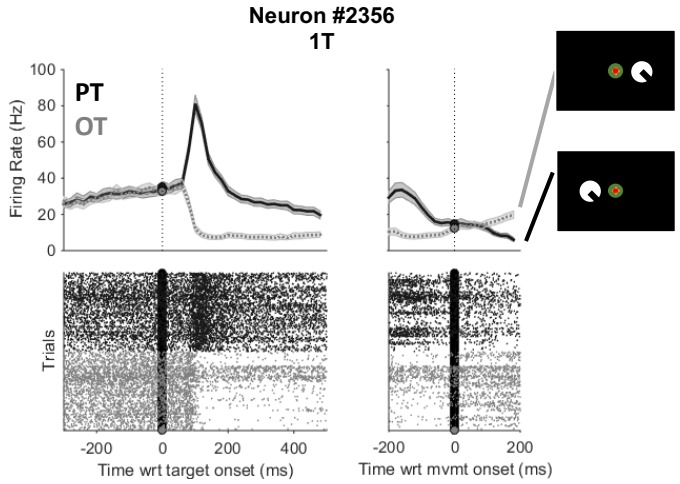

Figure 11. Example neuron during 1T trials

Peristimulus firing rate histogram with 20 ms sliding window and raster plot of an example PMd cell during single target (1T) trials. Dark lines represent the cell's response to its preferred target (PT), whereas the broken gray lines represent the cells' response to the non-preferred, opposite target (OT). Shaded area indicates 95% confidence interval.

increased, and their order was reversed following the movement onset. Although this neuron exhibited significant variability in its background firing rate in different recording sessions, its tuning and peak burst were consistent from day to day.

Figure 12 shows the same neuron's response during Easy-BU, Easy-TD and Easy-Both trials. In these trials, the time at which the neuron predicts the monkey's choice can differ from the initial response to target appearance. During Easy-BU trials, this neuron predicted the monkey's choice 90 ms after target onset. During Easy-TD trials, it predicted the monkey's choice 95 ms after target onset. During Easy-Both trials, it predicted the monkey's choice 90 ms after target onset. Similar to the 1T trials (Figure 11), the difference in the firing rates between PT and OT trials remained throughout the delay period and into the movement onset. In addition, there was a subtle increase at around 80 ms in both PT and

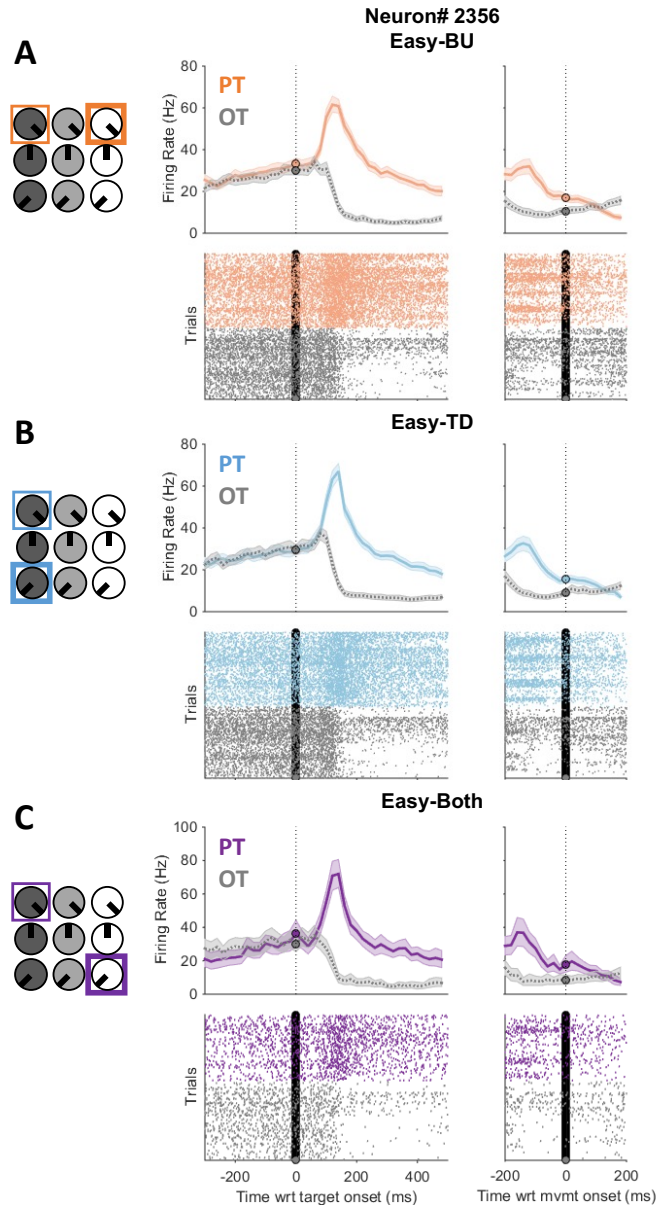

Figure 12. Example neuron during Easy trials

The same cell as Figure 11, during Easy trials. **(A)** Easy-BU, **(B)** Easy-TD, and **(C)** Easy-Both trials, with an example combination highlighted on the 3x3 target chart on the left. Colour and broken gray lines represent its response to PT and OT, respectively.

OT trials, which is the time this neuron discriminated PT and OT in 1T trials. This suggests that the neuron initially responded to the onset of two targets, which was followed by the decision based on the BU and/or TD features.

Figure 13A shows the same neuron's response during Twin trials. During Twin trials, this neuron's average firing rate was higher for PT than OT trials even *before* the target onset. This pre-stimulus baseline bias was not unique to this neuron. For this reason, we took the difference in the baseline firing rate into account when deciding on the latency of choice-related neural activity. By subtracting the difference between PT and OT trials during the pre-stimulus baseline period, we can see the neuron's response to the stimulus onset (Figure 13B). Based on this baseline subtraction procedure, during Twin trials, this neuron predicted the monkey's choice 100 ms after target onset (Figure 13B, dotted pink line).

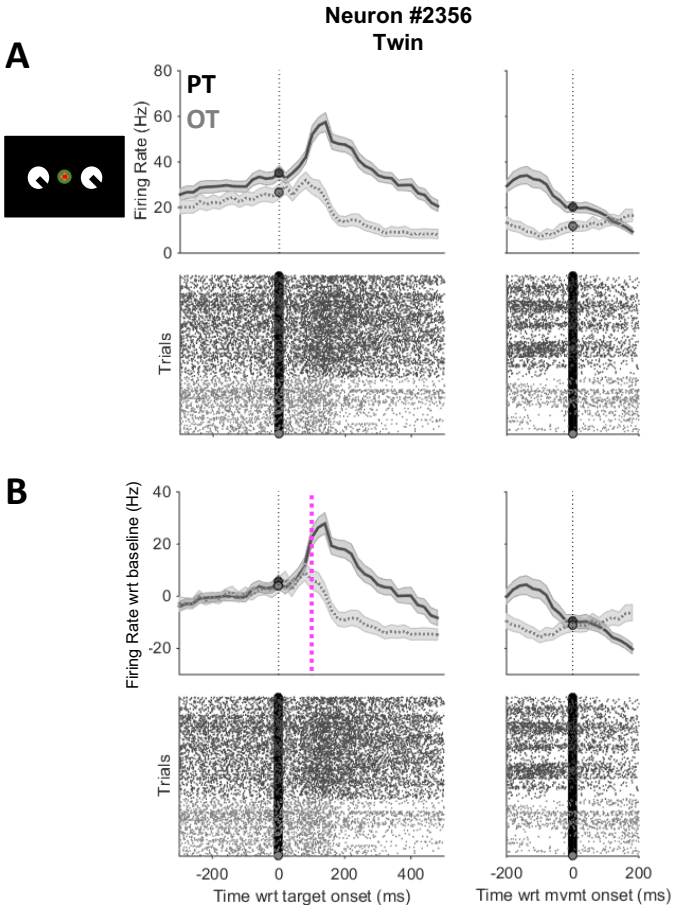

Figure 13. Example neuron during Twin trials

The same cell as Figure 11 during Twin trials. **(A)** Raw firing rate. **(B)** Firing rate adjusted by subtracting the mean during the baseline period (300 ms prior to target onset). Solid dark and broken gray lines represent its response to PT and OT, respectively. Dotted pink like indicates the choice latency.

Figure 14 shows the same neuron's response during two types of equivalued Conflict trials, ConS and ConM. Similar to the Twin trials (Figure 13), there was a separation in the baseline firing rate between the PT and OT trials, especially in ConS-BU (Figure 14A, PT trials had 10.25Hz higher baseline firing rate compared to OT trials). After subtracting the baseline mean, according to our choice latency criteria, this neuron's choice latency was 100 ms for ConS-BU (Figure 14A). For ConS-TD trials, our criteria initially detected the reversal in PT and OT firing rate at 120 ms after target onset (Figure 14B). For ConM-BU trials, the difference between PT and OT did not meet our choice criteria for the 500 ms time window we tested (Figure 14C). For ConM-TD trials, the choice latency was 125 ms (Figure 14D).

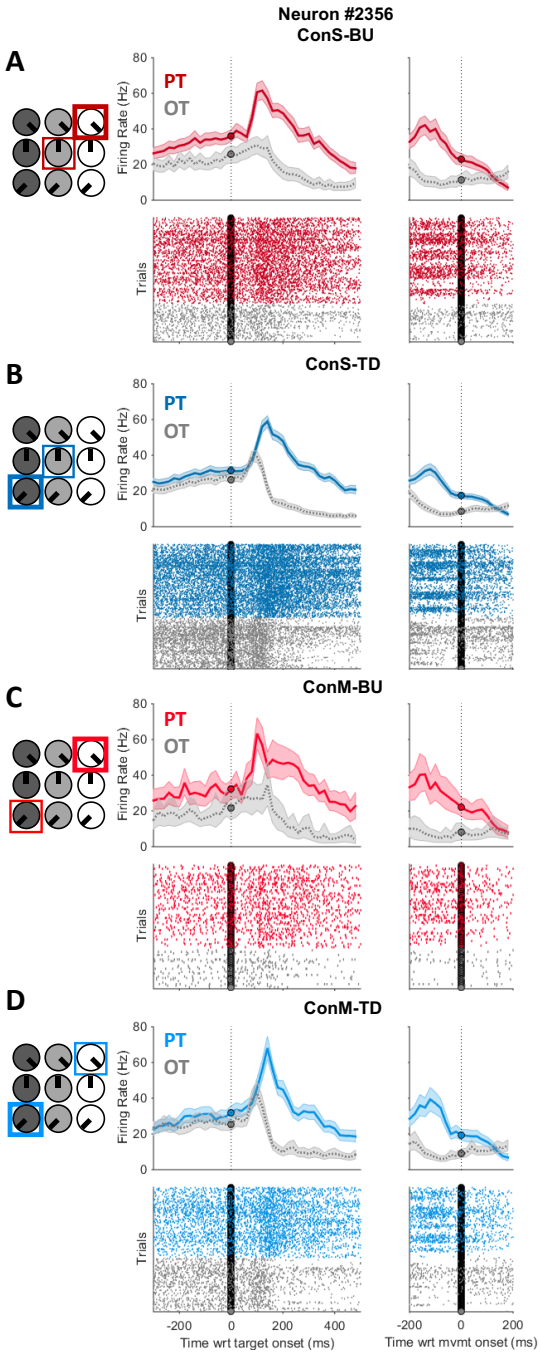

Figure 14. Example neuron during Conflict trials

The same cell as Figure 11 during **(A)** ConS-BU, **(B)** ConS-TD, **(C)** ConM-BU, and **(D)** ConM-TD trials. Solid colour and broken gray lines represent its response to PT and OT, respectively. An example combination of target appearances is highlighted on the 3x3 target chart on the left of each plot. The chosen target is highlighted with a thicker line.

One possible interpretation of the pre-stimulus baseline bias is that prior to the target onset, the monkey was already biased toward moving right or left, and this neuron's firing rate was already modulated by that bias. Such a bias will not be observed in 1T and Easy trials because these conditions come with a "correct" option that can appear on the left or the right with equal probability, averaging out any pre-stimulus activity for PT and OT trials. It was only revealed during the free choice conditions, such as Twin and equivalued Conflict trials, in which there is no "correct" option and the monkey could let the baseline bias drive his decision to choose the target he was predisposed to choose. In other words, this pre-stimulus baseline bias in PMd may reflect the underlying cause for when one "feels like" doing something without an externally motivated reason.

Population Latency Analysis

To investigate the choice latency at the population level, we focused on neurons that met the inclusion criteria described in the Neural Data Analysis section. In brief, we analysed only those cells that displayed the choice-related activity within 250 ms from target onset in 1T trials. This resulted in 24% of PMd (N=292) and 8% (N=71) of PRR neurons to be included in the population latency analysis. To determine the choice latency, we applied the same latency detection algorithm we used for individual cells. Thus, each population activity was divided based on the trial conditions (e.g., 1T, Easy-BU etc.) and the monkey's choice (PT and OT) trials. Choice latency was calculated by subtracting the mean baseline firing rate of each trial condition to remove the pre-stimulus baseline bias.

PMd Population Activity

Figure 15 shows the PMd population's average firing rate during 1T, Easy-BU, Easy-TD, and Easy-Both trials, aligned to the target and movement onset. During 1T trials, PMd population activity sharply increased for PT while it decreased below baseline for OT after target onset, predicting monkey's choice at 60 ms (Figure 15A). The peak for PT appeared to occur at around the same time as the drop to the lowest point for OT trials. During Easy-BU trials, it predicted the monkey's choice 60 ms after target onset (Figure 15B). During Easy-TD trials, the PMd population predicted the monkey's choice 80 ms after target onset (Figure 15C). During Easy-Both trials, the PMd population predicted the monkey's choice 60 ms after target onset (Figure 15D). In all of these conditions, the PMd population maintained its firing rate higher for PT and below baseline for OT trials during the

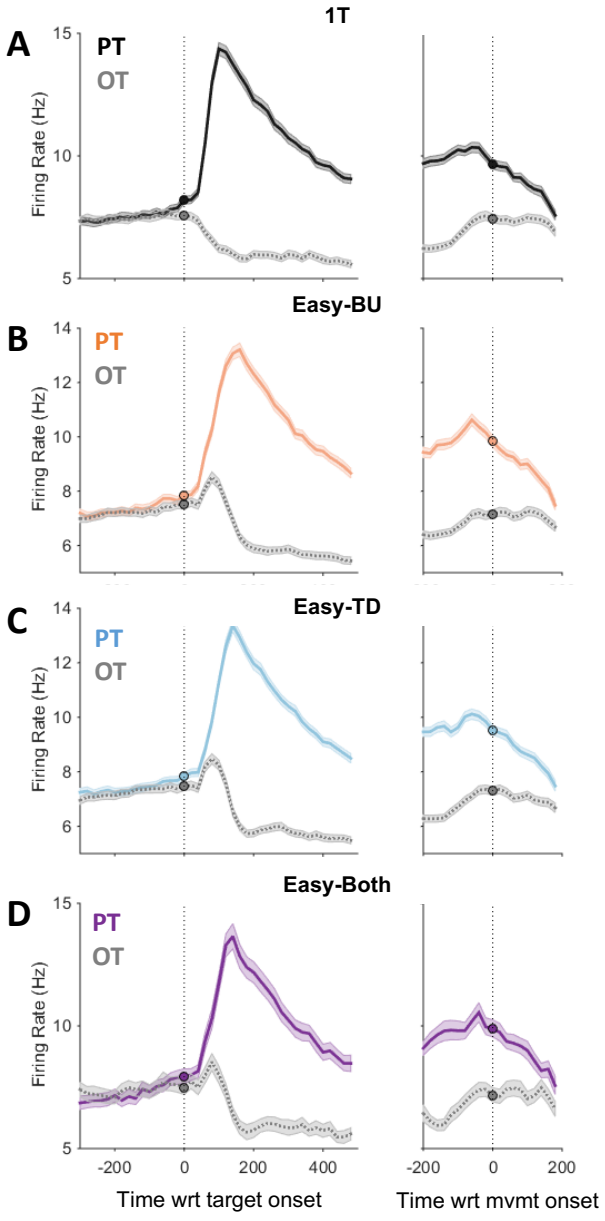

Figure 15. PMd population activity during 1T and Easy trials

Average firing rate of 292 PMd cells during **(A)** 1T, **(B)** Easy-BU, **(C)** Easy-TD, and **(D)** Easy-Both trials, aligned to target onset (left column) and movement onset (right column). Darker colour lines indicate trials in which the monkey chose the cell's preferred target (PT), and gray lines indicate trials in which the monkey chose the opposite target (OT).

delay period and past the onset of movement. The firing rate for PT had an additional peak just before the movement onset, which was followed by a slow decrease as the movement was executed. This may imply that the PMd population was maintaining the action plan during the delay period, and upon the GO signal, executed the movement via the downstream motor areas and let go of the plan.

Figure 16 shows the average activity of the same PMd population during Twin, ConS and ConM trials, aligned to the target onset and movement onset. During Twin trials, the PMd population predicted the monkey's choice 100 ms after target onset (Figure 16A). Note that as mentioned above, this calculation was performed after subtracting the baseline bias. During ConS trials, when the monkey chose the target favoured by the BU feature (ConS-BU), the PMd population predicted the monkey's

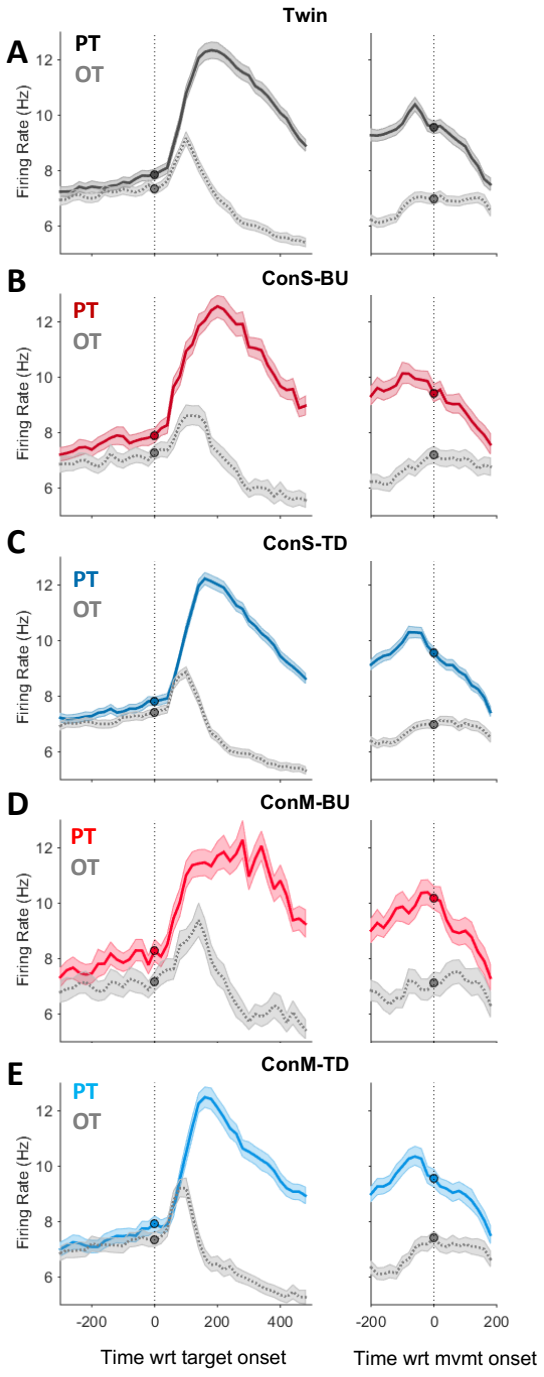

Figure 16. PMd population activity during Twin, ConS and ConM trials

Same population as Figure 15 during **(A)** Twin, **(B)** ConS-BU, **(C)** ConS-TD, **(D)** ConM-BU, and **(E)** ConM-TD trials, aligned to target onset (left column) and movement onset (right column).

choice 90 ms after target onset (Figure 16B). When the monkey chose the target favoured by the TD feature (ConS-TD) it predicted the monkey's choice 100 ms after target onset (Figure 16C). During ConM-BU trials, PMd predicted the monkey's choice 105 ms after target onset (Figure 16D). During ConM-TD trials, PMd predicted the monkey's choice 110 ms after target onset (Figure 16E).

During Twin, ConS and ConM trials, PMd activity separated for PT and OT *prior* to the target onset, reflecting the monkey's choice. This presence of the pre-stimulus baseline bias in PMd population suggests that, when a situation allows, random pre-stimulus fluctuation in PMd activity may play a causal role in making the monkey decide to choose a cell's preferred target.

During 1T and potentially Easy-TD trials (Figure 15A and C), the divergence of PT versus OT was observed at the moment of the target onset (i.e., t=0), which precedes the fastest stimulus onset responses and thus cannot be caused by the stimulus (Ledberg et al., 2007). This is likely an artefact due to our selection criteria, which strongly favour cells with early responses during 1T trials, increasing the likelihood of

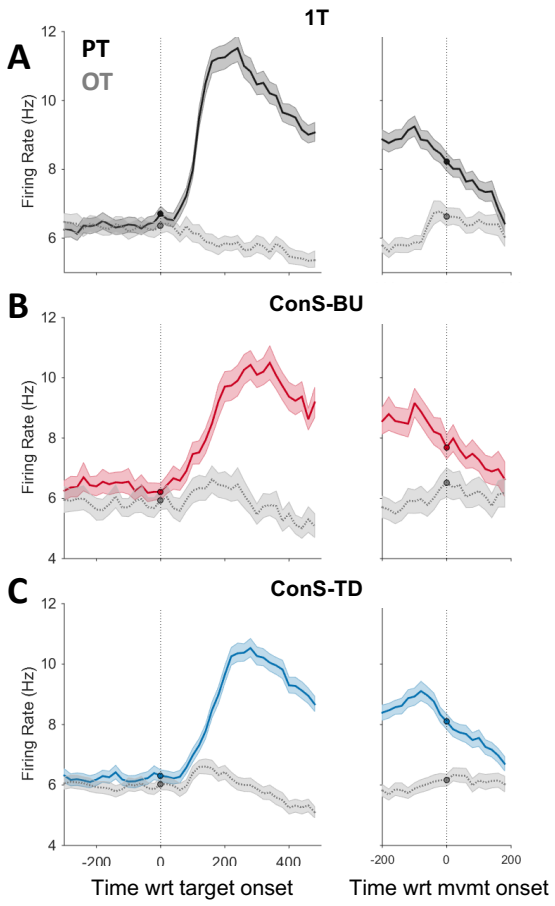

Figure 17. Activity of PMd Population without early cells during 1T and ConS trials

Average firing rate of 152 PMd cells tuned between 100-250 ms from target onset during **(A)** 1T, **(B)** ConS-BU, and **(C)** ConS-TD trials, aligned to target (left column) and movement onset (right column). Same colour coding as Figure 15 and Figure 16.

including cells whose pre-stimulus firing pattern *happen* to correlate with the target of choice. When the earliest cells (response within 100 ms from the target onset) were excluded from the population, the separation at time zero during 1T (Figure 17A) and Easy (data not shown) trials was not observed. Notably, in this subset of cells, the pre-stimulus baseline bias in Conflict trials was reduced but still present (Figure 17B-C).

PRR Population Activity

Figure 18 shows the average firing rate of the PRR population during 1T, Easy-BU, Easy-TD, and Easy-Both trials, aligned to the target and movement onset. During 1T trials, PRR population activity sharply increased for PT, whereas it remained around the baseline level for OT, predicting the monkey's reach direction 80 ms after the target appeared (Figure 18A). This was as fast as the PMd population. During Easy-BU trials, PRR population activity predicted the monkey's choice 100 ms after target onset (Figure 18B). During Easy-TD trials, PRR predicted the monkey's choice 75 ms after target onset (Figure 18C). During Easy-Both trials, PRR predicted the

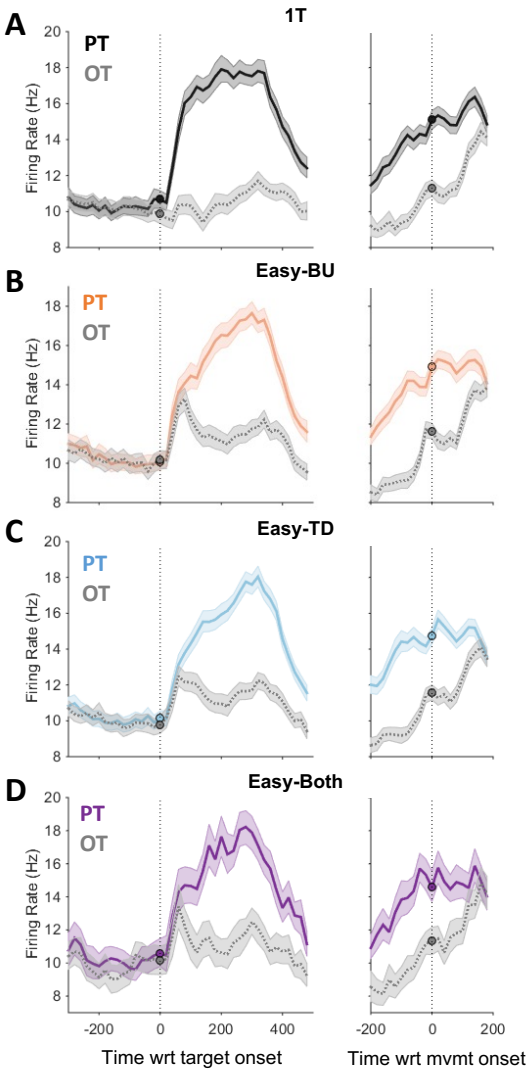

Figure 18. PRR Population activity during 1T, Easy-BU, Easy-TD and Twin trials

Average firing rate of 71 PRR cells during **(A)** 1T, **(B)** Easy-BU, **(C)** Easy-TD, and **(D)** Easy-Both trials, aligned to target (left column) and movement onset (right column). Same colour coding as Figure 15.

monkey's choice 115 ms after target onset (Figure 18D). When two targets were presented, PRR activity briefly increased for both PT and OT until 80 ms, followed a further increase for PT, leading to a divergence. Compared to PMd, whose firing rate during OT trials sharply decreased below its baseline, PRR activity for OT lingered around the same level as the initial increase, slightly dipping but never going below the baseline. During 1T, Easy-BU, Easy-TD and Easy-Both trials, PRR activity for OT displayed a secondary increase in the firing rate at around 300 ms, which appear to coincide with the peak for PT, followed by a decrease in the firing rate. In all these four conditions, PRR population activity displayed a pre-movement ramp-up which appeared to peak past the movement onset, after which the activity for OT caught up with PT and converged, approximately 200 ms after movement onset.

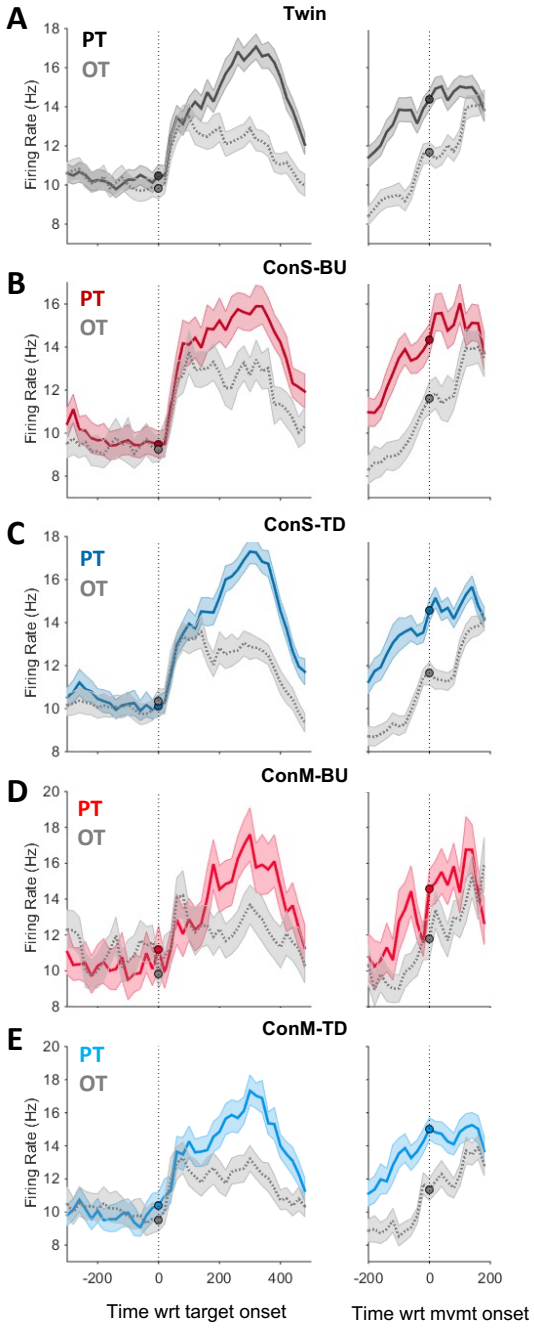

Figure 19. PRR Population activity during Twin, ConS and ConM trials

Same population as Figure 18 during **(A)** Twin, **(B)** ConS-BU, **(C)** ConS-TD, **(D)** ConM-BU, and **(E)** ConM-TD trials, aligned to target onset (left column) and movement onset (right column). Same colour coding as Figure 16.

Figure 19 shows the average activity of the same PRR population during Twin, ConS and ConM trials, aligned to the target onset and movement onset. During Twin trials, the PRR population predicted the monkey's choice 160 ms after target onset (Figure 19A). During ConS-BU, the PRR population predicted the monkey's choice 195 ms after target onset (Figure 19B). During ConS-TD trials, PRR predicted the monkey's choice 150 ms after target onset (Figure 19C). During ConM-BU trials, PRR predicted the monkey's choice 235 ms after target onset (Figure 19D). During ConM-TD trials, PRR predicted the monkey's choice 105 ms after target onset (Figure 19E). In all Twin and equivalued Conflict trials, the baseline firing rate for PT and OT overlapped. That is, unlike PMd, PRR activity did not display a pre-stimulus baseline bias. While the absence of evidence is not the evidence of absence, the apparent predictive activity in PMd in contrast to PRR suggests the possibility that the fluctuation of PMd activity has a more causal role in the monkey's choice than that of PRR activity.

The tuning latency of the PMd and PRR populations are summarised in Table 2. When one target was better than the other and the features were congruent (i.e., "easy" conditions), PMd predicted the monkey's choice in 60-80 ms. In the same situations, PRR predicted the monkey's choice in 75-115 ms, and the difference was particularly large during Easy-BU and Easy-Both trials. When

Condition	PMd	PRR
1T	60 ms	80 ms
Easy-BU	60 ms	100 ms
Easy-TD	80 ms	75 ms
Easy-Both	60 ms	115 ms
Mean "easy"	*65 ms*	*92.5 ms*

Condition	PMd	PRR
Twin	100 ms	160 ms
ConS-BU	90 ms	195 ms
ConS-TD	100 ms	150 ms
ConM-BU	105 ms	235 ms
ConM-TD	110 ms	105 ms
Mean equal value	*101 ms*	*169 ms*

Table 2. Summary of Population Tuning Latency

Tuning latencies of the PMd and PRR populations for different conditions and the mean of "easy" and equal value groups in millisecond.

the target values were equal and features were incongruent, PMd predicted the monkey's choice in approximately 100 ms, whereas PRR predicted the choice in 105-235 ms.

Frequency of Pre-stimulus Baseline Bias

Were PMd cells more likely to show the pre-stimulus baseline bias than PRR cells? To quantify the frequency of cells with the pre-stimulus baseline bias, we compared the difference in the baseline firing rate between PT and OT during a 300 ms pre-stimulus window of equivalued trials. Neurons were considered to show the bias at $p<0.05$ (Wilcoxon rank sum test). According to this criterion, in the PMd population, 23% of cells (280/1207) had the bias, and in the PRR population, 11% (99/871) had the bias. These frequencies were comparable to those reported in other studies in the analogous areas for eye movements; for example, Coe and colleagues reported that 49.1% (27/55) of SEF, 22.5% (25/111) of FEF, and 31.3% (10/32) of LIP neurons displayed a pre-stimulus anticipatory bias in a saccade task with variable reward rate (Coe et al., 2002).

PMd choice latency varied across trial conditions, whereas PRR did not.

Figure 20 shows the cumulative histogram of choice latency of PMd and PRR neurons that appeared within 500 ms from target onset when all trial types are considered. In the PMd population (N=529), the distribution of choice latency varied across conditions. 1T trials had the shortest latency, with more than 50% of the population reflecting the monkey's choice 120 ms after target onset. This was followed by Easy-TD at 140 ms, Easy-BU and Easy-Both at 150 ms, ConS-TD and ConM-TD at 170 ms, Twin at 180 ms, and ConS-BU at 190 ms finally ConM-BU trials at 200 ms after target onset. 1T trials were significantly different from all other trials (Wilcoxon rank sum test, 1T vs Easy-TD at $p=2.6\text{x}10^{-5}$, vs Easy-BU at $p=7.4\text{x}10^{-5}$, vs Easy-Both at $p=2.3\text{x}10^{-5}$, vs ConS-TD at $p=1.2\text{x}10^{-12}$, vs ConM-TD at $p=5.2\text{x}10^{-12}$, vs Twin at p=1.7x10-13, vs ConS-BU at $p=1.9\text{x}10^{-13}$, vs ConM-BU at $p=3.4\text{x}10^{-7}$). Decision latencies in Easy-BU, Easy-

TD and Easy-Both trials were not significantly different from each other (p>0.05), but they were faster than all equivalued conditions (Twin, ConS-BU, ConS-TD, ConM-BU, and ConM-TD, all at p<0.01, p<0.01, and p=0.01, respectively). ConS-BU, ConS-TD, ConM-BU, ConM-TD and Twin trials were not significantly different from each other (p>0.05). In the PRR population (N=194), 1T trials were significantly faster than Easy-TD, ConS-BU and Twin trials (1T vs Easy-TD at p=4.2x10^{-3}, vs ConS-BU at p=0.01, vs Twin at p=5.0x10^{-5}). Easy-Both, ConM-TD, Easy-BU and ConS-TD were faster than Twin trials (Twin vs Easy-Both at p=4.1x10^{-3}, vs ConM-TD at p=1.9x10^{-2}, vs Easy-BU at p=2.6x10^{-2}, vs ConS-TD at p=3.5x10^{-2}). The 1T, Easy-Both, ConM-TD, Easy-BU, ConS-TD, and ConM-BU were not significantly different from each other (p>0.05). Easy-TD, ConS-BU and Twin were not different from each other (p>0.05).

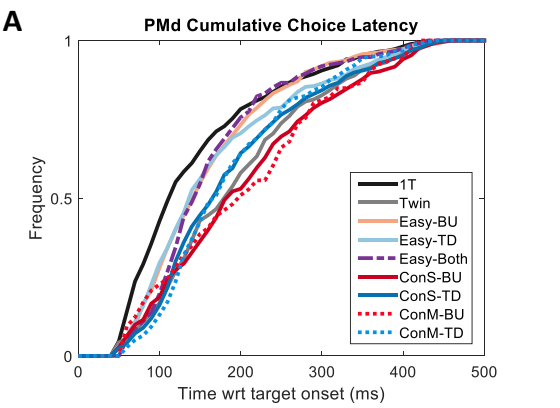

Condition	>50% predictive (ms)
1T	120
Easy-TD	140
Easy-BU	150
Easy-Both	150
ConS-TD	170
ConM-TD	170
Twin	180
ConS-BU	190
ConM-BU	200

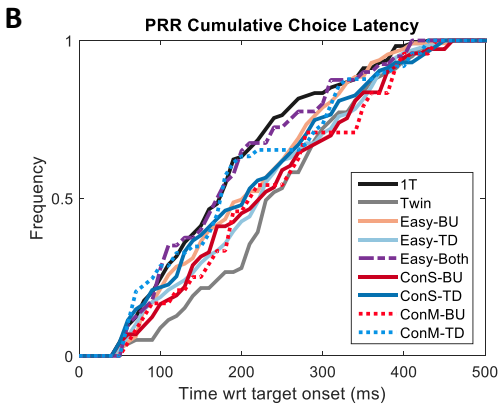

Condition	>50% predictive (ms)
1T	180
Easy-Both	180
ConM-TD	180
Easy-BU	210
ConS-TD	210
ConM-BU	220
Easy-TD	230
ConS-BU	230
Twin	240

Figure 20. Cumulative Choice Latency

Cumulative histogram of choice latency for **(A)** PMd (N=529) and **(B)** PRR population (N=194). Conditions are depicted with the same colour coding as Figure 15. Asterisks indicate statistical significance at p<0.05.

PMd was faster than PRR at predicting the monkey's choice

Figure 21 is the same data as Figure 20, separated by conditions to better visualise the comparison between PMd (lines with triangles) and PRR (lines with dots). The PMd population was faster than PRR at predicting the monkey's choice during 1T, Easy-BU, Easy-TD and Twin trials (Wilcoxon rank sum test, 1T at $p=5.5\times10^{-5}$, Easy-BU at 3.7×10^{-5}, Easy-TD at $p=9.5\times10^{-7}$ and Twin at p=8.9x10-5). There was no difference between PMd and PRR in Easy-Both, ConS-BU, ConS-TD, ConM-BU and ConM-TD trials ($p>0.05$). In most of the conditions, at the time when 50% of PMd population predicted the monkey's choice, less than 45% of PRR population did so (1T: 32%, Easy-BU: 36%,

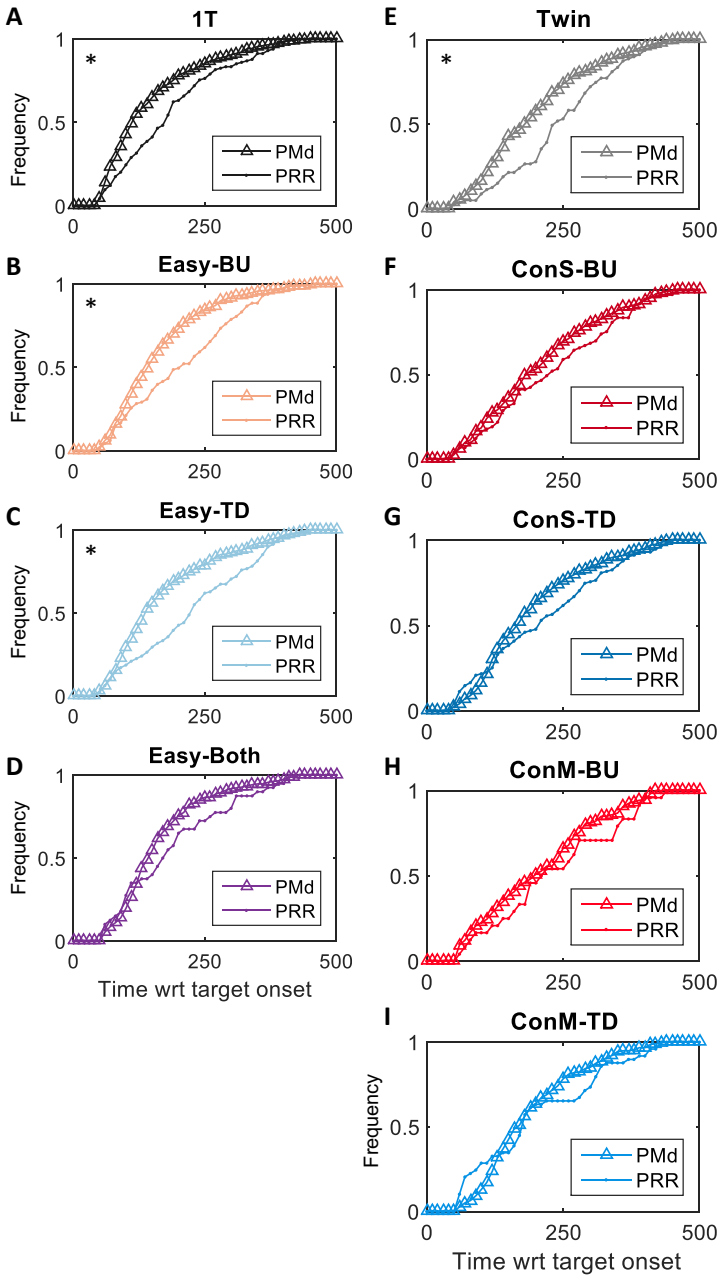

Figure 21. Cumulative Choice Latency by conditions

Cumulative histogram of choice latency of **(A)** 1T, **(B)** Easy-BU, **(C)** Easy-TD, **(D)** Easy-Both, **(E)** Twin, **(F)** ConS-BU, **(G)** ConS-TD, **(H)** ConM-BU, and **(I)** ConM-TD trials. Lines with triangles and dots represent PMd and PRR populations, respectively. Asterisks indicate statistical significance at $p<0.05$.

Easy-TD: 26%, Easy-Both: 40%, Twin: 27%, ConS-BU: 43%, ConS-TD: 43%, ConM-BU: 46%, ConM-TD: 45%).

Microstimulation

We used microstimulation to further investigate the causal roles of PMd and PPC in the ongoing reaching decision. We hypothesised that if an area is causally involved in ongoing decision processes, disrupting its neural activity would result in changes in the behavioural patterns, such as slowing or speeding of the decision process (Thura & Cisek, 2020). We stimulated (57 ms, 333 Hz, 70 μA) in 6 PMd and 6 PRR sites, chosen based on the presence of audibly or visually observable neural activity at the beginning of each session.

Microstimulation effects were location- and time-dependent

Figure 22 summarizes the effects of microstimulation. Out of 6 PMd sites, 2 sites had effects that were statistically significant, 3 sites had a trend of effects that did not meet statistical significance, and one site had no effects. Of these, 3 sites made the RTs longer and 2 sites had a mixed result (i.e., both longer and shorter RTs). Out of 6 PRR sites, 2 had effects that were statistically significant, 1 had a trend of effects that did not meet statistical significance, and 3 had no effects. Of these, 2 sites made

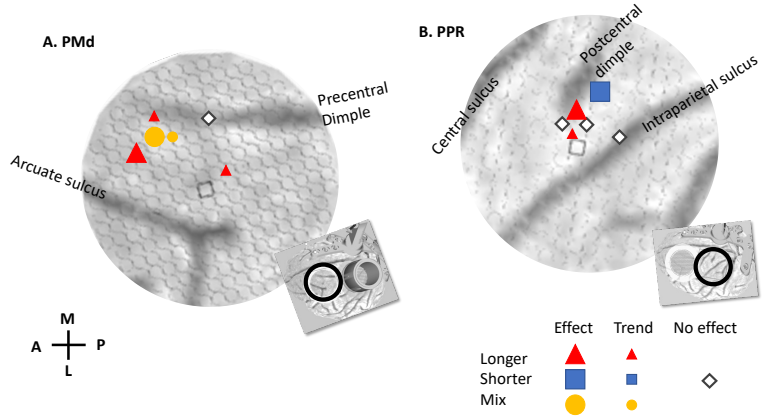

Figure 22. Microstimulation location

Penetration location of microstimulation on **(A)** PMd and **(B)** PRR. Different shapes indicate different effects on behavioural latency when stimulating the site. Red triangle: longer RT. Blue square: shorter RT. Yellow circle: longer and shorter RT depending on trial conditions, thus mixed effects. Larger shapes represent statistically significant changes. Smaller shapes represent a trend that did not meet statistical significance. A: anterior. P: posterior. M: medial. L: lateral.

the RTs longer, and one site made it shorter. In total, 5/6 PMd and 3/6 PRR sites had some effects on the behavioural latency.

Figure 23 shows the effects of an example site in PMd (indicated by the large yellow circle in Figure 22A), which had a mixed result. Microstimulation of this site at 150 ms after target onset made the RT shorter during 1T trials (Wilcoxon rank sum test, $p<0.01$), but did not have an effect in other trials. In contrast, microstimulation at 100 ms made the RT *longer* in several trial types (significant at $p<0.01$ in Easy-BU, Twin, and ConS-TD, and nearly significant at $p=0.051$ in ConS-BU).

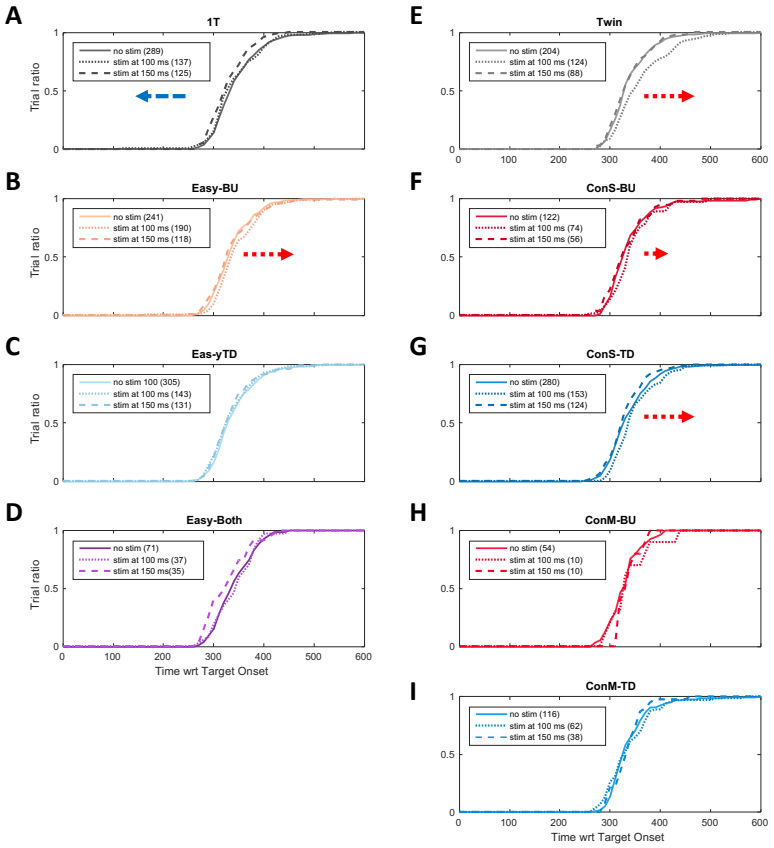

Figure 23. Example microstimulation effects

Cumulative histogram of RTs of different conditions with and without microstimulation on a PMd site. **(A)** 1T, **(B)** Easy-BU, **(C)** Easy-TD, **(D)** Easy-Both, **(E)** Twin, **(F)** ConS-BU, **(G)** ConS-TD, **(H)** ConM-BU, and **(I)** ConM-TD. Dotted and dashed lines represent RT of trials with microstimulation at 100 ms and 150 ms after target onset, respectively. Solid lines represent control trials (i.e., no stimulation). This site had mixed effects.

Table 3 shows the effects of all microstimulation sites. In most conditions, there was no effect of microstimulation regardless of the timing. When there was an effect, stimulation at 100 ms after target onset mostly increased the RTs, whereas stimulation at 150 ms had more mixed effects. All but one of the PMd sites had some stimulation effects, whereas

half of the PRR sites had no effects. This again points towards the possibility that PMd has a stronger causal role on ongoing decisions compared to that of PRR.

	PMd						PRR					
Condition	12	17	7	4	26	6	49	60	38	55	40	50
1T	↓*	-	-	-	-	-	-	-	-	-	-	-
Twin	↑*	-	-	-	-	-	-	↑	-	-	-	-
Easy-BU	↑	-	-	-	-	-	-	-	-	-	-	-
Easy-TD	-	-	-	-	↑	-	↑	-	-	-	-	-
Easy-Both	-	↑*	↑	-	-	-	-	-	-	-	-	-
ConS-BU	↑	-	-	-	-	-	-	-	-	-	-	-
ConS-TD	↑*	-	-	-	↑↓	↑	-	-	-	-	-	-
ConM-BU	-	-	-	-	-	-	-	↑	↓*↓*	-	-	-
ConM-TD	-	-	↓	-	-	-	-	-	-	-	-	-

Table 3. Microstimulation effect details

Top 6 sites are in PMd, and bottom 6 sites are in PRR. Upward arrows indicate increase in RT (i.e., slower). Downward arrows indicate decrease in RT (i.e., faster). Arrows with an asterisk mean the effect met statistical significance at p=0.05 in Wilcoxon ranksum test. Red and blue arrows represent effects of stimulations delivered at 100 ms and 150 ms after target onset, respectively.

Neural Space Analysis

To explore how the firing rate of the whole neuronal population varied during the task, we created a hyperdimensional space using each neuron's firing rate as one dimension and performed dimensionality reduction using Principal Component Analysis (PCA). Figure 24 shows the first 9 principal components (PCs) of all isolated neurons, which together account for 76.44% of the variance explained. PC1 explains almost 30% of the variance in the firing rate, capturing the transition between deliberation (which we estimated as being until approximately 110 ms after target onset) and commitment. PC2 explains approximately 17% of the variance, and it reflects the direction of the upcoming choice movement (i.e., left vs right) and differs for different trial

conditions. Specifically, the divergence reflecting the directional choice appears the earliest in 1T (black), second earliest in Easy-BU (orange) and Easy-TD (light blue), and the latest in ConS-BU (dark red), ConS-TD (dark blue), and Twin (gray) trials. PC3 explains approximately 13% of the variance, and it reflects the trial types and the elapsing time. The distinction of trial types varied from PC2, such that ConS-BU had the highest amplitude, separating itself from ConS-TD and Twin. PC4 explains less than 4% of the variance, yet it appears to reflect the baseline bias that was the most prominent in ConS-BU trials, diverging prior to target onset.

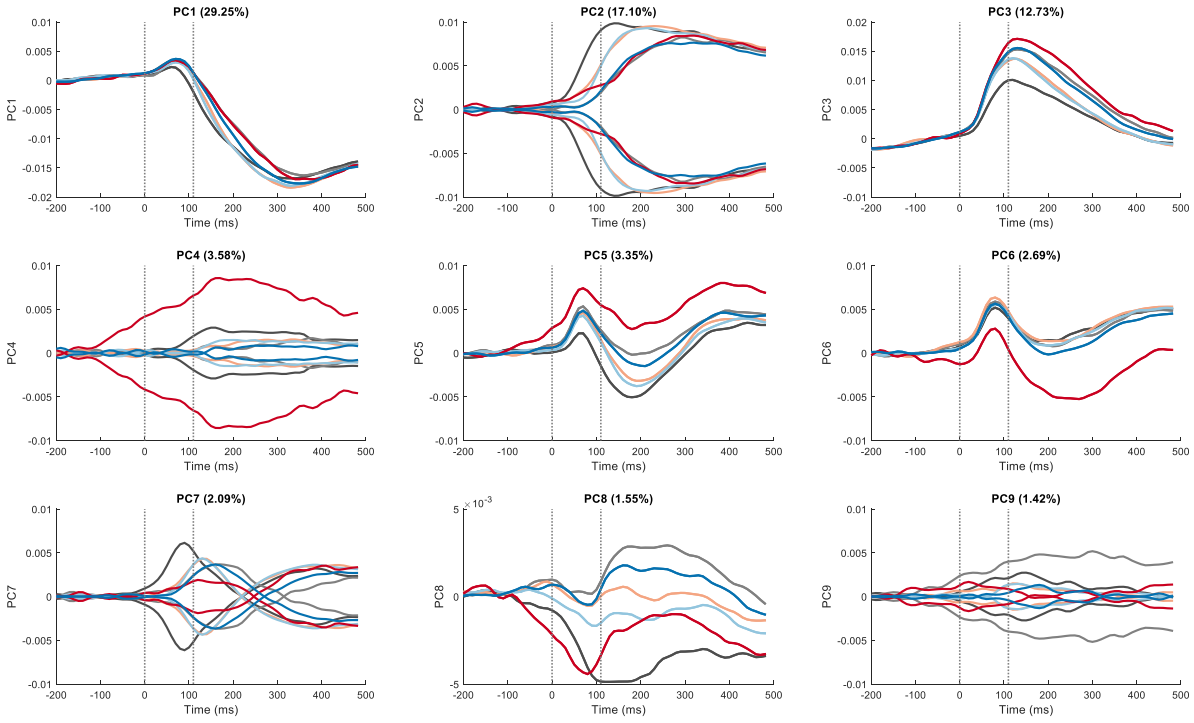

Figure 24. Principal Components of Neural Space Analysis, all neurons

Trajectories of the principal components plotted against time, aligned to target onset. Different colours represent different trial conditions. Black: 1T, orange: Easy-BU, light blue: Easy-TD, dark red: ConS-BU, dark blue: ConS-TD, gray: Twin.

Figure 25 shows the activity of PMd (Figure 25A) and PRR (Figure 25B) separately projected on the same PC spaces. At a glance, the trajectories of both PMd and PRR population appear similar to that of the whole population. However, PC1 of the PMd population appears to distinguish different trial types clearly within 50 ms, while PRR does not do so until much later, approximately 300 ms after target onset. Furthermore, PC1 of the PRR population lacks the initial increase seen in PMd that reflects the presence of a second target. PC2 of the PRR population also diverges in a different order than that of PMd. In particular, while both areas distinguished 1T from the rest of the trial types, PMd trajectory had the Easy trials followed by the Conflict and

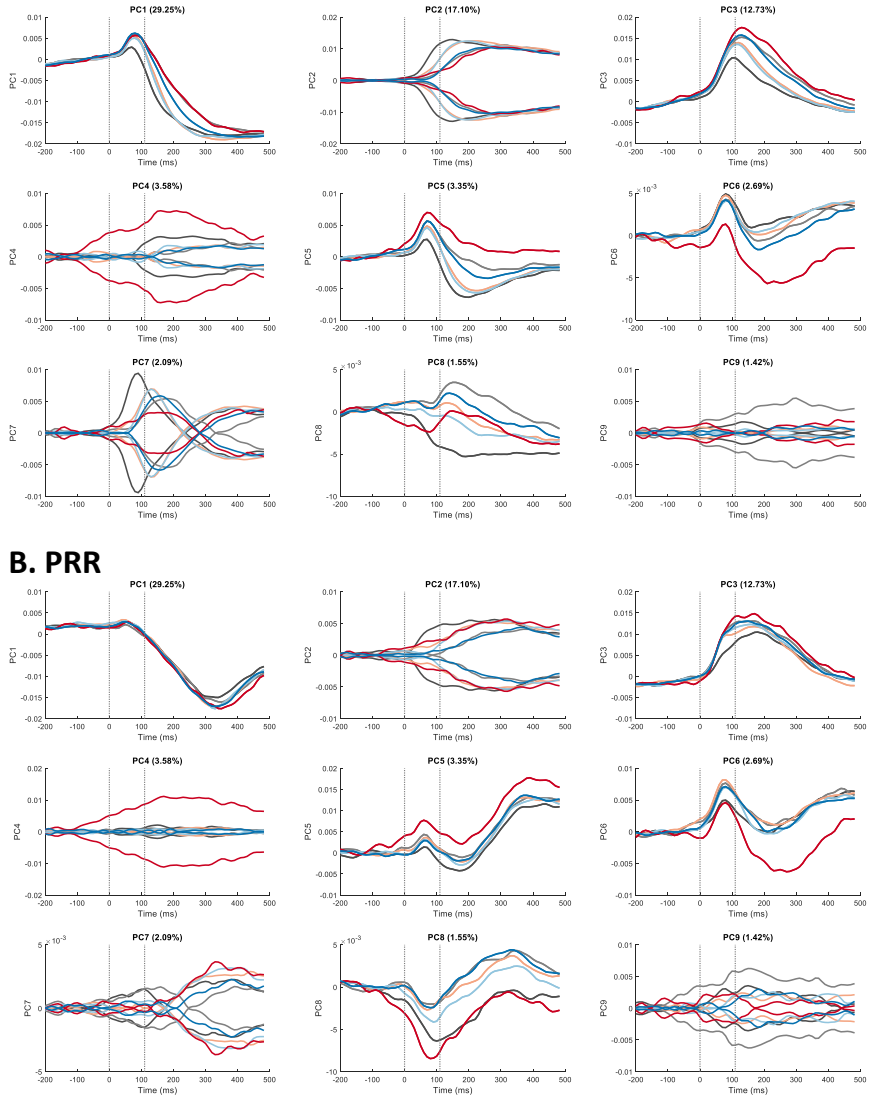

Figure 25. Neural Space Analysis, Monkey Y

The first 9 principal components of **(A)** PMd and **(B)** PRR neurons. Colour coding is the same as in Figure 24.

Twin trials, whereas PRR trajectory had ConS-BU as the second earliest with the baseline bias, followed by Easy trials and finally ConS-TD and Twin. While activity in both regions reflect key aspects of the task, their differences were not uniformly explained by the different components. In other words, PMd and PRR seem to be affected by different trial conditions at different timepoints during the task.

Interestingly, if we focus only on PC2, the divergence of activity during ConS-BU trials appears earlier in PRR than in PMd, while the opposite is the case in ConS-TD trials. This is in agreement with the prediction of the hypothesis that both regions are part of a Distributed Consensus. However, the statistical significance of this observation remains to be established and as such, must be considered with caution.

Local Field Potential (LFP) Analysis

In addition to the spiking data, we collected local field potentials (LFPs), which are believed to be a proxy of a summation of synaptic activities around the recording electrode (Pesaran et al., 2008; Sanes & Donoghue, 1993; Scherberger et al., 2005). The preliminary results are described elsewhere (Lusignan, 2022). In brief, the LFP signal was recorded at approximately 1017 Hz from electrodes that had audible, visible or isolatable neural activities. The analyses focused on data from 8 PMd and 10 PPC electrodes in which the largest number of consecutive sessions were recorded, which were averaged across each region for spectrogram and frequency band analyses. The main findings were discussed around three bandwidths. First, the alpha band (15-22 Hz) displayed a rapid and transient burst following target onset, which was present in all but single target trials. Second, the low gamma band (40-55 Hz) showed suppression following target onset and rebound into the delay period. Finally, high gamma band (70-90 Hz) activity discriminated right versus left choices in a subset of trial conditions. In both PMd and PPC, alpha, low gamma

and high gamma bands were all modulated by the choice directions. In PMd, low gamma and high gamma bands additionally discriminated different trial types, particularly between the Easy and Conflict trials. Future work will include a more detailed analyses on a larger dataset, including the LFPs from the second monkey, to obtain a more complete picture.

CONCLUSION

This chapter showed the results from the Dual Feature task performed by a monkey while we recorded electrophysiological data from the dorsal premotor cortex and parietal reach region. Behaviourally, the reaction time distributions between the human participants and one of the monkeys showed very similar trends. Neurally, both PMd and PRR population activity reflected the monkey's directional choice shortly after target onset. In 1T, Easy-BU, Easy-Both, Twin, ConS-BU, ConS-TD and ConM-BU trials, the earliest choice-related activities appeared in PMd at least 20 ms faster than that of PRR. In the Easy-TD and ConM-TD trials, PRR was faster than PMd, but only by 5 ms. The analysis of the latency distributions showed that this choice-related activity appeared earlier in PMd than in PRR in 1T, Easy-BU, Easy-TD and Twin trails. In Easy-Both, ConS-BU, ConS-TD, ConM-BU and ConM-TD trials, PMd and PRR latencies were similar. Furthermore, there was a significant pre-stimulus bias in the PMd baseline activity, which was absent in the PRR baseline activity. The analysis of cumulative histograms of choice latency showed that while the latency distribution in PMd discriminated different trial conditions, that of PRR reflected essentially only the difference between 1T trials and the rest (trials with two targets). The microstimulation section showed that, while the effects are not straightforward, stimulation of PMd appear to affect the monkey's reaction time more often than stimulation of PRR. Neural space analysis on the larger populations including cells with later tuning property showed that despite the strong reciprocal connections, the components that explained the variance of PMd activities

were not equally present in PRR activities. Preliminary LFP analyses suggest that while directional information is present in both PMd and PPC, additional information such as trial conditions were seen in PMd but not in PPC.

One of our original aims was to investigate whether separate neural substrates exist for processing bottom-up and top-down information, and how conflicts between these are resolved. We drew inspiration from previous studies and chose two specific attributes: the target brightness as BU and the angle of an overlaid line as TD, and recorded from two sensorimotor regions, PMd and PRR. We expected that during BU-based decisions, neural activity predicting the monkey's choice would appear first in PRR and then in PMd. In contrast, we expected that during TD-based decisions, choice-related activity would appear first in PMd and then in PRR. In other words, we aimed to replicate what Buschman and Miller reported, that LIP preceded FEF when bottom-up information was dominant, and FEF preceded LIP when top-down information was dominant (Buschman & Miller, 2007), even when both kinds of information were present simultaneously. So far, our results point towards a different story. Instead of the attribute-based latency reversal, we found that PMd almost always preceded PRR in predicting the monkey's choice. If the latency difference existed in Easy but not in Conflict trials, the results could have been interpreted as reflecting the visual attribute without necessarily contributing to the decision processes. However, the latency order was consistent not only in the Twin and Conflict trials, but also during decisions based on both BU and TD attributes. Thus, our results are more in line with studies that argue against PRR having a causal role, at least in our task (Katz et al., 2016; Westendorff et al., 2010).

In contrast to PRR, our results suggests that PMd does have a causal role in the decision process we investigated. One notable finding from our results was the speed in which the PMd population predicted the monkey's choice. In all conditions we analysed, the PMd population showed

directional tuning within 110 ms from target onset. When the choice was "easy", this tuning appeared within 60-80 ms from target onset. Not only is this comparative to the FEF latency reported by Buschman and Miller, it is almost as fast as the latency of the event-related potential locked to stimulus onset (but not response predictive, which was typically at or later than 150 ms from stimulus onset) by Ledberg and colleagues (Buschman & Miller, 2007; Ledberg et al., 2007). Furthermore, the difference in latency between PMd and PRR was not constant across trials, as would be predicted if both regions lie outside a Central Executive from which they receive decision-related information. Instead, PMd activity showed choice-predictive latencies that differed for decisions made on the basis of different kinds of information, while PRR latencies were similar in all 2-target trials. This is consistent with the proposal that PMd lies within the decision-making circuit even if PRR does not.

Finally, the baseline activity of the PMd population was predictive of the upcoming choice in Twin and Conflict trials, that is, when the trial condition contained no "correct" answer. Because the trial conditions were randomized in our task, it is unlikely that the monkey was anticipating any specific condition in a given trial. This is in line with the fact that there is no clear difference in the pre-stimulus baseline activity in 1T and Easy trials, as any fluctuation prior to the stimulus onset will be overwritten once information arrives about the "correct" option, which can appear on the left or on the right with equal likelihood. It other words, this bias was revealed only when the trials were classified on the basis of direction in trials when the monkey was given an opportunity to freely choose, in which the baseline fluctuation could influence the upcoming choice. The lack of such pre-stimulus baseline bias in the PRR population additionally suggests that PRR does not have a causal role in this decision paradigm.

Taken together, our results provide support for the hypothesis that PMd plays a causal role in the decision process, but do not support a causal role of PRR, at least in the task we studied.

Strictly speaking, our findings do not conclusively reject either the Central Executive or Distributed Consensus theories, and instead simply argue against their most extreme variations. For example, the classical Central Executive theory does not include sensorimotor areas as part of the decision-making network, yet our results suggest a causal role of PMd in action decisions and thus argue against the classical notion of a Central Executive. Notably, the possibility that the Central Executive may not be a single brain area, and could instead be comprised of multiple neural substrates, has been proposed previously (Baddeley, 1996). Conversely, a Distributed Consensus theory that implicates the entire sensorimotor circuit in decision-making would also include PRR (Cisek, 2012), yet our results argue against a causal role for PRR in our task. Instead, our results are best interpreted as support for a third alternative: a decision network that includes PMd, but not PRR (at least not for the attribute we chose), when making value-based action choices. This third alternative will be examined in more depth in the final chapter of this thesis: General Discussion.

CHAPTER 5 GENERAL DISCUSSION

SUMMARY

The goal of this thesis was to examine how the brain makes action decisions. To do so, we focused on two alternative hypotheses:

1. All decisions are made in a Central Executive

2. Decisions about actions are made through a Distributed Consensus

The crucial difference between these hypotheses lies in their implication for neural substrates of decision making. If all decisions are made in a Central Executive, one would expect that the brain region or regions included in the Central Executive would reflect decision-related variables during deliberation, be causally involved in determining a choice, and would broadcast that choice to regions outside the Central Executive, including the sensorimotor areas responsible for implementing the selected actions. Numerous studies provided data supporting this view, and suggested the prefrontal cortex as the Central Executive area (Goodwin et al., 2012; Juechems et al., 2017; Kim & Shadlen, 1999; Padoa-Schioppa, 2011; Tanji & Hoshi, 2008; Wallis & Miller, 2003). In contrast, if some decisions are made through a Distributed Consensus that involves many regions, including those outside of the prefrontal cortex, then one would expect those regions to also be involved in ongoing decision processes. This notion has been supported by other studies, which have proposed that sensorimotor areas such as superior colliculus, lateral intra parietal area, parietal reach area, primary motor cortex and premotor cortex are included in the distributed decision network (Basso & Wurtz, 1998; Gail & Andersen, 2006; Pastor-Bernier & Cisek, 2011; Platt & Glimcher, 1999; Shadlen & Newsome, 2001; Thura & Cisek, 2014). These two hypotheses suggest different roles for different brain areas, and combined with the notion of dorsal and ventral

streams, predict different sequences in which decision-related information can flow in the brain. However, in most decision experiments, the tasks are not designed to completely dissociate the two. This is because in most studies there is almost always a correct answer, a situation in which the predictions of the two hypotheses are difficult to distinguish. Therefore, we designed a decision task with two independent attributes, which allows us to create a situation of conflict, in which the two hypotheses predict different patterns and latencies of neural responses.

We used "bottom-up" (BU) brightness and "top-down" (TD) line orientation features to jointly indicate the reward value in a two-alternative forced-choice reaching task. The BU feature was aimed to activate the saliency network through the dorsal occipital-to-parietal pathway, whereas the TD feature was aimed to activate a more knowledge-based categorization network through the ventral temporal-to-prefrontal pathway (Buschman & Miller, 2007). The two hypotheses made the most distinct predictions when the features were in conflict, but the total reward values of the choices were equal. In this incongruent free-choice condition, a pure Central Executive model predicted that behavioural and neural latency will reflect the serial flow of decision-related activity in the brain. That is, the shortest choice latency should be in the prefrontal cortex, where the decision happens, and slower responses should be found in sensorimotor areas, where the final decision is converted into behavioural outputs – but with a constant latency difference between different regions regardless of how the decision is made (Figure 1A). For the same situation, the Distributed Consensus model predicted that, if a region is part of the distributed decision network, its choice latency will vary as a function of its role in the ongoing decision. That is, shorter latencies are expected when a region is faster to receive the information on which the choice is based, whereas longer latencies are expected when a decision was made in a different region on the basis

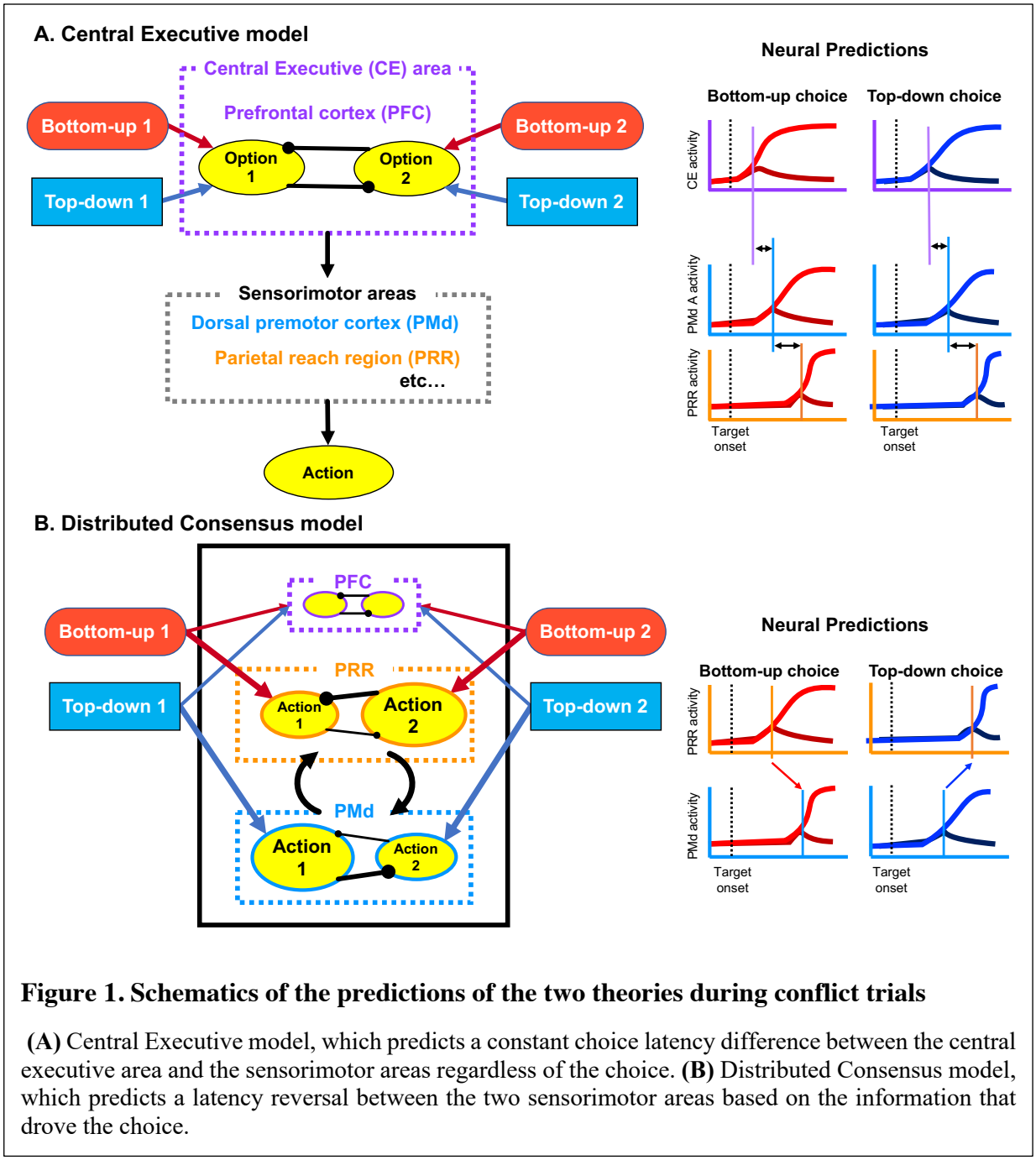

Figure 1. Schematics of the predictions of the two theories during conflict trials

(A) Central Executive model, which predicts a constant choice latency difference between the central executive area and the sensorimotor areas regardless of the choice. **(B)** Distributed Consensus model, which predicts a latency reversal between the two sensorimotor areas based on the information that drove the choice.

of other kinds of information. (Figure 1B) We collected behavioural data from human participants, and behavioural and neural data from two macaque monkeys.

The human project was purely behavioural, which means it cannot directly address the distinction between the two main hypotheses. However, it was informative for comparing the behavioural

patterns of monkeys to that of humans. Furthermore, it allowed us to address a question relevant to the Central Executive hypothesis: do we always integrate everything before making a decision, or can we sometimes jump the gun? Here, we report that human participants made decisions with different latencies depending on conditions, and the order of the latencies suggested that decisions were sometimes made before all of the attributes were integrated. Importantly, all of the trial types were randomly interleaved, making it impossible for participants to simply choose different policies for "Easy" versus "Conflict" trials because one could not know whether a given trial involved conflict until both kinds of information (BU and TD) were received. Thus, our findings were inconsistent with the "integrate-and-compare" model, which postulates that decision processes are a comparison between singular, integral units of desirability (FitzGerald et al., 2009; Lim et al., 2013). Instead, our findings were more in line with other studies, supporting the theory that decision-making is a hierarchical process in which multiple aspects can influence each other beyond their conceptual boundaries (Diederich, 2003; Hunt et al., 2014).

If decisions can be made without fully integrating all the information, what are the neural substrates of the relevant processes? Does everything happen in a single Central Executive area, such as the prefrontal cortex, or can other areas trigger choices, especially when made on partial information? Given that decisions can be made without full integration of all information, we anticipated to observe differential neural activations in regions that play a causal role in ongoing action decisions.

The core of this thesis was the monkey project, and its objective was to find patterns of neural activity that dissociate the two hypotheses. Here, we report that choice-predictive activity was present in both sensorimotor areas we recorded, PMd and PRR, but many of our findings suggest that PMd, but not PRR, has a causal role in the current decision task. First, the choice-predictive activity of the PMd population preceded that of PRR in 1T, Easy-BU, Easy-Both, Twin, ConS-

BU, ConS-TD, and ConM-BU trials by a minimum of 20 ms, whereas PRR preceded PMd in Easy-TD and ConM-TD but only by 5 ms. Second, PMd displayed a pre-stimulus baseline bias in Twin and Conflict trials, whereas PRR did not. Third, the latency of choice-predictive activities in PMd varied with trial conditions, whereas that of PRR only discriminated whether the trial contained single versus multiple targets. Fourth, preliminary microstimulation results showed more consistent effects when microstimulating PMd, compared to PRR where effects were found in only 50% of stimulation sites. Fifth, preliminary LFP analyses suggest that different bandwidths in PMd reflect different trial conditions, whereas that of PPC (i.e., PRR and LIP combined) did not. Together, our results suggest that PMd activity, especially during free-choice conditions, plays a causal role in the upcoming decisions. In comparison, our results did not support a causal role for PRR in our multi-attribute action decision task. As for the two hypotheses, our results argue against both of them, at least in their more extreme versions, and instead favor an alternative model that lies somewhere in-between.

ON "PREMOTOR, BUT NOT PARIETAL"

How do our results compare with previous findings? We interpreted our results to indicate that PMd, but not PRR, has a causal role in our multi-attribute decision task. However, our initial prediction was that both PMd and PRR will have a causal role, based on a plethora of studies demonstrating that both LIP and PRR activities reflect decision variables (Buschman & Miller, 2007; Kubanek & Snyder, 2015; Pesaran et al., 2008, 2008; Platt & Glimcher, 1999; Shadlen & Newsome, 2001; Snyder et al., 1997; T. Yang & Shadlen, 2007). Before we refer to this apparent inconsistency as such, it is important to note that previous studies were reporting neural correlates of decision variables, such as the change in the neuronal activity with respect to experimentally manipulated parameters. With those kinds of correlations, it is difficult to distinguish whether the

observed effects imply that a region is causally related to a choice versus simply receiving a reflection of decision processes happening elsewhere. In this regard, our results are consistent with previous studies, as we did observe choice-related neural modulation in both PMd and PRR activity, albeit almost always slower in the latter region.

To address the gap between the correlation and causation of neural correlates of decision-making, some studies used stimulation techniques to probe the causal role of a target brain area. For example, Hanks and colleagues showed that microstimulation of LIP affected the saccade choice ratio, arguing that LIP is one of the regions playing a causal role when choosing between multiple options (Hanks et al., 2006). However, Katz and colleagues showed that pharmacological inactivation of monkey LIP did not affect the performance of a random dot motion task, thus suggesting that an intact LIP is not necessary for choosing where to look based on perceptual input (Katz et al., 2016). Mooshagian and Snyder also showed that during bimanual reaching, neither LIP nor PRR activity reflected the order of targets the monkeys looked at (Mooshagian & Snyder, 2018). These findings, albeit about saccades and not arm reaches, suggest that while PPC activity reflects variables pertinent to the ongoing processes, and may even have some influence on certain decision processes, its presence may not be indispensable. While the issue of whether parietal cortex is or is not causally involved in decisions is far from resolved, our results can be seen as favoring the latter view.

INTERPRETING THE PRE-STIMULUS BASELINE BIAS

What does the pre-stimulus baseline bias mean? One of the most puzzling of our results was the difference in the firing rate between when the monkey was to choose the cell's preferred target (PT) versus the opposite target (OT) *prior* to target onset, observed clearly in the PMd population

during the conditions in which both targets were equally valued. We interpreted this phenomenon as indicative of PMd activity having a causal role.

Here is a colloquial analogy that may help understand our conjecture: Imagine that you happen to feel like having some vanilla ice cream. You walk into an ice cream parlour but on that day, they happen to only have mango ice cream. So, you take the mango. This is analogous to 1T trials, in which there are no options to choose from. On a different day, you walk into the ice cream parlour and may initially be dazzled as you see the variety of flavours. This is potentially what is happening as the firing rate briefly increases for both PT and OT when there is more than one target, and converges in case of Twin trials, as the neural activity is modulated by the presence of two options. After that, if you notice that the mango flavour is on a special promo and sold at 2 scoops for 1, you will probably choose the mango ice-cream. This is analogous to the Easy trials, in which one option is clearly better than the other, and whatever you were "feeling like" is overwritten by information about the presence of the better option. In contrast, if all flavours are at the same price, you are more likely to choose vanilla based on your original gut feeling. This is analogous to Twin and equi-valued conflict trials. These trials contain no persuasive information to choose one target over the other, so the neural activity is less influenced by external information and may continue to reflect its original state. This allows the baseline fluctuation to affect the decision process to choose the neuron's preferred target. That is, when all options are equally valued, we can act based on what we "felt like" and choose the vanilla ice cream.

Other studies have reported similar pre-stimulus biases in superior colliculus, caudate nucleus, and substantia niagra pars reticulara, which can be experimentally manipulated and predictably influence behavioural outcome (Basso & Wurtz, 1998; Ikeda & Hikosaka, 2003; Lauwereyns et al., 2002; Platt & Glimcher, 1999; M. Sato & Hikosaka, 2002; Takikawa et al., 2002). For example,

Shadlen and Newsome showed that during a random dot motion task, LIP activity prior to the stimulus onset already predicts the monkey's choice when the motion coherence is low (Shadlen & Newsome, 2001). In another example, Coe and colleagues showed that during a free choice saccade task, a subset of neurons in monkey supplementary eye field, LIP and FEF displayed anticipatory activities that predicted the choice prior to target presentation (Coe et al., 2002). In our task, trials were interleaved, thus any spatial reward contingency the monkey perceived was coincidental. Nonetheless, it is possible that the monkey decided to favour one direction over the other, due to the biased input from cortical and subcortical regions to the sensorimotor neurons representing respective directions (Hikosaka & Watanabe, 2000; Kawagoe et al., 1998; Mogenson et al., 1980; Samejima et al., 2005).

LATENCY AND CAUSALITY

We observed that PMd population activity predicted the monkey's choice as early as 60 ms from target onset, even in the presence of multiple targets, if the targets varied in the BU feature. According to a study by Maunsell and Gibson in awake and behaving monkeys, the lateral geniculate nucleus cells respond within 30 to 50 ms from the visual stimulus onset, with the shortest latency ranging from 20 to 31 ms (J. H. Maunsell & Gibson, 1992). In a comment to the study by Buschman and Miller, Schall and colleagues noted that the conventional pop-out search task evoked choice-predictive activities within 140 ms from stimulus onset in FEF, lateral PFC, LIP and SC (Schall et al., 2007). Accordingly, one may consider that our PMd population's choice latency is too early to be taken as a neural correlate of choice. However, in another study on event related potentials, Ledberg and colleagues reported that premotor, primary motor and prefrontal areas showed early, stimulus-nonspecific activation comparative to that of V1, suggesting that these areas need not wait for the whole occipital lobe to complete visual processing before they

receive stimulus input (Ledberg et al., 2007). Our PMd results are in line with their claim that decision processes involve multiple brain areas, ranging from sensorimotor to the executive regions.

What was striking was the long latency of our PRR cells, not only because Ledberg and colleagues reported consistently earlier activations in parietal regions, but because it is known that PRR is heavily interconnected with PMd (Johnson et al., 1996; Markov et al., 2014; Morecraft et al., 2012). However, a study using a memory-guided anti-reach task showed that the order of activation during anti-reach trials was always PMd before PRR, with a difference of 27 ms between the two areas (Westendorff et al., 2010). While the latency difference between the two areas is not the same, our results are in line with that of Westendorff and colleagues, further supporting the implication of PMd having more of a causal role in decision processes compared to PRR.

BETWEEN A CENTRAL EXECUTIVE AND A DISTRIBUTED CONSENSUS

In our experiment, PRR activities did predict the monkey's choice, sometimes as quickly as that of PMd. However, it preceded PMd in doing so in only one condition: Easy-TD, and only by 5 ms. These results fit neither of our original predictions. However, it must be acknowledged that those original neural predictions were based on somewhat "extreme" versions of the Central Executive and Distributed Consensus models, and that our results are best interpreted as pointing toward an alternative that falls on the gradient between the two theories.

We predicted that, if decisions are made in a Central Executive, choice-predictive activity in PMd and PRR will appear at a constant latency difference across different trial conditions. First, the

visual input arrives at the occipital cortex, and the information is distributed throughout the brain, including the canonical dorsal and ventral visual pathways, creating the bottom-up and top-down flows of information (Figure 2A). The bottom-up information refers to the saliency-based features, such as the stimulus onset, and in our experiment's case, also the brightness of the target in addition to the visual onset. This information is expected to arrive at the parietal areas for attention-related processes as well as to the central executive areas for the decision processes (Figure 2A, red arrow). The top-down information refers to features that are not inherently salient, such as a learnt mapping of arbitrary cues, which is expected to go through the temporal lobe to trigger memory-related processes and arrive at the executive areas (Figure 2A, blue arrow). Eventually, all information is gathered in the central executive area, converted into a unified "common currency", integrated, and

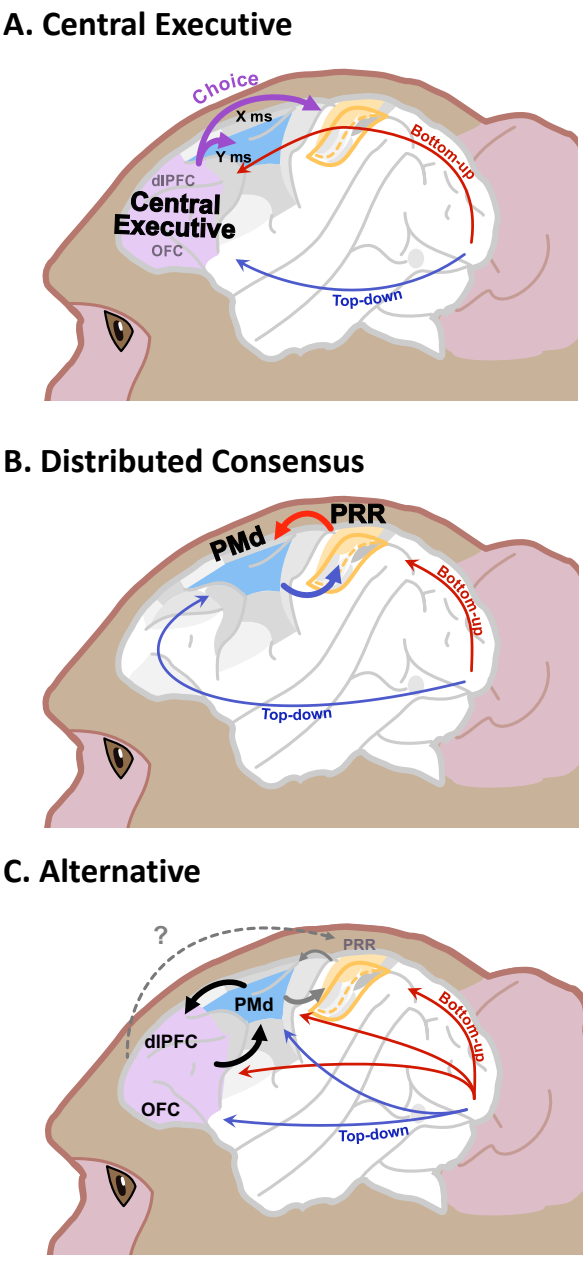

Figure 2. Schematics of the three theories

Two original theories, **(A)** Central Executive and **(B)** Distributed Consensus, and **(C)** Alternative third theory based on our results. Thin lines indicate information pathways. Thick lines indicate decision pathways. The dotted gray line is a hypothesized frontal-to-parietal decision pathway.

compared at an abstract level to make decisions. The resulting choice is then realised via activating the sensorimotor regions (Figure 2A, purple arrows). This prediction was based on an assumption that these sensorimotor areas are not part of the Central Executive network, which traditionally implies prefrontal cortex (Tanji & Hoshi, 2008). Thus, however the Central Executive arrives at its choice, that choice will be broadcast to other regions with constant delays (e.g., X ms for PRR, Y ms for PMd), such that the relative latency difference between PMd and PRR remains constant. In other words, while the decisions may be faster in Easy-BU trials than Easy-TD trials, and faster in Easy than Conflict trials, the time when PMd and PRR predict the monkey's choice will be always the same duration apart. In contrast, if decisions are made through a Distributed Consensus which includes *both* PMd and PRR, we predicted that the choice-predictive activity in PMd and PRR will have a latency reversal as a function of chosen target attributes (Figure 2B). This was based on the assumption that PRR receives "bottom-up" information before PMd, while PMd receives "top-down" information before PRR. In a conflict trial, for example, once PRR decides based on its bottom-up information, this resolution of a within-region competition influences the ongoing competition elsewhere in favour of its decision, such that the competition in PMd gets an additional boost to the option whose bottom-up feature is favourable. Our results had neither a constant temporal difference between the two regions, nor a temporal reversal in the order of choice-predictive activity. The variable latency differences between PMd and PRR argue against the idea that both are simply receiving the final decision. Instead, they suggest that PRR may be receiving a multitude of inputs from different regions, and its activity only reflects the final decision when other regions broadcast the resolution of competition between options. For example, Figure 2C depicts a possible alternative model in which PMd, dlPFC and OFC, all of which receive both BU and TD input, comprise parts of a distributed decision network. Projections from dlPFC

and OFC to PRR are suggested as a potential pathway for the delayed decision input, although not all tracing studies support these connections (Bakola et al., 2013; Markov et al., 2014; Shipp et al., 1998).

Another question is whether PMd is part of the decision circuit, or whether it simply happens to receive a preview of the ongoing decision processes occurring elsewhere. According to Baddeley, a Central Executive is just a theoretical concept and not to be taken to imply a unitary neural substrate, much like the functional implications of prefrontal areas are far from unitary (Baddeley, 1998). In this view, the distinction between the Central Executive and Distributed Consensus models becomes a continuum, and PMd may fall somewhere in the middle as a non-traditionally "executive" sensorimotor area with a causal influence. If so, one would expect to see other neural substrates with comparative latency, predicting the monkey's choice equally or more quickly in certain conditions. Likewise, it is possible that PMd is simply receiving and reflecting the final output from executive regions, such as prefrontal areas. In this view, one would expect to find neural substrates with consistently shorter latency than that of PMd. In fact, our second monkey's recording chamber includes prefrontal areas for this very reason. Our aim is to investigate the neural correlates of several other candidate executive regions, such as dlPFC and dACC during the same task, to see if the activity in these areas precedes PMd in predicting the monkey's choice. A potentially interesting case is if some frontal regions consistently reflect the information pertinent to the decisions but not sensitive to the choice made, which implies their role in providing decision variables without the causal role.

LIMITATIONS

"There is nothing wrong with not knowing, but there is something wrong with not learning."

- Sara A. Solla, at the Montreal AI & Neuroscience meeting (MAIN), December 2020

Below are some of the limitations of this thesis, what they may imply, and possible ways of mitigation for future.

Sample Sizes

Both human and monkey experiments consist of small sample sizes. The human behavioural data come from 14 participants. Their median RT distribution did not systematically cluster, but their cumulative RT distributions for ConS-BU and ConS-TD trials suggest that there are two subgroups within the sampled population, one with 8 and the other with 5 participants (Chapter 3, Figure 4). Furthermore, one participant did not provide us with any trials in one of the trial conditions: ConS-BU, as all the initially ConS-BU trials eventually became ConS-TD trials (i.e., started to reach for BU-favoured target, but course-corrected for TD-favoured target). This was not completely unexpected, as the Dual Feature task is a free choice task that does not penalise such one-sided choice behaviour. According to a power analysis on our data (alpha: 0.5, desired power: 0.8), future replication attempts require a minimum of 12 participants if we are to focus on the subgroup with an RT difference between ConS-BU and ConS-TD, but for a full assessment of individual differences, one would require a minimum of 68 participants.

The electrophysiological data presented here come from one monkey and the second monkey's data are only mentioned in Table 1. This was due to the low yield in task-related cells in the second monkey, which did not merit population analysis. One may ponder that, if the percentage of task-related neurons in monkey Y was a representative of neuronal population, then we should have

collected approximately 38 PMd and 4 PRR neurons that are task-related in monkey K. However, we only collected 7 PMd and 0 PRR neurons to date. One possible explanation for this difference is that the two monkeys are performing the task with different heuristics, which affected the firing patterns of neurons in monkey K. Another possible explanation stems from the technical difference in the recording techniques between the two monkeys. We implemented a different approach to finding neurons in monkey K, in which we descended the electrodes first into deeper layers and then attempted to find isolatable units as we pulled up. This approach did not yield as many task-related isolatable neurons as we did with monkey Y, in which we slowly descended the electrodes to isolate units from shallow layers. In fact, a preliminary analysis showed that cells recorded in shallow layers in monkey Y had shorter choice latency compared to those recorded in deep layers, and all PMd cells from monkey K to date were recorded in deep layers. Nevertheless, we are currently analysing more data from the second monkey, and hope to replicate the finding from the first monkey.

The premise and corresponding predictions assumed extreme cases

The second limitation is in the fundamental assumptions that led to the original prediction of the Distributed Consensus theory. Based on previous literature, we designed the experiment assuming that the outcome would support either 1) neither PMd nor PRR has a causal role, or 2) both PMd and PRR have a causal role. The data from the first monkey suggested a third alternative, that is, 3) one of the two sensorimotor areas (i.e., PMd) has a causal role, but not the other (i.e., PRR). While this is itself interesting and important, it makes it impossible to use latency differences to conclusively establish a causal role for PMd without comparing it to other regions that are putatively causally involved.

Consequently, we extended our recording regions in the second monkey. In addition to replicating the data from the first monkey, our aim is to investigate the choice latency of other frontal regions, including dorsolateral prefrontal cortex and dorsal anterior cingulate cortex. We predict that if the Central Executive theory holds, the prefrontal regions will always precede PMd with their choice latency. Alternatively, if PMd is part of the frontal decision-making network, its choice latency will be comparable to that of the prefrontal regions.

Limited Attributes

A simple explanation for the absence of an effect is that the experimental manipulation did not yield appropriate conditions for comparison. In case of this project, it is possible that the attributes we chose, particularly the "bottom-up" brightness feature of the targets, may have been an inadequate attribute for effectively engaging PRR neurons to play a causal role in ongoing decisions. In other words, perhaps PRR can be causally involved in decisions, but not in decisions based on attributes such as stimulus brightness. In fact, a study has shown that monkey PRR is capable of "ignoring" salience-driven response, when the task demands so (Kubanek et al., 2013). What are the other attributes that could allow PRR to play a causal role? One possibility is that PRR is instead more concerned with spatial attributes, such as location. Damage in the parietal cortex, as well as pharmacological inactivation of the same area, can lead to hemi-spatial neglect, a symptom characterised by reduced or lack of awareness on one side of space (Kubanek et al., 2015; Parton et al., 2004). In that regard, one could consider replacing the target brightness with a spatial feature, so that certain parts of space or limbs are associated with high or low reward magnitude (Larry Snyder, personal communication), to see if such information leads PRR to play a causal role in decisions. In fact, Mooshagian and Snyder showed that LIP activity is sensitive to response modality condition, such that the classically observed saccade-predictive activity during

saccade tasks (Andersen, Bracewell, et al., 1990) were abolished when the monkeys made natural saccades prior to reaching with both arms (Mooshagian & Snyder, 2018).

Overtraining

An inherent limitation of monkey electrophysiology is that in most cases, monkeys are extremely overtrained by the time the recordings are performed. This project was no exception, as both monkeys have been performing the same task for over a year before we implanted the recording chambers. In the result section of chapter 4, we reported that initially, monkey Y's reaction time distribution was comparable to that of humans. However, the observed difference between different trials conditions collapsed and disappeared following a few more sessions, likely due to overtraining. This raises concerns about the interpretation of the neural results. For example, if the monkey stopped treating the features as independent and instead memorised all of the combinations, the neural data would reflect the fact that each target is treated as one of 9 different categories (e.g., dim target with line at 4 o'clock = 1 drop, bright target with line at 8 o'clock = 3 drops, and so on). If the monkeys were performing the task with perfect categorisation, one would predict that there will be no difference in the choice latency between trial conditions, since a comparison of any pair of target categories should take the same duration regardless of the particular combination of features that define each category. It is also possible that their response times would vary as a function of the difficulty of the comparison, in which case we predict longer choice latency in conflict trials. The fact the reaction time distributions collapsed makes it difficult to test these possibilities, albeit the observed differences in the neural latencies suggest that trial conditions had an impact, at least in PMd.

FUTURE DIRECTIONS

Reversible Inactivation

Based on our results, we predict that reversible inactivation of PMd and PRR to have distinct effects on the behavioural responses. For example, pharmacological inactivation of PRR may reduce the likelihood of choosing the target in its receptive field during equivalued trials without affecting "easy" trials, similar to what has been reported by Katz and colleagues (Katz et al., 2016). In contrast, inactivation of PMd may reduce the likelihood of choosing targets based on "top-down" information.

Additional Attributes

In our project, the brightness attribute did not influence the PRR activity as much as we expected. An obvious mitigation strategy is to choose a different attribute that is likely to be processed in PRR, such as spatial attribute mentioned above. Another way to expand the project is to record from additional brain regions and introduce additional attributes. For example, studies have shown that neurons in dACC reflect action effort (Walton et al., 2003). Accordingly, we can predict that effort attribute may affect dACC more than other areas. Other possible attributes include target size, effector (e.g., arm vs eye), reward probability, reward palatability and reward delivery delay. It is also possible that a simultaneous presentation of all the attributes may result in the neural activity being dominated by salient features, thus one may consider sequentially revealing each attribute to investigate the influence of each attribute on different brain areas. Careful manipulation of the timing of stimulus presentation and the GO signal could reveal how different attributes are integrated, and may allow well-trained monkeys to change their mind mid-reach.

Closing the Loop

Similar to previous studies, our results revealed an internal anticipatory activity in a form of pre-stimulus baseline bias (Basso & Wurtz, 1998; Coe et al., 2002; Shadlen & Newsome, 2001). This suggests an opportunity to create a closed loop, such that the baseline fluctuation of multiple regions is monitored online, and a GO signal is given when one region is clearly leaning toward one option versus the other. If this manipulation affects choice ratio as a function of the fluctuation and bias magnitude, and if experimentally silencing this region reduces the decision in favour of its bias, one can interpret them as evidence supporting the role of baseline fluctuation in a particular region as causally affecting a subsequent decision.

The Rich Club

The concept of a "rich club" suggests that, in a recurrent network, certain hubs can be heavily connected to other nodes, resulting in a small subset of nodes having larger than expected influence on the network (Zamora-López et al., 2010). One curious question is whether those neurons with pre-stimulus baseline bias belong to the cortical rich club. A simple and feasible approach would be to analyse their spike-field coherency, to see if they have stronger connection within and between regions. A more ambitious approach involves techniques such as high-density probes, to see if the rich club has preferred connectivity depths and projection patterns.

CONCLUSION

We designed a task with the goal to dissociate two models explaining how decisions are made. Our results were incompatible with both models and pointed towards a third alternative that can be seen as lying in-between the two proposed models. Our behavioral results suggest that action decisions can sometimes occur before all available information is integrated. Our neural results suggest that PMd activity plays a causal role in decisions about actions, whereas PRR activity

reflects the ongoing decision but does not appear to play a causal role. Our rich results raise more questions than they answer, many of which are worth pursuing in future studies.

REFERENCES

Abballe, L., & Asari, H. (2022). Natural image statistics for mouse vision. *PLOS ONE*, *17*(1), e0262763. https://doi.org/10.1371/journal.pone.0262763

Allman, J. M., Tetreault, N. A., Hakeem, A. Y., & Park, S. (2011). The von economo neurons in apes and humans. *American Journal of Human Biology*, *23*(1), 5–21. https://doi.org/10.1002/ajhb.21136

Amiez, C., Joseph, J. P., & Procyk, E. (2006). Reward encoding in the monkey anterior cingulate cortex. *Cerebral Cortex*, *16*(7), 1040–1055. https://doi.org/10.1093/cercor/bhj046

Andersen, R. A., Asanuma, C., Essick, G., & Siegel, R. M. (1990). Corticocortical connections of anatomically and physiologically defined subdivisions within the inferior parietal lobule. *Journal of Comparative Neurology*, *296*(1), 65–113. https://doi.org/10.1002/cne.902960106

Andersen, R. A., Bracewell, R. M., Barash, S., Gnadt, J. W., & Fogassi, L. (1990). Eye position effects on visual, memory, and saccade-related activity in areas LIP and 7a of macaque. *Journal of Neuroscience*, *10*(4), 1176–1196.

Andersen, R. A., Snyder, L. H., Batista, A. P., Buneo, C. A., & Cohen, Y. E. (1998). Posterior parietal areas specialized for eye movements (LIP) and reach (PRR) using a common coordinate frame. *Novartis Foundation Symposium*, *218*, 109–122; discussion 122-128, 171–175.

Azevedo, F. A. C., Carvalho, L. R. B., Grinberg, L. T., Farfel, J. M., Ferretti, R. E. L., Leite, R. E. P., Filho, W. J., Lent, R., & Herculano-Houzel, S. (2009). Equal numbers of neuronal and nonneuronal cells make the human brain an isometrically scaled-up primate brain. *Journal of Comparative Neurology*, *513*(5), 532–541. https://doi.org/10.1002/cne.21974

Baddeley, A. D. (1992). Working memory. *Science*, *255*(5044), 556–559. https://doi.org/10.1126/science.1736359

Baddeley, A. D. (1996). Exploring the Central Executive. *The Quarterly Journal of Experimental Psychology Section A*, *49*(1), 5–28. https://doi.org/10.1080/713755608

Baddeley, A. D. (1998). The central executive: A concept and some misconceptions. *Journal of the International Neuropsychological Society*, *4*(5), 523–526.

Baddeley, A. D. (2003). Working memory: Looking back and looking forward. *Nature Reviews Neuroscience*, *4*(10), 829–839. https://doi.org/10.1038/nrn1201

Baddeley, A. D., Della Sala, S., Papagno, C., & Spinnler, H. (1997). Dual-task performance in dysexecutive and nondysexecutive patients with a frontal lesion. *Neuropsychology*, *11*(2), 187–194. https://doi.org/10.1037/0894-4105.11.2.187

Baddeley, A. D., & Hitch, G. (1974). Working Memory. In G. H. Bower (Ed.), *Psychology of Learning and Motivation* (Vol. 8, pp. 47–89). Academic Press. https://doi.org/10.1016/S0079-7421(08)60452-1

Baker, S. C., Rogers, R. D., Owen, A. M., Frith, C. D., Dolan, R. J., Frackowiak, R. S. J., & Robbins, T. W. (1996). Neural systems engaged by planning: A PET study of the Tower of London task. *Neuropsychologia*, *34*(6), 515–526. https://doi.org/10.1016/0028-3932(95)00133-6

Bakola, S., Passarelli, L., Gamberini, M., Fattori, P., & Galletti, C. (2013). Cortical connectivity suggests a role in limb coordination for macaque area PE of the superior parietal cortex. *Journal of Neuroscience*, *33*(15), 6648–6658. https://doi.org/10.1523/JNEUROSCI.4685-12.2013

Barrett, R. L. C., Dawson, M., Dyrby, T. B., Krug, K., Ptito, M., D'Arceuil, H., Croxson, P. L., Johnson, P. J., Howells, H., Forkel, S. J., Dell'Acqua, F., & Catani, M. (2020). Differences in Frontal Network Anatomy Across Primate Species. *Journal of Neuroscience*, *40*(10), 2094–2107. https://doi.org/10.1523/JNEUROSCI.1650-18.2019

Barsalou, L. W., Dutriaux, L., & Scheepers, C. (2018). Moving beyond the distinction between concrete and abstract concepts. *Philosophical Transactions of the Royal Society B: Biological Sciences*. https://royalsocietypublishing.org/doi/abs/10.1098/rstb.2017.0144

Basso, M. A., & Wurtz, R. H. (1998). Modulation of neuronal activity in superior colliculus by changes in target probability. *Journal of Neuroscience*, *18*(18), 7519–7534.

Basten, U., Biele, G., Heekeren, H. R., & Fiebach, C. J. (2010). How the brain integrates costs and benefits during decision making. *Proceedings of the National Academy of Sciences*, *107*(50), 21767–21772. https://doi.org/10.1073/pnas.0908104107

Blackwell, A. A., Köppen, J. R., Whishaw, I. Q., & Wallace, D. G. (2018). String-pulling for food by the rat: Assessment of movement, topography and kinematics of a bilaterally skilled forelimb act. *Learning and Motivation*, *61*, 63–73. https://doi.org/10.1016/j.lmot.2017.03.010

Bliss-Moreau, E., Costa, V. D., & Baxter, M. G. (2022). A pragmatic reevaluation of the efficacy of nonhuman primate optogenetics for psychiatry. *Oxford Open Neuroscience*, *1*. https://doi.org/10.1093/oons/kvac006

Borra, E., & Luppino, G. (2017). Functional anatomy of the macaque temporo-parieto-frontal connectivity. *Cortex*, *97*, 306–326. https://doi.org/10.1016/j.cortex.2016.12.007

Borutaite, V. (2010). Mitochondria as decision-makers in cell death. *Environmental and Molecular Mutagenesis*, *51*(5), 406–416. https://doi.org/10.1002/em.20564

Boyden, E. S., Zhang, F., Bamberg, E., Nagel, G., & Deisseroth, K. (2005). Millisecond-timescale, genetically targeted optical control of neural activity. *Nature Neuroscience*, *8*(9), Article 9. https://doi.org/10.1038/nn1525

Bruce, C. J., Goldberg, M. E., Bushnell, M. C., & Stanton, G. B. (1985). Primate frontal eye fields. II. Physiological and anatomical correlates of electrically evoked eye movements. *Journal of Neurophysiology*, *54*(3), 714–734. https://doi.org/10.1152/jn.1985.54.3.714

Buneo, C. A., Jarvis, M. R., Batista, A. P., & Andersen, R. A. (2002). Direct visuomotor transformations for reaching. *Nature*, *416*(6881), 632. https://doi.org/10.1038/416632a

Buschman, T. J., & Miller, E. K. (2007). Top-Down Versus Bottom-Up Control of Attention in the Prefrontal and Posterior Parietal Cortices. *Science*, *315*(5820), 1860–1862. https://doi.org/10.1126/science.1138071

Busemeyer, J. R., Gluth, S., Rieskamp, J., & Turner, B. M. (2019). Cognitive and Neural Bases of Multi-Attribute, Multi-Alternative, Value-based Decisions. *Trends in Cognitive Sciences*, *23*(3), 251–263. https://doi.org/10.1016/j.tics.2018.12.003

Busemeyer, J. R., & Townsend, J. T. (1993). Decision field theory: A dynamic-cognitive approach to decision making in an uncertain environment. *Psychological Review*, *100*(3), 432–459. https://doi.org/10.1037/0033-295x.100.3.432

Cai, X., & Padoa-Schioppa, C. (2019). Neuronal evidence for good-based economic decisions under variable action costs. *Nature Communications*, *10*(1), 393. https://doi.org/10.1038/s41467-018-08209-3

Caminiti, R., Ferraina, S., & Johnson, P. B. (1996). The sources of visual information to the primate frontal lobe: A novel role for the superior parietal lobule. *Cerebral Cortex*, *6*(3), 319–328. https://doi.org/10.1093/cercor/6.3.319

Caplette, L. (2023). *Simple RM/Mixed ANOVA for any design* [Computer software]. https://www.mathworks.com/matlabcentral/fileexchange/64980-simple-rm-mixed-anova-for-any-design

Carandini, M., & Heeger, D. J. (2012). Normalization as a canonical neural computation. *Nature Reviews Neuroscience*, *13*(1), Article 1. https://doi.org/10.1038/nrn3136

Caselli, L., & Chelazzi, L. (2011). Does the Macaque Monkey Provide a Good Model for Studying Human Executive Control? A Comparative Behavioral Study of Task Switching. *PLOS ONE*, *6*(6), e21489. https://doi.org/10.1371/journal.pone.0021489

Cecala, A. L., Kozak, R. A., Pruszynski, J. A., & Corneil, B. D. (2023). Done in 65 ms: Express Visuomotor Responses in Upper Limb Muscles in Rhesus Macaques. *eNeuro*, *10*(8). https://doi.org/10.1523/ENEURO.0078-23.2023

Chang, S. W. C., Gariépy, J.-F., & Platt, M. L. (2013). Neuronal reference frames for social decisions in primate frontal cortex. *Nature Neuroscience*, *16*(2), 243–250. https://doi.org/10.1038/nn.3287

Chang, S. W. C., & Snyder, L. H. (2012). The representations of reach endpoints in posterior parietal cortex depend on which hand does the reaching. *Journal of Neurophysiology*, *107*(9), 2352–2365. https://doi.org/10.1152/jn.00852.2011

Chen, C.-Y., Matrov, D., Veale, R., Onoe, H., Yoshida, M., Miura, K., & Isa, T. (2021). Properties of visually guided saccadic behavior and bottom-up attention in marmoset, macaque, and human. *Journal of Neurophysiology*, *125*(2), 437–457. https://doi.org/10.1152/jn.00312.2020

Christopoulos, V. N., Bonaiuto, J., Kagan, I., & Andersen, R. A. (2015). Inactivation of Parietal Reach Region Affects Reaching but not Saccade Choices in Internally Guided Decisions.

Journal of Neuroscience, *35*(33), 11719–11728. https://doi.org/10.1523/JNEUROSCI.1068-15.2015

Churchland, M. M., Santhanam, G., & Shenoy, K. V. (2006). Preparatory Activity in Premotor and Motor Cortex Reflects the Speed of the Upcoming Reach. *Journal of Neurophysiology*, *96*(6), 3130–3146. https://doi.org/10.1152/jn.00307.2006

Cisek, P. (1999). Beyond the Computer Metaphor: Behavior as Interaction. *Journal of Consciousness Studies*, *6*(11–12), 125–142.

Cisek, P. (2007). Cortical Mechanisms of Action Selection: The Affordance Competition Hypothesis. *Philosophical Transactions of the Royal Society B: Biological Sciences*, *362*(1485), 1585–1599. https://doi.org/10.1098/rstb.2007.2054

Cisek, P. (2012). Making decisions through a distributed consensus. *Current Opinion in Neurobiology*, *22*(6), 927–936. https://doi.org/10.1016/j.conb.2012.05.007

Cisek, P. (2019). Resynthesizing behavior through phylogenetic refinement. *Attention, Perception & Psychophysics*, *81*(7), 2265–2287. https://doi.org/10.3758/s13414-019-01760-1

Cisek, P., & Kalaska, J. F. (2005). Neural Correlates of Reaching Decisions in Dorsal Premotor Cortex: Specification of Multiple Direction Choices and Final Selection of Action. *Neuron*, *45*(5), 801–814. https://doi.org/10.1016/j.neuron.2005.01.027

Clarke, H., Walker, S., Dalley, J., Robbins, T., & Roberts, A. (2007). Cognitive Inflexibility after Prefrontal Serotonin Depletion Is Behaviorally and Neurochemically Specific. *Cerebral Cortex*, *17*(1), 18–27. https://doi.org/10.1093/cercor/bhj120

Coe, B., Tomihara, K., Matsuzawa, M., & Hikosaka, O. (2002). Visual and Anticipatory Bias in Three Cortical Eye Fields of the Monkey during an Adaptive Decision-Making Task.

Journal of Neuroscience, *22*(12), 5081–5090. https://doi.org/10.1523/JNEUROSCI.22-12-05081.2002

Colby, C. L., Duhamel, J. R., & Goldberg, M. E. (1996). Visual, presaccadic, and cognitive activation of single neurons in monkey lateral intraparietal area. *Journal of Neurophysiology*, *76*(5), 2841–2852.

Colby, C. L., & Goldberg, M. E. (1999). Space and Attention in Parietal Cortex. *Annual Review of Neuroscience*, *22*(1), 319–349. https://doi.org/10.1146/annurev.neuro.22.1.319

Collin, S. P., Knight, M. A., Davies, W. L., Potter, I. C., Hunt, D. M., & Trezise, A. E. O. (2003). Ancient colour vision: Multiple opsin genes in the ancestral vertebrates. *Current Biology*, *13*(22), R864–R865. https://doi.org/10.1016/j.cub.2003.10.044

Constantinidis, C., Franowicz, M. N., & Goldman-Rakic, P. S. (2001). The sensory nature of mnemonic representation in the primate prefrontal cortex. *Nature Neuroscience*, *4*(3), 311. https://doi.org/10.1038/85179

Contemori, S., Loeb, G. E., Corneil, B. D., Wallis, G., & Carroll, T. J. (2022). Symbolic cues enhance express visuomotor responses in human arm muscles at the motor planning rather than the visuospatial processing stage. *Journal of Neurophysiology*, *128*(3), 494–510. https://doi.org/10.1152/jn.00136.2022

Cos, I., Bélanger, N., & Cisek, P. (2011). The influence of predicted arm biomechanics on decision making. *Journal of Neurophysiology*, *105*(6), 3022–3033. https://doi.org/10.1152/jn.00975.2010

Critchley, H. D., & Rolls, E. T. (1996). Hunger and satiety modify the responses of olfactory and visual neurons in the primate orbitofrontal cortex. *Journal of Neurophysiology*, *75*(4), 1673–1686.

Croxson, P. L., Forkel, S. J., Cerliani, L., & Thiebaut de Schotten, M. (2018). Structural Variability Across the Primate Brain: A Cross-Species Comparison. *Cerebral Cortex*, *28*(11), 3829–3841. https://doi.org/10.1093/cercor/bhx244

Croxson, P. L., Johansen-Berg, H., Behrens, T. E. J., Robson, M. D., Pinsk, M. A., Gross, C. G., Richter, W., Richter, M. C., Kastner, S., & Rushworth, M. F. S. (2005). Quantitative Investigation of Connections of the Prefrontal Cortex in the Human and Macaque using Probabilistic Diffusion Tractography. *Journal of Neuroscience*, *25*(39), 8854–8866. https://doi.org/10.1523/JNEUROSCI.1311-05.2005

Croxson, P. L., Walton, M. E., O'Reilly, J. X., Behrens, T. E. J., & Rushworth, M. F. S. (2009). Effort-based cost-benefit valuation and the human brain. *Journal of Neuroscience*, *29*(14), 4531–4541. https://doi.org/10.1523/JNEUROSCI.4515-08.2009

Cui, H., & Andersen, R. A. (2007). Posterior Parietal Cortex Encodes Autonomously Selected Motor Plans. *Neuron*, *56*(3), 552–559. https://doi.org/10.1016/j.neuron.2007.09.031

Cunningham, J. P., & Yu, B. M. (2014). Dimensionality reduction for large-scale neural recordings. *Nature Neuroscience*, *17*(11), Article 11. https://doi.org/10.1038/nn.3776

Curtis, C. E., & D'Esposito, M. (2003). Persistent activity in the prefrontal cortex during working memory. *Trends in Cognitive Sciences*, *7*(9), 415–423. https://doi.org/10.1016/S1364-6613(03)00197-9

Dacey, D. M. (2000). Parallel Pathways for Spectral Coding in Primate Retina. *Annual Review of Neuroscience*, *23*(1), 743–775. https://doi.org/10.1146/annurev.neuro.23.1.743

de Schotten, M. T., Dell'Acqua, F., Forkel, S. J., Simmons, A., Vergani, F., Murphy, D. G. M., & Catani, M. (2011). A lateralized brain network for visuospatial attention. *Nature Neuroscience*, *14*(10), 1245–1246. https://doi.org/10.1038/nn.2905

Del Bene, F., & Wyart, C. (2012). Optogenetics: A new enlightenment age for zebrafish neurobiology. *Developmental Neurobiology*, *72*(3), 404–414. https://doi.org/10.1002/dneu.20914

Delgado, M. R., Beer, J. S., Fellows, L. K., Huettel, S. A., Platt, M. L., Quirk, G. J., & Schiller, D. (2016). Viewpoints: Dialogues on the functional role of the ventromedial prefrontal cortex. *Nature Neuroscience*, *19*(12), 1545–1552. https://doi.org/10.1038/nn.4438

Della Sala, S., Baddeley, A. D., Papagno, C., & Spinnler, H. (1995). Dual-task paradigm: A means to examine the central executive. *Annals of the New York Academy of Sciences*, *769*, 161–171.

Desimone, R., & Duncan, J. (1995). Neural Mechanisms of Selective Visual Attention. *Annual Review of Neuroscience*, *18*, 193–222. https://doi.org/10.1146/annurev.ne.18.030195.001205

Dias, R., Robbins, T. W., & Roberts, A. C. (1996). Dissociation in prefrontal cortex of affective and attentional shifts. *Nature*, *380*(6569), 69–72. https://doi.org/10.1038/380069a0

DiCarlo, J. J., Zoccolan, D., & Rust, N. C. (2012). How does the brain solve visual object recognition? *Neuron*, *73*(3), 415–434. https://doi.org/10.1016/j.neuron.2012.01.010

Diederich, A. (2003). MDFT account of decision making under time pressure. *Psychonomic Bulletin & Review*, *10*(1), 157–166. https://doi.org/10.3758/BF03196480

Donner, T. H., Kettermann, A., Diesch, E., Ostendorf, F., Villringer, A., & Brandt, S. A. (2002). Visual Feature and Conjunction Searches of Equal Difficulty Engage Only Partially Overlapping Frontoparietal Networks. *NeuroImage*, *15*(1), 16–25. https://doi.org/10.1006/nimg.2001.0951

Dum, R. P., & Strick, P. L. (2002). Motor areas in the frontal lobe of the primate. *Physiology & Behavior*, *77*(4), 677–682. https://doi.org/10.1016/S0031-9384(02)00929-0

Engel, A. K., Maye, A., Kurthen, M., & König, P. (2013). Where's the action? The pragmatic turn in cognitive science. *Trends in Cognitive Sciences*, *17*(5), 202–209. https://doi.org/10.1016/j.tics.2013.03.006

Evans, N. J., & Hawkins, G. E. (2019). When humans behave like monkeys: Feedback delays and extensive practice increase the efficiency of speeded decisions. *Cognition*, *184*, 11–18. https://doi.org/10.1016/j.cognition.2018.11.014

Evrard, H. C., Forro, T., & Logothetis, N. K. (2012). Von Economo neurons in the anterior insula of the macaque monkey. *Neuron*, *74*(3), 482–489. https://doi.org/10.1016/j.neuron.2012.03.003

Falótico, T. (2022). Robust capuchin tool use cognition in the wild. *Current Opinion in Behavioral Sciences*, *46*, 101170. https://doi.org/10.1016/j.cobeha.2022.101170

Fechner, G. T. (1948). Elements of psychophysics, 1860. In *Readings in the history of psychology* (pp. 206–213). Appleton-Century-Crofts. https://doi.org/10.1037/11304-026

Ferstl, E. C., Neumann, J., Bogler, C., & Cramon, D. Y. von. (2008). The extended language network: A meta-analysis of neuroimaging studies on text comprehension. *Human Brain Mapping*, *29*(5), 581–593. https://doi.org/10.1002/hbm.20422

FitzGerald, T. H. B., Seymour, B., & Dolan, R. J. (2009). The Role of Human Orbitofrontal Cortex in Value Comparison for Incommensurable Objects. *Journal of Neuroscience*, *29*(26), 8388–8395. https://doi.org/10.1523/JNEUROSCI.0717-09.2009

Fogassi, L., Ferrari, P. F., Gesierich, B., Rozzi, S., Chersi, F., & Rizzolatti, G. (2005). Parietal lobe: From action organization to intention understanding. *Science*, *308*(5722), 662–667. https://doi.org/10.1126/science.1106138

Freedman, D. J., Riesenhuber, M., Poggio, T., & Miller, E. K. (2002). Visual Categorization and the Primate Prefrontal Cortex: Neurophysiology and Behavior. *Journal of Neurophysiology*, *88*(2), 929–941. https://doi.org/10.1152/jn.2002.88.2.929

Funahashi, S., Bruce, C. J., & Goldman-Rakic, P. S. (1989). Mnemonic coding of visual space in the monkey's dorsolateral prefrontal cortex. *Journal of Neurophysiology*, *61*(2), 331–349. https://doi.org/10.1152/jn.1989.61.2.331

Gail, A., & Andersen, R. A. (2006). Neural Dynamics in Monkey Parietal Reach Region Reflect Context-Specific Sensorimotor Transformations. *Journal of Neuroscience*, *26*(37), 9376–9384. https://doi.org/10.1523/JNEUROSCI.1570-06.2006

Gallagher, M., McMahan, R. W., & Schoenbaum, G. (1999). Orbitofrontal Cortex and Representation of Incentive Value in Associative Learning. *Journal of Neuroscience*, *19*(15), 6610–6614.

Galletti, C., & Fattori, P. (2018). The dorsal visual stream revisited: Stable circuits or dynamic pathways? *Cortex*, *98*, 203–217. https://doi.org/10.1016/j.cortex.2017.01.009

Ganel, T., Chajut, E., & Algom, D. (2008). Visual coding for action violates fundamental psychophysical principles. *Current Biology*, *18*(14), R599–R601. https://doi.org/10.1016/j.cub.2008.04.052

Gesemann, M., & Neuhauss, S. C. F. (2023). Evolution of visual guanylyl cyclases and their activating proteins with respect to clade and species-specific visual system adaptation.

Frontiers in Molecular Neuroscience, *16*. https://www.frontiersin.org/articles/10.3389/fnmol.2023.1131093

Gharbawie, O. A., Gonzalez, C. L. R., & Whishaw, I. Q. (2005). Skilled reaching impairments from the lateral frontal cortex component of middle cerebral artery stroke: A qualitative and quantitative comparison to focal motor cortex lesions in rats. *Behavioural Brain Research*, *156*(1), 125–137. https://doi.org/10.1016/j.bbr.2004.05.015

Gibson, J. J. (1979). *The Ecological Approach to Visual Perception*. Houghton Mifflin. https://doi.org/10.4324/9781315740218

Glimcher, P. W., & Sparks, D. L. (1992). Movement selection in advance of action in the superior colliculus. *Nature*, *355*(6360), 542–545. https://doi.org/10.1038/355542a0

Gold, J. I., & Shadlen, M. N. (2007). The Neural Basis of Decision Making. *Annual Review of Neuroscience*, *30*(1), 535–574. https://doi.org/10.1146/annurev.neuro.29.051605.113038

Goodale, M. A., & Milner, A. D. (1992). Separate visual pathways for perception and action. *Trends in Neurosciences*, *15*(1), 20–25. https://doi.org/10.1016/0166-2236(92)90344-8

Goodwin, S. J., Blackman, R. K., Sakellaridi, S., & Chafee, M. V. (2012). Executive Control Over Cognition: Stronger and Earlier Rule-Based Modulation of Spatial Category Signals in Prefrontal Cortex Relative to Parietal Cortex. *Journal of Neuroscience*, *32*(10), 3499–3515. https://doi.org/10.1523/JNEUROSCI.3585-11.2012

Gottfried, J. A., O'Doherty, J., & Dolan, R. J. (2003). Encoding Predictive Reward Value in Human Amygdala and Orbitofrontal Cortex. *Science*, *301*(5636), 1104–1107. https://doi.org/10.1126/science.1087919

Gottlieb, J. (2007). From Thought to Action: The Parietal Cortex as a Bridge between Perception, Action, and Cognition. *Neuron*, *53*(1), 9–16. https://doi.org/10.1016/j.neuron.2006.12.009

Hackett, T. A., Preuss, T. M., & Kaas, J. H. (2001). Architectonic identification of the core region in auditory cortex of macaques, chimpanzees, and humans. *Journal of Comparative Neurology*, *441*(3), 197–222. https://doi.org/10.1002/cne.1407

Hadland, K. A. (2002). The Anterior Cingulate and Reward-Guided Selection of Actions. *Journal of Neurophysiology*, *89*(2), 1161–1164. https://doi.org/10.1152/jn.00634.2002

Hall, N. J., Herzfeld, D. J., & Lisberger, S. G. (2021). Evaluation and resolution of many challenges of neural spike sorting: A new sorter. *Journal of Neurophysiology*, *126*(6), 2065–2090. https://doi.org/10.1152/jn.00047.2021

Hanes, D. P., & Schall, J. D. (1996). Neural Control of Voluntary Movement Initiation. *Science*, *274*(5286), 427–430. https://doi.org/10.1126/science.274.5286.427

Hanks, T. D., Ditterich, J., & Shadlen, M. N. (2006). Microstimulation of macaque area LIP affects decision-making in a motion discrimination task. *Nature Neuroscience*, *9*(5), 682–689. https://doi.org/10.1038/nn1683

Harris, Z. S. (1970). From Phoneme to Morpheme. In Z. S. Harris (Ed.), *Papers in Structural and Transformational Linguistics* (pp. 32–67). Springer Netherlands. https://doi.org/10.1007/978-94-017-6059-1_2

He, S. Q., Dum, R. P., & Strick, P. L. (1993). Topographic organization of corticospinal projections from the frontal lobe: Motor areas on the lateral surface of the hemisphere. *Journal of Neuroscience*, *13*(3), 952–980. https://doi.org/10.1523/JNEUROSCI.13-03-00952.1993

Herculano-Houzel, S., Collins, C. E., Wong, P., & Kaas, J. H. (2007). Cellular scaling rules for primate brains. *Proceedings of the National Academy of Sciences*, *104*(9), 3562–3567. https://doi.org/10.1073/pnas.0611396104

Hernández, A., Zainos, A., & Romo, R. (2000). Neuronal correlates of sensory discrimination in the somatosensory cortex. *Proceedings of the National Academy of Sciences*, *97*(11), 6191–6196. https://doi.org/10.1073/pnas.120018597

Hikosaka, K., & Watanabe, M. (2000). Delay Activity of Orbital and Lateral Prefrontal Neurons of the Monkey Varying with Different Rewards. *Cerebral Cortex*, *10*(3), 263–271. https://doi.org/10.1093/cercor/10.3.263

Hitch, G. J., Hu, Y., Allen, R. J., & Baddeley, A. D. (2018). Competition for the focus of attention in visual working memory: Perceptual recency versus executive control. *Annals of the New York Academy of Sciences*, *1424*(1), 64–75. https://doi.org/10.1111/nyas.13631

Hogan, N. (1985). Impedance control—An approach to manipulation. I - Theory. II - Implementation. III - Applications. *ASME Journal of Dynamic Systems and Measurement Control B*, *107*, 1–24.

Hosokawa, T., Kato, K., Inoue, M., & Mikami, A. (2007). Neurons in the macaque orbitofrontal cortex code relative preference of both rewarding and aversive outcomes. *Neuroscience Research*, *57*(3), 434–445. https://doi.org/10.1016/j.neures.2006.12.003

Hunt, L. T., Dolan, R. J., & Behrens, T. E. J. (2014). Hierarchical competitions subserving multi-attribute choice. *Nature Neuroscience*, *17*(11), Article 11. https://doi.org/10.1038/nn.3836

Hurley, S. (2001). Perception And Action: Alternative Views. *Synthese*, *129*(1), 3–40. https://doi.org/10.1023/A:1012643006930

Iba, M., & Sawaguchi, T. (2003). Involvement of the Dorsolateral Prefrontal Cortex of Monkeys in Visuospatial Target Selection. *Journal of Neurophysiology*, *89*(1), 587–599. https://doi.org/10.1152/jn.00148.2002

Ikeda, T., & Hikosaka, O. (2003). Reward-Dependent Gain and Bias of Visual Responses in Primate Superior Colliculus. *Neuron*, *39*(4), 693–700. https://doi.org/10.1016/S0896-6273(03)00464-1

Jacobs, G. H., Deegan, J. F., Crognale, M. A., & Fenwick, J. A. (1993). Photopigments of dogs and foxes and their implications for canid vision. *Visual Neuroscience*, *10*(1), 173–180. https://doi.org/10.1017/S0952523800003291

Jacobs, I., & Osvath, M. (2023). Tool use and tooling in ravens (Corvus corax): A review and novel observations. *Ethology*, *129*(3), 169–181. https://doi.org/10.1111/eth.13352

Janik, V. M. (2014). Cetacean vocal learning and communication. *Current Opinion in Neurobiology*, *28*, 60–65. https://doi.org/10.1016/j.conb.2014.06.010

Jarvis, E. D. (2007). Neural systems for vocal learning in birds and humans: A synopsis. *Journal of Ornithology*, *148*(1), 35–44. https://doi.org/10.1007/s10336-007-0243-0

Johnson, P. B., Ferraina, S., Bianchi, L., & Caminiti, R. (1996). Cortical Networks for Visual Reaching: Physiological and Anatomical Organization of Frontal and Parietal Lobe Arm Regions. *Cerebral Cortex*, *6*(2), 102–119. https://doi.org/10.1093/cercor/6.2.102

Jonas, E., & Kording, K. P. (2017). Could a Neuroscientist Understand a Microprocessor? *PLOS Computational Biology*, *13*(1), e1005268. https://doi.org/10.1371/journal.pcbi.1005268

Jones, J. P., & Palmer, L. A. (1987). An evaluation of the two-dimensional Gabor filter model of simple receptive fields in cat striate cortex. *Journal of Neurophysiology*, *58*(6), 1233–1258.

Juechems, K., Balaguer, J., Ruz, M., & Summerfield, C. (2017). Ventromedial Prefrontal Cortex Encodes a Latent Estimate of Cumulative Reward. *Neuron*, *93*(3), 705-714.e4. https://doi.org/10.1016/j.neuron.2016.12.038

Kable, J. W., & Glimcher, P. W. (2007). The neural correlates of subjective value during intertemporal choice. *Nature Neuroscience*, *10*(12), Article 12. https://doi.org/10.1038/nn2007

Kable, J. W., & Glimcher, P. W. (2009). The Neurobiology of Decision: Consensus and Controversy. *Neuron*, *63*(6), 733–745. https://doi.org/10.1016/j.neuron.2009.09.003

Kahnt, T., Heinzle, J., Park, S. Q., & Haynes, J.-D. (2011). Decoding different roles for vmPFC and dlPFC in multi-attribute decision making. *NeuroImage*, *56*(2), 709–715. https://doi.org/10.1016/j.neuroimage.2010.05.058

Katz, L., Yates, J., Pillow, J. W., & Huk, A. (2016). Dissociated functional significance of choice-related activity across the primate dorsal stream. *Nature*, *535*(7611), Salt Lake City USA. https://doi.org/10.1038/nature18617

Kaufman, L. D., Pratt, J., Levine, B., & Black, S. E. (2012). Executive Deficits Detected in Mild Alzheimer's Disease Using the Antisaccade Task. *Brain and Behavior*, *2*(1), 15–21. https://doi.org/10.1002/brb3.28

Kawagoe, R., Takikawa, Y., & Hikosaka, O. (1998). Expectation of reward modulates cognitive signals in the basal ganglia. *Nature Neuroscience*, *1*(5), 411–416. https://doi.org/10.1038/1625

Kennerley, S. W., Walton, M. E., Behrens, T. E. J., Buckley, M. J., & Rushworth, M. F. S. (2006). Optimal decision making and the anterior cingulate cortex. *Nature Neuroscience*, *9*(7), Article 7. https://doi.org/10.1038/nn1724

Khan, A. Z., Munoz, D. P., Takahashi, N., Blohm, G., & McPeek, R. M. (2016). Effects of a pretarget distractor on saccade reaction times across space and time in monkeys and humans. *Journal of Vision*, *16*(7), 5. https://doi.org/10.1167/16.7.5

Killeen, P. R., Cate, H., & Tran, T. (1993). Scaling Pigeons' Choice of Feeds: Bigger Is Better. *Journal of the Experimental Analysis of Behavior*, *60*(1), 203–217. https://doi.org/10.1901/jeab.1993.60-203

Kim, J.-N., & Shadlen, M. N. (1999). Neural correlates of a decision in the dorsolateral prefrontal cortex of the macaque. *Nature Neuroscience*, *2*(2), 176. https://doi.org/10.1038/5739

Kingstone, A., & Klein, R. M. (1993). What are human express saccades? *Perception & Psychophysics*, *54*(2), 260–273. https://doi.org/10.3758/BF03211762

Klaes, C., Westendorff, S., Chakrabarti, S., & Gail, A. (2011). Choosing Goals, Not Rules: Deciding among Rule-Based Action Plans. *Neuron*, *70*(3), 536–548. https://doi.org/10.1016/j.neuron.2011.02.053

Klein-Flügge, M. C., Kennerley, S. W., Friston, K., & Bestmann, S. (2016). Neural Signatures of Value Comparison in Human Cingulate Cortex during Decisions Requiring an Effort-Reward Trade-off. *Journal of Neuroscience*, *36*(39), 10002–10015. https://doi.org/10.1523/JNEUROSCI.0292-16.2016

Komatsu, H., & Suzuki, H. (1985). Projections from the functional subdivisions of the frontal eye field to the superior colliculus in the monkey. *Brain Research*, *327*(1), 324–327. https://doi.org/10.1016/0006-8993(85)91528-8

Kondrashev, S. L. (2023). Trichromatic vision in toads: Evidence from preference for colour objects during mate choice. *Behaviour*, *160*(8–9), 753–784. https://doi.org/10.1163/1568539X-bja10233

Krajbich, I., & Rangel, A. (2011). Multialternative drift-diffusion model predicts the relationship between visual fixations and choice in value-based decisions. *Proceedings of the National Academy of Sciences*, *108*(33), 13852–13857. https://doi.org/10.1073/pnas.1101328108

Kravitz, D. J., Saleem, K. S., Baker, C. I., Ungerleider, L. G., & Mishkin, M. (2013). The ventral visual pathway: An expanded neural framework for the processing of object quality. *Trends in Cognitive Sciences*, *17*(1), 26–49. https://doi.org/10.1016/j.tics.2012.10.011

Kubanek, J., Li, J. M., & Snyder, L. H. (2015). Motor role of parietal cortex in a monkey model of hemispatial neglect. *Proceedings of the National Academy of Sciences of the United States of America*, *112*(16), E2067–E2072. https://doi.org/10.1073/pnas.1418324112

Kubanek, J., & Snyder, L. H. (2015). Reward-Based Decision Signals in Parietal Cortex Are Partially Embodied. *Journal of Neuroscience*, *35*(12), 4869–4881. https://doi.org/10.1523/JNEUROSCI.4618-14.2015

Kubanek, J., Wang, C., & Snyder, L. H. (2013). Neuronal responses to target onset in oculomotor and somatomotor parietal circuits differ markedly in a choice task. *Journal of Neurophysiology*, *110*(10), 2247–2256. https://doi.org/10.1152/jn.00968.2012

Kunita, K., & Fujiwara, K. (2022). Influence of sports experience on distribution of pro-saccade reaction time under gap condition. *Journal of Physiological Anthropology*, *41*(1), 4. https://doi.org/10.1186/s40101-022-00277-1

Lauwereyns, J., Watanabe, K., Coe, B., & Hikosaka, O. (2002). A neural correlate of response bias in monkey caudate nucleus. *Nature*, *418*(6896), Article 6896. https://doi.org/10.1038/nature00892

Ledberg, A., Bressler, S. L., Ding, M., Coppola, R., & Nakamura, R. (2007). Large-Scale Visuomotor Integration in the Cerebral Cortex. *Cerebral Cortex*, *17*(1), 44–62. https://doi.org/10.1093/cercor/bhj123

Lee, C., Rohrer, W. H., & Sparks, D. L. (1988). Population coding of saccadic eye movements by neurons in the superior colliculus. *Nature*, *332*(6162), 357–360. https://doi.org/10.1038/332357a0

Levy, D. J., & Glimcher, P. W. (2012). The root of all value: A neural common currency for choice. *Current Opinion in Neurobiology*, *22*(6), 1027–1038. https://doi.org/10.1016/j.conb.2012.06.001

Lewis, J. W., & Van Essen, D. C. (2000). Corticocortical connections of visual, sensorimotor, and multimodal processing areas in the parietal lobe of the macaque monkey. *Journal of Comparative Neurology*, *428*(1), 112–137. https://doi.org/10.1002/1096-9861(20001204)428:1<112::AID-CNE8>3.0.CO;2-9

Li, C.-S. R., Padoa-Schioppa, C., & Bizzi, E. (2001). Neuronal Correlates of Motor Performance and Motor Learning in the Primary Motor Cortex of Monkeys Adapting to an External Force Field. *Neuron*, *30*(2), 593–607. https://doi.org/10.1016/S0896-6273(01)00301-4

Li, L., Hu, X., Preuss, T. M., Glasser, M. F., Damen, F. W., Qiu, Y., & Rilling, J. (2013). Mapping putative hubs in human, chimpanzee and rhesus macaque connectomes via diffusion tractography. *NeuroImage*, *80*, 462–474. https://doi.org/10.1016/j.neuroimage.2013.04.024

Lim, S.-L., O'Doherty, J. P., & Rangel, A. (2013). Stimulus Value Signals in Ventromedial PFC Reflect the Integration of Attribute Value Signals Computed in Fusiform Gyrus and Posterior Superior Temporal Gyrus. *Journal of Neuroscience*, *33*(20), 8729–8741. https://doi.org/10.1523/JNEUROSCI.4809-12.2013

Louie, K., & Glimcher, P. W. (2010). Separating Value from Choice: Delay Discounting Activity in the Lateral Intraparietal Area. *Journal of Neuroscience*, *30*(16), 5498–5507. https://doi.org/10.1523/JNEUROSCI.5742-09.2010

Luppino, G., & Rizzolatti, G. (2000). The Organization of the Frontal Motor Cortex. *Physiology*, *15*(5), 219–224. https://doi.org/10.1152/physiologyonline.2000.15.5.219

Lusignan, T. (2022). *Potentiels de champ locaux lors d'une prise de décision à plusieurs facteurs*. https://papyrus.bib.umontreal.ca/xmlui/handle/1866/27206

MacDonald, A. W., Cohen, J. D., Stenger, V. A., & Carter, C. S. (2000). Dissociating the Role of the Dorsolateral Prefrontal and Anterior Cingulate Cortex in Cognitive Control. *Science*, *288*(5472), 1835–1838. https://doi.org/10.1126/science.288.5472.1835

Marino, L. (1998). A Comparison of Encephalization between Odontocete Cetaceans and Anthropoid Primates. *Brain Behavior and Evolution*, *51*(4), 230–238. https://doi.org/10.1159/000006540

Markov, N. T., Ercsey-Ravasz, M. M., Ribeiro Gomes, A. R., Lamy, C., Magrou, L., Vezoli, J., Misery, P., Falchier, A., Quilodran, R., Gariel, M. A., Sallet, J., Gamanut, R., Huissoud, C., Clavagnier, S., Giroud, P., Sappey-Marinier, D., Barone, P., Dehay, C., Toroczkai, Z., … Kennedy, H. (2014). A weighted and directed interareal connectivity matrix for macaque cerebral cortex. *Cerebral Cortex*, *24*(1), 17–36. https://doi.org/10.1093/cercor/bhs270

Marks, L. E., & Algom, D. (1998). Chapter 2—Psychophysical Scaling. In M. H. Birnbaum (Ed.), *Measurement, Judgment and Decision Making* (pp. 81–178). Academic Press. https://doi.org/10.1016/B978-012099975-0.50004-X

Matelli, M., Luppino, G., & Rizzolatti, G. (1985). Patterns of cytochrome oxidase activity in the frontal agranular cortex of the macaque monkey. *Behavioural Brain Research*, *18*(2), 125–136. https://doi.org/10.1016/0166-4328(85)90068-3

Maunsell, J. H., & Gibson, J. R. (1992). Visual response latencies in striate cortex of the macaque monkey. *Journal of Neurophysiology*, *68*(4), 1332–1344. https://doi.org/10.1152/jn.1992.68.4.1332

Maunsell, J. H. R., Ghose, G. M., Assad, J. A., McADAMS, C. J., Boudreau, C. E., & Noerager, B. D. (1999). Visual response latencies of magnocellular and parvocellular LGN neurons in macaque monkeys. *Visual Neuroscience*, *16*(1), 1–14.

McPeek, R. M., & Keller, E. L. (2002). Saccade Target Selection in the Superior Colliculus During a Visual Search Task. *Journal of Neurophysiology*, *88*(4), 2019–2034. https://doi.org/10.1152/jn.2002.88.4.2019

Mesgarani, N., David, S. V., Fritz, J. B., & Shamma, S. A. (2014). Mechanisms of noise robust representation of speech in primary auditory cortex. *Proceedings of the National Academy of Sciences of the United States of America*, *111*(18), 6792–6797. https://doi.org/10.1073/pnas.1318017111

Messier, J., & Kalaska, J. F. (2000). Covariation of Primate Dorsal Premotor Cell Activity With Direction and Amplitude During a Memorized-Delay Reaching Task. *Journal of Neurophysiology*, *84*(1), 152–165. https://doi.org/10.1152/jn.2000.84.1.152

Metz, G. A. S., & Whishaw, I. Q. (2000). Skilled reaching an action pattern: Stability in rat (Rattus norvegicus) grasping movements as a function of changing food pellet size. *Behavioural Brain Research*, *116*(2), 111–122. https://doi.org/10.1016/S0166-4328(00)00245-X

Miller, E. K., Erickson, C. A., & Desimone, R. (1996). Neural Mechanisms of Visual Working Memory in Prefrontal Cortex of the Macaque. *Journal of Neuroscience*, *16*(16), 5154–5167. https://doi.org/10.1523/JNEUROSCI.16-16-05154.1996

Milosavljevic, M., Malmaud, J., Huth, A., Koch, C., & Rangel, A. (2010). The Drift Diffusion Model can account for the accuracy and reaction time of value-based choices under high and low time pressure. *Judgment and Decision Making*, *5*(6), 437–449. https://doi.org/10.1017/S1930297500001285

Mishkin, M., & Ungerleider, L. G. (1982). Contribution of striate inputs to the visuospatial functions of parieto-preoccipital cortex in monkeys. *Behavioural Brain Research*, *6*(1), 57–77. https://doi.org/10.1016/0166-4328(82)90081-X

Mogenson, G. J., Jones, D. L., & Yim, C. Y. (1980). From motivation to action: Functional interface between the limbic system and the motor system. *Progress in Neurobiology*, *14*(2), 69–97. https://doi.org/10.1016/0301-0082(80)90018-0

Monosov, I. E., & Hikosaka, O. (2012). Regionally Distinct Processing of Rewards and Punishments by the Primate Ventromedial Prefrontal Cortex. *Journal of Neuroscience*, *32*(30), 10318–10330. https://doi.org/10.1523/JNEUROSCI.1801-12.2012

Mooshagian, E., & Snyder, L. H. (2018). Spatial eye–hand coordination during bimanual reaching is not systematically coded in either LIP or PRR. *Proceedings of the National Academy of Sciences of the United States of America*, *115*(16), E3817–E3826. https://doi.org/10.1073/pnas.1718267115

Morecraft, R. J., Stilwell-Morecraft, K. S., Cipolloni, P. B., Ge, J., McNeal, D. W., & Pandya, D. N. (2012). Cytoarchitecture and cortical connections of the anterior cingulate and adjacent

somatomotor fields in the rhesus monkey. *Brain Research Bulletin*, *87*(4), 457–497. https://doi.org/10.1016/j.brainresbull.2011.12.005

Munoz, D. P., & Wurtz, R. H. (1993). Fixation cells in monkey superior colliculus. II. Reversible activation and deactivation. *Journal of Neurophysiology*, *70*(2), 576–589.

Nakahashi, A., & Cisek, P. (2023). Parallel processing of value-related information during multi-attribute decisions. *Journal of Neurophysiology*, *130*(4), 967–979. https://doi.org/10.1152/jn.00230.2023

Nakahashi, A., & Cisek, P. (2016). *How is neural activity in premotor and parietal cortex influenced by bottom-up and top-down information about the value of reach choices?* [Poster, Program No. 81.13]. Society for Neuroscience, 2016, San Diego. https://www.abstractsonline.com/pp8/index.html#!/4071/presentation/22376

Nakahashi, A., & Cisek, P. (2020). *Neural space trajectories of macaque dorsal premotor and posterior parietal cortex activity during multi-attribute decision-making* [E-Poster]. FENS Forum, 2020.

Nakahashi, A., Lusignan, T., & Cisek, P. (2018). *Fronto-parietal neural activity during multi-attribute decision-making with conflicting value information* [Poster, Program No. 401.14]. Society for Neuroscience, 2018, San Diego. https://www.abstractsonline.com/pp8/#!/4649/presentation/3658

Nassi, J. J., & Callaway, E. M. (2009). Parallel processing strategies of the primate visual system. *Nature Reviews Neuroscience*, *10*(5), 360–372. https://doi.org/10.1038/nrn2619

Neitz, J., Geist, T., & Jacobs, G. H. (1989). Color vision in the dog. *Visual Neuroscience*, *3*(2), 119–125. https://doi.org/10.1017/S0952523800004430

Neitz, J., & Jacobs, G. H. (1986). Reexamination of spectral mechanisms in the rat (Rattus norvegicus). *Journal of Comparative Psychology*, *100*(1), 21–29.

Nestler, E. J. (2005). The Neurobiology of Cocaine Addiction. *Science & Practice Perspectives*, *3*(1), 4–10.

Orban, G. A., Van Essen, D., & Vanduffel, W. (2004). Comparative Mapping of Higher Visual Areas in Monkeys and Humans. *Trends in Cognitive Sciences*, *8*(7), 315–324. https://doi.org/10.1016/j.tics.2004.05.009

Padoa-Schioppa, C. (2009). Range-Adapting Representation of Economic Value in the Orbitofrontal Cortex. *Journal of Neuroscience*, *29*(44), 14004–14014. https://doi.org/10.1523/JNEUROSCI.3751-09.2009

Padoa-Schioppa, C. (2011). Neurobiology of economic choice: A good-based model. *Annual Review of Neuroscience*, *34*, 333–359. https://doi.org/10.1146/annurev-neuro-061010-113648

Padoa-Schioppa, C., & Assad, J. A. (2006). Neurons in the orbitofrontal cortex encode economic value. *Nature*, *441*(7090), 223–226. https://doi.org/10.1038/nature04676

Padoa-Schioppa, C., & Assad, J. A. (2008). The representation of economic value in the orbitofrontal cortex is invariant for changes of menu. *Nature Neuroscience*, *11*(1), Article 1. https://doi.org/10.1038/nn2020

Pal, A., & Sinha, A. (2022). Beyond food for thought: Tool use and manufacture by wild nonhuman primates in nonforaging contexts. *Current Opinion in Behavioral Sciences*, *47*, 101201. https://doi.org/10.1016/j.cobeha.2022.101201

Pandya, D. N., & Seltzer, B. (1982). Intrinsic connections and architectonics of posterior parietal cortex in the rhesus monkey. *Journal of Comparative Neurology*, *204*(2), 196–210. https://doi.org/10.1002/cne.902040208

Papagno, C., Comi, A., Riva, M., Bizzi, A., Vernice, M., Casarotti, A., Fava, E., & Bello, L. (2017). Mapping the brain network of the phonological loop. *Human Brain Mapping*, *38*(6), 3011–3024. https://doi.org/10.1002/hbm.23569

Parton, A., Malhotra, P., & Husain, M. (2004). Hemispatial neglect. *Journal of Neurology, Neurosurgery, and Psychiatry*, *75*(1), 13–21.

Pasley, B. N., David, S. V., Mesgarani, N., Flinker, A., Shamma, S. A., Crone, N. E., Knight, R. T., & Chang, E. F. (2012). Reconstructing Speech from Human Auditory Cortex. *PLOS Biology*, *10*(1), e1001251. https://doi.org/10.1371/journal.pbio.1001251

Pastor-Bernier, A., & Cisek, P. (2011). Neural Correlates of Biased Competition in Premotor Cortex. *Journal of Neuroscience*, *31*(19), 7083–7088. https://doi.org/10.1523/JNEUROSCI.5681-10.2011

Pesaran, B., Nelson, M. J., & Andersen, R. A. (2008). Free choice activates a decision circuit between frontal and parietal cortex. *Nature*, *453*(7193), 406–409. https://doi.org/10.1038/nature06849

Petrides, M., & Pandya, D. N. (2009). Distinct parietal and temporal pathways to the homologues of Broca's area in the monkey. *PLoS Biology*, *7*(8), e1000170. https://doi.org/10.1371/journal.pbio.1000170

Petrides, M., Tomaiuolo, F., Yeterian, E. H., & Pandya, D. N. (2012). The prefrontal cortex: Comparative architectonic organization in the human and the macaque monkey brains. *Cortex*, *48*(1), 46–57. https://doi.org/10.1016/j.cortex.2011.07.002

Philiastides, M. G., Biele, G., & Heekeren, H. R. (2010). A mechanistic account of value computation in the human brain. *Proceedings of the National Academy of Sciences*, *107*(20), 9430–9435. https://doi.org/10.1073/pnas.1001732107

Piccinini, G., & Bahar, S. (2013). Neural Computation and the Computational Theory of Cognition. *Cognitive Science*, *37*(3), 453–488. https://doi.org/10.1111/cogs.12012

Pierrot-Deseilligny, C., Müri, R. M., Nyffeler, T., & Milea, D. (2005). The Role of the Human Dorsolateral Prefrontal Cortex in Ocular Motor Behavior. *Annals of the New York Academy of Sciences*, *1039*(1), 239–251. https://doi.org/10.1196/annals.1325.023

Pierrot-Deseilligny, C., Müri, R. M., Ploner, C. J., Gaymard, B., Demeret, S., & Rivaud-Pechoux, S. (2003). Decisional role of the dorsolateral prefrontal cortex in ocular motor behaviour. *Brain*, *126*(6), 1460–1473. https://doi.org/10.1093/brain/awg148

Platt, M. L., & Glimcher, P. W. (1999). Neural correlates of decision variables in parietal cortex. *Nature*, *400*(6741), 233–238. https://doi.org/10.1038/22268

Pritchard, T. C., Nedderman, E. N., Edwards, E. M., Petticoffer, A. C., Schwartz, G. J., & Scott, T. R. (2008). Satiety-responsive neurons in the medial orbitofrontal cortex of the macaque. *Behavioral Neuroscience*, *122*(1), 174–182. https://doi.org/10.1037/0735-7044.122.1.174

Ramnani, N., Behrens, T. E. J., Johansen-Berg, H., Richter, M. C., Pinsk, M. A., Andersson, J. L. R., Rudebeck, P., Ciccarelli, O., Richter, W., Thompson, A. J., Gross, C. G., Robson, M. D., Kastner, S., & Matthews, P. M. (2006). The evolution of prefrontal inputs to the cortico-pontine system: Diffusion imaging evidence from Macaque monkeys and humans. *Cerebral Cortex*, *16*(6), 811–818. https://doi.org/10.1093/cercor/bhj024

Rayner, K. (1998). Eye movements in reading and information processing: 20 years of research. *Psychological Bulletin*, *124*(3), 372–422. https://doi.org/10.1037/0033-2909.124.3.372

Rilling, J. K. (2006). Human and nonhuman primate brains: Are they allometrically scaled versions of the same design? *Evolutionary Anthropology: Issues, News, and Reviews*, *15*(2), 65–77. https://doi.org/10.1002/evan.20095

Ringach, D. L. (2004). Mapping receptive fields in primary visual cortex. *Journal of Physiology*, *558*(3), 717–728. https://doi.org/10.1113/jphysiol.2004.065771

Rizzolatti, G., & Luppino, G. (2001). The Cortical Motor System. *Neuron*, *31*(6), 889–901. https://doi.org/10.1016/S0896-6273(01)00423-8

Rizzolatti, G., Luppino, G., & Matelli, M. (1998). The organization of the cortical motor system: New concepts. *Electroencephalography and Clinical Neurophysiology*, *106*(4), 283–296. https://doi.org/10.1016/S0013-4694(98)00022-4

Roe, R. M., Busemeyer, J. R., & Townsend, J. T. (2001). Multialternative decision field theory: A dynamic connectionist model of decision making. *Psychological Review*, *108*(2), 370–392. https://doi.org/10.1037/0033-295x.108.2.370

Rolls, E. T., Hornak, J., Wade, D., & McGrath, J. (1994). Emotion-related learning in patients with social and emotional changes associated with frontal lobe damage. *Journal of Neurology, Neurosurgery, and Psychiatry*, *57*(12), 1518–1524.

Rudebeck, P. H., Behrens, T. E., Kennerley, S. W., Baxter, M. G., Buckley, M. J., Walton, M. E., & Rushworth, M. F. S. (2008). Frontal Cortex Subregions Play Distinct Roles in Choices between Actions and Stimuli. *Journal of Neuroscience*, *28*(51), 13775–13785. https://doi.org/10.1523/JNEUROSCI.3541-08.2008

Rushworth, M. F., Kolling, N., Sallet, J., & Mars, R. B. (2012). Valuation and decision-making in frontal cortex: One or many serial or parallel systems? *Current Opinion in Neurobiology*, *22*(6), 946–955. https://doi.org/10.1016/j.conb.2012.04.011

Samejima, K., Ueda, Y., Doya, K., & Kimura, M. (2005). Representation of Action-Specific Reward Values in the Striatum. *Science*, *310*(5752), 1337–1340. https://doi.org/10.1126/science.1115270

Sanes, J. N., & Donoghue, J. P. (1993). Oscillations in local field potentials of the primate motor cortex during voluntary movement. *Proceedings of the National Academy of Sciences of the United States of America*, *90*(10), 4470–4474. https://doi.org/10.1073/pnas.90.10.4470

Sato, M., & Hikosaka, O. (2002). Role of Primate Substantia Nigra Pars Reticulata in Reward-Oriented Saccadic Eye Movement. *Journal of Neuroscience*, *22*(6), 2363–2373. https://doi.org/10.1523/JNEUROSCI.22-06-02363.2002

Sato, T. R., & Schall, J. D. (2003). Effects of stimulus-response compatibility on neural selection in frontal eye field. *Neuron*, *38*(4), 637–648.

Saur, D., Schelter, B., Schnell, S., Kratochvil, D., Küpper, H., Kellmeyer, P., Kümmerer, D., Klöppel, S., Glauche, V., Lange, R., Mader, W., Feess, D., Timmer, J., & Weiller, C. (2010). Combining functional and anatomical connectivity reveals brain networks for auditory language comprehension. *NeuroImage*, *49*(4), 3187–3197. https://doi.org/10.1016/j.neuroimage.2009.11.009

Schall, J. D., Paré, M., & Woodman, G. F. (2007). Comment on "Top-Down Versus Bottom-Up Control of Attention in the Prefrontal and Posterior Parietal Cortices." *Science*, *318*(5847), 44–44. https://doi.org/10.1126/science.1144865

Schall, J. D., & Thompson, K. G. (1999). Neural Selection and Control of Visually Guided Eye Movements. *Annual Review of Neuroscience*, *22*(1), 241–259. https://doi.org/10.1146/annurev.neuro.22.1.241

Scherberger, H., Jarvis, M. R., & Andersen, R. A. (2005). Cortical Local Field Potential Encodes Movement Intentions in the Posterior Parietal Cortex. *Neuron*, *46*(2), 347–354. https://doi.org/10.1016/j.neuron.2005.03.004

Schiffer, S. (1991). Ceteris paribus laws. *Mind*, *C*(397), 1–17. https://doi.org/10.1093/mind/C.397.1

Schmahmann, J. D., Pandya, D. N., Wang, R., Dai, G., D'Arceuil, H. E., de Crespigny, A. J., & Wedeen, V. J. (2007). Association fibre pathways of the brain: Parallel observations from diffusion spectrum imaging and autoradiography. *Brain*, *130*(3), 630–653. https://doi.org/10.1093/brain/awl359

Schmolesky, M. T., Wang, Y., Hanes, D. P., Thompson, K. G., Leutgeb, S., Schall, J. D., & Leventhal, A. G. (1998). Signal timing across the macaque visual system. *Journal of Neurophysiology*, *79*(6), 3272–3278. https://doi.org/10.1152/jn.1998.79.6.3272

Schnupp, J., King, A., Walker, K., & Bizley, J. (2010). The Representation of the Pitch of Vowel Sounds in Ferret Auditory Cortex. In E. A. Lopez-Poveda, A. R. Palmer, & R. Meddis (Eds.), *The Neurophysiological Bases of Auditory Perception* (pp. 407–416). Springer. https://doi.org/10.1007/978-1-4419-5686-6_38

Schultz, W., Tremblay, L., & Hollerman, J. R. (2000). Reward Processing in Primate Orbitofrontal Cortex and Basal Ganglia. *Cerebral Cortex*, *10*(3), 272–283. https://doi.org/10.1093/cercor/10.3.272

Schweimer, J., & Hauber, W. (2005). Involvement of the rat anterior cingulate cortex in control of instrumental responses guided by reward expectancy. *Learning & Memory*, *12*(3), 334–342. https://doi.org/10.1101/lm.90605

Scott, J. A., Grayson, D., Fletcher, E., Lee, A., Bauman, M. D., Schumann, C. M., Buonocore, M. H., & Amaral, D. G. (2016). Longitudinal analysis of the developing rhesus monkey brain using magnetic resonance imaging: Birth to adulthood. *Brain Structure and Function*, *221*(5), 2847–2871. https://doi.org/10.1007/s00429-015-1076-x

Seltzer, B., & Pandya, D. N. (1986). Posterior parietal projections to the intraparietal sulcus of the rhesus monkey. *Experimental Brain Research*, *62*(3), 459–469. https://doi.org/10.1007/BF00236024

Sergio, L. E., Hamel-Pâquet, C., & Kalaska, J. F. (2005). Motor Cortex Neural Correlates of Output Kinematics and Kinetics During Isometric-Force and Arm-Reaching Tasks. *Journal of Neurophysiology*, *94*(4), 2353–2378. https://doi.org/10.1152/jn.00989.2004

Shadlen, M. N., & Newsome, W. T. (2001). Neural Basis of a Perceptual Decision in the Parietal Cortex (Area LIP) of the Rhesus Monkey. *Journal of Neurophysiology*, *86*(4), 1916–1936. https://doi.org/10.1152/jn.2001.86.4.1916

Shallice, T. (1982). Specific Impairments of Planning. *Philosophical Transactions of the Royal Society of London B: Biological Sciences*, *298*(1089), 199–209. https://doi.org/10.1098/rstb.1982.0082

Shallice, T., & Burgess, P. W. (1991). Deficits in strategy application following frontal lobe damage in man. *Brain*, *114*(2), 727–741. https://doi.org/10.1093/brain/114.2.727

Shevlin, B. R. K., Smith, S. M., Hausfeld, J., & Krajbich, I. (2022). High-value decisions are fast and accurate, inconsistent with diminishing value sensitivity. *Proceedings of the National Academy of Sciences of the United States of America*, *119*(6), e2101508119. https://doi.org/10.1073/pnas.2101508119

Shidara, M., & Richmond, B. J. (2002). Anterior Cingulate: Single Neuronal Signals Related to Degree of Reward Expectancy. *Science*, *296*(5573), 1709–1711. https://doi.org/10.1126/science.1069504

Shipp, S., Blanton, M., & Zeki, S. (1998). A visuo-somatomotor pathway through superior parietal cortex in the macaque monkey: Cortical connections of areas V6 and V6A. *European Journal of Neuroscience*, *10*(10), 3171–3193. https://doi.org/10.1046/j.1460-9568.1998.00327.x

Shizgal, P. (1997). Neural basis of utility estimation. *Current Opinion in Neurobiology*, *7*(2), 198–208. https://doi.org/10.1016/S0959-4388(97)80008-6

Shoham, D., & Grinvald, A. (2001). The Cortical Representation of the Hand in Macaque and Human Area S-I: High Resolution Optical Imaging. *Journal of Neuroscience*, *21*(17), 6820–6835. https://doi.org/10.1523/JNEUROSCI.21-17-06820.2001

Siegel, M., Buschman, T. J., & Miller, E. K. (2015). Cortical information flow during flexible sensorimotor decisions. *Science*, *348*(6241), 1352–1355. https://doi.org/10.1126/science.aab0551

Smeets, J. B. J., & Brenner, E. (2008). Grasping Weber's law. *Current Biology*, *18*(23), R1089–R1090. https://doi.org/10.1016/j.cub.2008.10.008

Smith, D. V., Hayden, B. Y., Truong, T.-K., Song, A. W., Platt, M. L., & Huettel, S. A. (2010). Distinct Value Signals in Anterior and Posterior Ventromedial Prefrontal Cortex. *Journal of Neuroscience*, *30*(7), 2490–2495. https://doi.org/10.1523/JNEUROSCI.3319-09.2010

Smith, E. E., & Jonides, J. (1997). Working Memory: A View from Neuroimaging. *Cognitive Psychology*, *33*(1), 5–42. https://doi.org/10.1006/cogp.1997.0658

Snyder, L. H., Batista, A. P., & Andersen, R. A. (1997). Coding of intention in the posterior parietal cortex. *Nature*, *386*(6621), Article 6621. https://doi.org/10.1038/386167a0

Snyder, L. H., Batista, A. P., & Andersen, R. A. (2000). Saccade-Related Activity in the Parietal Reach Region. *Journal of Neurophysiology*, *83*(2), 1099–1102.

Song, J.-H., & McPeek, R. M. (2010). Roles of Narrow- and Broad-Spiking Dorsal Premotor Area Neurons in Reach Target Selection and Movement Production. *Journal of Neurophysiology*, *103*(4), 2124–2138. https://doi.org/10.1152/jn.00238.2009

Sparks, D. L. (1978). Functional properties of neurons in the monkey superior colliculus: Coupling of neuronal activity and saccade onset. *Brain Research*, *156*(1), 1–16. https://doi.org/10.1016/0006-8993(78)90075-6

Stevens, S. S. (1957). On the Psychophysical Law. *Psychological Review*, *64*, 153–181. https://doi.org/10.1037/h0046162

Stoet, G., & Snyder, L. H. (2004). Single Neurons in Posterior Parietal Cortex of Monkeys Encode Cognitive Set. *Neuron*, *42*(6), 1003–1012. https://doi.org/10.1016/j.neuron.2004.06.003

Suchan, B., Yágüez, L., Wunderlich, G., Canavan, A. G. M., Herzog, H., Tellmann, L., Hömberg, V., & Seitz, R. J. (2002). Hemispheric dissociation of visual-pattern processing and visual rotation. *Behavioural Brain Research*, *136*(2), 533–544. https://doi.org/10.1016/S0166-4328(02)00204-8

Sugrue, L. P., Corrado, G. S., & Newsome, W. T. (2004). Matching Behavior and the Representation of Value in the Parietal Cortex. *Science*, *304*(5678), 1782–1787. https://doi.org/10.1126/science.1094765

Sugrue, L. P., Corrado, G. S., & Newsome, W. T. (2005). Choosing the greater of two goods: Neural currencies for valuation and decision making. *Nature Reviews Neuroscience*, *6*(5), 363–375. https://doi.org/10.1038/nrn1666

Supèr, H., Spekreijse, H., & Lamme, V. A. F. (2001). A Neural Correlate of Working Memory in the Monkey Primary Visual Cortex. *Science*, *293*(5527), 120–124. https://doi.org/10.1126/science.1060496

Swaminathan, S. K., Masse, N. Y., & Freedman, D. J. (2013). A Comparison of Lateral and Medial Intraparietal Areas during a Visual Categorization Task. *Journal of Neuroscience*, *33*(32), 13157–13170. https://doi.org/10.1523/JNEUROSCI.5723-12.2013

Taira, M., Boline, J., Smyrnis, N., Georgopoulos, A. P., & Ashe, J. (1996). On the relations between single cell activity in the motor cortex and the direction and magnitude of three-dimensional static isometric force. *Experimental Brain Research*, *109*(3), 367–376. https://doi.org/10.1007/BF00229620

Takikawa, Y., Kawagoe, R., & Hikosaka, O. (2002). Reward-Dependent Spatial Selectivity of Anticipatory Activity in Monkey Caudate Neurons. *Journal of Neurophysiology*, *87*(1), 508–515. https://doi.org/10.1152/jn.00288.2001

Talmi, D., Dayan, P., Kiebel, S. J., Frith, C. D., & Dolan, R. J. (2009). How Humans Integrate the Prospects of Pain and Reward during Choice. *Journal of Neuroscience*, *29*(46), 14617–14626. https://doi.org/10.1523/JNEUROSCI.2026-09.2009

Tan, Y., & Li, W.-H. (1999). Trichromatic vision in prosimians. *Nature*, *402*(6757), Article 6757. https://doi.org/10.1038/46947

Tanji, J., & Hoshi, E. (2008). Role of the lateral prefrontal cortex in executive behavioral control. *Physiological Reviews*, *88*(1), 37–57. https://doi.org/10.1152/physrev.00014.2007

Tanné-Gariépy, J., Rouiller, E. M., & Boussaoud, D. (2002). Parietal inputs to dorsal versus ventral premotor areas in the macaque monkey: Evidence for largely segregated visuomotor pathways. *Experimental Brain Research*, *145*(1), 91–103. https://doi.org/10.1007/s00221-002-1078-9

Thiebaut de Schotten, M., Dell'Acqua, F., Valabregue, R., & Catani, M. (2012). Monkey to human comparative anatomy of the frontal lobe association tracts. *Cortex*, *48*(1), 82–96. https://doi.org/10.1016/j.cortex.2011.10.001

Thura, D., Cabana, J.-F., Feghaly, A., & Cisek, P. (2022). Integrated neural dynamics of sensorimotor decisions and actions. *PLOS Biology*, *20*(12), e3001861. https://doi.org/10.1371/journal.pbio.3001861

Thura, D., & Cisek, P. (2014). Deliberation and Commitment in the Premotor and Primary Motor Cortex during Dynamic Decision Making. *Neuron*, *81*(6), 1401–1416. https://doi.org/10.1016/j.neuron.2014.01.031

Thura, D., & Cisek, P. (2020). Microstimulation of dorsal premotor and primary motor cortex delays the volitional commitment to an action choice. *Journal of Neurophysiology*, *123*(3), 927–935. https://doi.org/10.1152/jn.00682.2019

Treisman, A. M., & Gelade, G. (1980). A feature-integration theory of attention. *Cognitive Psychology*, *12*(1), 97–136. https://doi.org/10.1016/0010-0285(80)90005-5

Trueblood, J. S., Brown, S. D., & Heathcote, A. (2014). The multiattribute linear ballistic accumulator model of context effects in multialternative choice. *Psychological Review*, *121*, 179–205. https://doi.org/10.1037/a0036137

Turken, A. U., & Swick, D. (1999). Response selection in the human anterior cingulate cortex. *Nature Neuroscience*, *2*(10), Article 10. https://doi.org/10.1038/13224

Utz, K. S., Hesse, C., Aschenneller, N., & Schenk, T. (2015). Biomechanical factors may explain why grasping violates Weber's law. *Vision Research*, *111*, 22–30. https://doi.org/10.1016/j.visres.2015.03.021

Vargas-Irwin, C. E., Shakhnarovich, G., Yadollahpour, P., Mislow, J. M. K., Black, M. J., & Donoghue, J. P. (2010). Decoding Complete Reach and Grasp Actions from Local Primary Motor Cortex Populations. *Journal of Neuroscience*, *30*(29), 9659–9669. https://doi.org/10.1523/JNEUROSCI.5443-09.2010

Wallis, J. D. (2007). Orbitofrontal Cortex and Its Contribution to Decision-Making. *Annual Review of Neuroscience*, *30*, 31–56. https://doi.org/10.1146/annurev.neuro.30.051606.094334

Wallis, J. D., & Miller, E. K. (2003). Neuronal activity in primate dorsolateral and orbital prefrontal cortex during performance of a reward preference task. *European Journal of Neuroscience*, *18*(7), 2069–2081. https://doi.org/10.1046/j.1460-9568.2003.02922.x

Walton, M. E., Bannerman, D. M., Alterescu, K., & Rushworth, M. F. S. (2003). Functional Specialization within Medial Frontal Cortex of the Anterior Cingulate for Evaluating Effort-Related Decisions. *Journal of Neuroscience*, *23*(16), 6475–6479. https://doi.org/10.1523/JNEUROSCI.23-16-06475.2003

Wang, P., & Nikolic, D. (2011). An LCD Monitor with Sufficiently Precise Timing for Research in Vision. *Frontiers in Human Neuroscience*, *5*. https://doi.org/10.3389/fnhum.2011.00085

Watanabe, M. (1996). Reward expectancy in primate prefrontal neurons. *Nature*, *382*(6592), 629–632. https://doi.org/10.1038/382629a0

Westendorff, S., Klaes, C., & Gail, A. (2010). The Cortical Timeline for Deciding on Reach Motor Goals. *Journal of Neuroscience*, *30*(15), 5426–5436. https://doi.org/10.1523/JNEUROSCI.4628-09.2010

Wong, B. B. M., & Candolin, U. (2015). Behavioral responses to changing environments. *Behavioral Ecology*, *26*(3), 665–673. https://doi.org/10.1093/beheco/aru183

Yan, Y., Sobinov, A. R., & Bensmaia, S. J. (2022). Prehension kinematics in humans and macaques. *Journal of Neurophysiology*, *127*(6), 1669–1678. https://doi.org/10.1152/jn.00522.2021

Yan, Y., Wei, R., Zhang, Q., Jin, Z., Li, L., Burnham, B. P., Rauschenberger, R., Knudsen, E. I., Kiss, M., Eimer, M., Mueller, H. J., Geyer, T., Zehetleitner, M., Krummenacher, J., Proulx, M. J., Egeth, H. E., Wang, M., Corbetta, M., Shulman, G. L., … Peleman, K. (2016). Differential roles of the dorsal prefrontal and posterior parietal cortices in visual search: A TMS study. *Scientific Reports*, *6*, 30300. https://doi.org/10.1038/srep30300

Yang, T., & Shadlen, M. N. (2007). Probabilistic reasoning by neurons. *Nature*, *447*(7148), Article 7148. https://doi.org/10.1038/nature05852

Yang, X., & Krajbich, I. (2022). A dynamic computational model of gaze and choice in multi-attribute decisions. *Psychological Review*. https://doi.org/10.1037/rev0000350

Yep, R., Smorenburg, M. L., Riek, H. C., Calancie, O. G., Kirkpatrick, R. H., Perkins, J. E., Huang, J., Coe, B. C., Brien, D. C., & Munoz, D. P. (2022). Interleaved Pro/Anti-saccade Behavior Across the Lifespan. *Frontiers in Aging Neuroscience*, *14*. https://www.frontiersin.org/articles/10.3389/fnagi.2022.842549

Zamora-López, G., Zhou, C., & Kurths, J. (2010). Cortical hubs form a module for multisensory integration on top of the hierarchy of cortical networks. *Frontiers in Neuroinformatics*, *4*. https://www.frontiersin.org/articles/10.3389/neuro.11.001.2010

Zilles, K., Schlaug, G., Matelli, M., Luppino, G., Schleicher, A., Qü, M., Dabringhaus, A., Seitz, R., & Roland, P. E. (1995). Mapping of human and macaque sensorimotor areas by integrating architectonic, transmitter receptor, MRI and PET data. *Journal of Anatomy*, *187*(Pt 3), 515–537.